



IChF

Institute of Physical Chemistry PAS

Ph.D. Dissertation

**Chemical Characterization of Isoprene
Secondary Organic Aerosol in the Atmosphere
using LC-MS/MS Approaches**

Paulina Wach

Ph.D. Thesis

***Chemical Characterization of Isoprene Secondary
Organic Aerosol in the Atmosphere using LC-MS/MS
Approaches***

Paulina Wach, M.Sc.

Supervisor:

prof. dr hab. Rafał Szmigielski, Ph.D., D.Sc.

Biblioteka Instytutu Chemii Fizycznej PAN

F-B.575/24



10000000116289

A-21-7

K-c-123

H-63

The thesis was prepared within the International Doctoral Studies
at the Institute of Physical Chemistry, Polish Academy of Sciences, Warsaw, Poland

Warsaw, June 2023



B.575/24

*I dedicate this work to my Beloved ones, who showed great patience during my entire
adventure with my doctorate studies.*

Zosia, Staś, Grzegorz, Mom, Dad and my Sister - thank you!

Acknowledgments

There is a group of people without whom, despite the greatest willingness, this work would not have been created, which is why I would like to thank them here.

My supervisor, Prof. Rafał Szmigielski, thank you for inviting me to your research group, introducing me to the world of atmospheric aerosol, many valuable scientific talks, and help in the preparation of this work.

Special thanks are due to the Institute of Organic Chemistry of the Polish Academy of Sciences and to Professor Witold Danikiewicz for providing the measurement equipment used for all UHPLC-MS measurements described in this work. Professor, thank you for showing me the beauty of mass spectrometry, discussions on the results obtained and valuable substantive tips during the research covered by the scope of this thesis.

Professor Magda Claeys and Willy Meenhaut, thank you for your willingness to share your vast knowledge in the field of atmospheric aerosols and the analytical techniques used to study them. I would also like to thank you for the great support and warmth you always have for your co-workers. It was an honor and pleasure for me to work with you.

Dr. Krzysztof Rudzinski, thank you for your warmth, many conversations - both scientific and non-scientific ones, for help in preparing experiments in the aqueous phase, and for always valuable substantive comments.

I would also like to thank Professor Jason Suratt and Ying-Hsuan Lin for the smog chamber experiments and Teflon filter samples, as well as for valuable scientific discussions.

I would like to thank Krzysztof Skotak and other colleagues from The Institute of Environmental Protection – National Research Institute for providing fine ambient PM_{2.5} aerosol samples and for enjoyable work together during field campaigns.

I would like to thank my colleagues from the Environmental Chemistry Group for the joint scientific adventure and the atmosphere during it.

My colleagues from the Mass Spectrometry Group of the Institute of Organic Chemistry of the Polish Academy of Sciences in the years 2014-2020 I would like to thank you for

accepting me into your "mass-spec" family and for the disinterested help and kindness that I could always count on from you.

Ewelina, Ilona, Damian, Emil and Sandra – thank you for your support, lots of laughter, and hours spent learning together during our Ph.D. studies.

And finally, a special thanks go to Grzegorz Spólnik – for the fun and excitement with smaller and larger scientific discoveries, all the crazy ideas, gathering hail in a storm, hours spent together at the Synapt mass spectrometer and on analyzing fragmentation spectra, and for immeasurable support, love and faith in my abilities.

Funding

This thesis was partially supported by funds from the National Science Centre of Poland within OPUS8 Grant no. 2014/15/B/ST10/04276.



NATIONAL SCIENCE CENTRE
POLAND

Scientific achievements

Publications

The Ph.D. thesis is based on the following peer-reviewed publications (1-4):

1. Spolnik, Grzegorz; **Wach, Paulina**; Rudzinski, Krzysztof J.; Szmigielski, Rafal; Danikiewicz, Witold*; „Tracing the biogenic secondary organic aerosol markers in rain, snow and hail”, *Chemosphere*, 2020, 251, 126435.
2. **Wach, Paulina***; Spolnik, Grzegorz; Surratt, Jason D.; Blaziak, Kacper; Rudzinski, Krzysztof J.; Lin, Ying-Hsuan; Maenhaut, Willy; Danikiewicz, Witold; Claeys, Magda; Szmigielski, Rafal*; “Structural Characterization of Lactone-Containing MW 212 Organosulfates Originating from Isoprene Oxidation in Ambient Fine Aerosol”; *Environmental Science & Technology*, 2020, 54, 3, 1415-1424.
3. **Wach, Paulina***; Spolnik, Grzegorz; Rudzinski, Krzysztof J; Skotak, Krzysztof; Claeys, Magda; Danikiewicz, Witold; Szmigielski, Rafal*; „Radical oxidation of methyl vinyl ketone and methacrolein in aqueous droplets: characterization of organosulfates and atmospheric implications”, *Chemosphere*, 2019, 214, 1-9.
4. Spolnik, Grzegorz*; **Wach, Paulina**; Rudzinski, Krzysztof J; Skotak, Krzysztof; Danikiewicz, Witold; Szmigielski, Rafal*; „Improved UHPLC-MS/MS Methods for Analysis of Isoprene-Derived Organosulfates”, *Analytical Chemistry* 2018, 90(5), 3416-3423.

* corresponding authors

Other publications in which the author participated:

5. Spolnik, Grzegorz; **Wach, Paulina**; Wrobel, Zbigniew; Danikiewicz, Witold; „2-Iodomalondialdehyde is an abundant component of soluble organic iodine in atmospheric wet precipitation”, *Science of the Total Environment*, 2020, 730, 139175.
6. Rudzinski, Krzysztof J.; Szmigielski, Rafal; Kuznietsova, Inna; **Wach, Paulina**; Staszek, Dorota; "Aqueous-phase story of isoprene - A mini-review and reaction with HONO", *Atmospheric Environment* 2016, 130, 163-171.
7. Krasowska, Dorota; Zajac, Adrian; **Wach, Paulina**; Ciesielski, Wojciech; Michalski, Oskar; Kulawik, Damian; Pyzalska, Magdalena; Dudzinski, Bogdan; Pokora-Sobczak, Patrycja; Makowski, Tomasz; Janicka, Magdalena; “A Stereogenic

viii

Heteroatom-Containing Substituent as an Inducer of Chirality in the Derivatives of Thiophenes (Mono, Oligo and Poly), Fullerenes C60 and Multiwalled Nanotubes”, *Phosphorus, Sulfur and Silicon and the Related Elements* 2016, 191(3), 211-219.

8. Drabowicz, Józef; Pokora-Sobczak, Patrycja; Zając, Adrian; **Wach-Panfilow Paulina**; “A new procedure for the synthesis of optically active *t*-butylphenylphosphinothioic acid”, *Heteroatom Chemistry* 2014, 25(6), 674-677;

Chapter in the Monography

1. Drabowicz, Józef; Kielbasiński, Piotr; Zając, Adrian; **Wach-Panfilow, Paulina**; “Synthesis of sulfides, sulfoxides and sulfones” in *Comprehensive Organic Synthesis*, Gary A. Molander and Paul Knochel, Eds., 2nd Edition, Vol. 6, Oxford: Elsevier: 2014, pp. 131-174;

Patents

1. "Method for producing ionic liquids derivatives of organic phosphorous thioacids, involves dissolving thioacids in organic solvent, treating with desired amine and isolating resulting salts to ammonium by evaporation of solvent"; Inventor(s): DRABOWICZ J; POKORA-SOBCZAK P; KRASOWSKA D; et al.; Patent Number: PL406986-A1;
2. "Producing optically active *tert*-butylphenylthiophosphonic acid comprises treating racemic mixture of *tert*-butyl phenyl phosphine oxide with elemental sulfur in presence of alpha-phenylethylamine, isolating diastereomers and resolving"; Inventor(s): DRABOWICZ J; POKORA-SOBCZAK P; ZAJAC A; et al.; Patent Number: PL405141-A1;

Oral Presentations

1. **P. Wach**, G. Spólnik, J.D. Surratt, K. Błaziak, K.J. Rudziński; Lin, Ying-Hsuan; W. Meanhaut, W. Danikiewicz, M. Claeys, R. Szmigielski; “Structural Characterization of Lactone-Containing MW 212 Organosulfates Originating from Isoprene Oxidation in Ambient Fine Aerosol”, European Aerosol Conference 2020, Aachen, Germany
2. **P. Wach**, G. Spólnik, K.J. Rudziński, W. Meanhaut, M. Claeys, R. Szmigielski; „Identyfikacja organosiarczanów jako składników wtórnego aerozolu

atmosferycznego z wykorzystaniem techniki UHPLC-MS/MS”; Book of Abstracts: ISBN 978-83-60988-23-7, str. 265, S09K09

Posters

1. J. Drabowicz, D. Krasowska, A. Zając, **P. Wach-Panfilow**, E. Rozycka-Sokolowska, B. Marciniak, “Fullerene C₆₀ and mono- and oligo(poly)thiophenes containing a stereogenic heteroatom: Attempted syntheses and structural determinations”, 6th International Symposium on Molecular Electronics, December 3- 7. 2012, Grenoble (France), Symposium Materials, Chapter 3, Posters, pp. 163-164, T5-PC23.
2. D. Krasowska, A. Zając, **P. Wach-Panfilow**, J. Drabowicz, ” Synthesis and structural studies of fullerene C₆₀ and thiophenes [mono- Or oligo(poly)] functionalized with a stereogenic heteroatom”, 14th International Conference on Chiroptical Spectroscopy, June 9-13, 2013, Nashville, USA, Program and Abstracts: P57;
3. **P. Wach-Panfilow**, A. Zając, J. Drabowicz, “Pochodne fulerenu C₆₀ funkcjonalizowane podstawnikiem ze stereogenicznym heteroatomem – syntezy i struktura”, 56. Zjazd PTChem i SITPChem, 16-20. Września 2013, Siedlce, Book of Abstracts: S01P96, p. 175;
4. **P. Wach-Panfilow**, J. Drabowicz, A. Zając, “Próby syntezy pochodnych fulerenu C₆₀ funkcjonalizowanych grupami zawierającymi heterogeniczny heteroatom”, Winter Session SS PTChem, 7. Grudnia 2013, Łódź, P98;
5. Zając, **P. Wach-Panfilow**, J. Drabowicz, “Attempts on the synthesis and structural studies of fullerene C₆₀ functionalized with a chiral sulfur atom containing group”, 26th International Symposium on Organic Chemistry of Sulfur, 24-29 August 2014, Istanbul, Turkey, Abstracts: p. 61, PP-A14;
6. Zając, **P. Wach-Panfilow**, J. Drabowicz, “Synteza i struktura pochodnych fulerenu C₆₀ funkcjonalizowanych grupami posiadającymi stereogeniczny heteroatom”, 57. Zjazd Naukowy PTChem i SITPChem, 14-18. Września 2014, Częstochowa, Abstracts: S01-P85, p. 103;
7. **P. Wach-Panfilow**, G. Spólnik, K. J. Rudziński, M. S. Shalamzari, W. Maenhaut, M. Claeys and R. Szmigielski, “Exploration of aqueous organosulfates from isoprene by LC/MS/MS”, 33rd Informal Meeting on Mass Spectroscopy, 10-13,05,2015 r, Szczyrk, Poland, Book of Abstracts: ISBN 978-83-940417-1-7, TuPo05, p. 14;

8. G. Spólnik, **P. Wach**, K.J. Rudziński, W. Danikiewicz, J.D. Surrat, W. Meanhaut, M. Claeys and R. Szmigielski, "Atmospheric Organic Aerosol: Challenging the organosulphates analysis with LC-MS approaches", 34th Informal Meeting on Mass Spectroscopy, 15-18.05.2016, Fiera di Primiero, Italy, Books of Abstracts: ISBN 978-88-89-884-31-7
9. M. Sojka, **P. Wach**, K. Nestorowicz, K.J. Rudziński, W. Danikiewicz, A. degórska, K. Skotak and R. Szmigielski, "Secondary Organic Aerosol (SOA) in Poland: molecular characterization of summer and winter samples with high resolution mass spectrometry", 34th Informal Meeting on Mass Spectroscopy, 15-18.05.2016 r, Fiera di Primiero, Italy, Books of Abstracts: ISBN 978-88-89-884-31-7
10. **P. Wach**, G. Spólnik, K.J. Rudziński, W. Danikiewicz, K. Skotak, and R. Szmigielski „Probing the chemical composition of the fine ambient aerosol, rainwater, and hailstone with UHPLC-MS technique. Is there anything in common?"; European Aerosol Conference 2017 Zurich 27.08.-01.09.2017 r.; T216N20e
11. G. Spólnik, **P. Wach**, K. Rudzinski, K. Nestorowicz, K. Skotak, W. Danikiewicz, and R. Szmigielski; "Improving LC-MS methods for a detailed SOA characterization" European Aerosol Conference 2017 Zurich 27.08.-01.09.2017 r.; T216N280

Professional Experience

04.2021 – Molecule.one, analytical chemist

analytical method development for High Throughput Experimentation applications; quantitative and qualitative analysis of organic compounds (LC-ESI-MS); data managing; workflow planning

05.2021 – 08.2021 Institute of Mother and Child, Laboratory of Biochemistry, Department of Screening and Metabolic Diagnostics; assistant - specialist

quantitative and qualitative analysis of amino- and organic acids in biological samples (LC, LC-ESI-MS)

11.2018 – 04.2021 Institute of Organic Chemistry, PAS, Mass Spectrometry Group; chemist

commercial qualitative and quantitative analysis on small organic compounds as well as complex structures, structure confirmations and identification of contaminants in drugs for the pharmaceutical industry (LC-ESI-MS, IM-ESI-MS)

08.2014 – 01.2018 Institute of Physical Chemistry, PAS, Environmental Chemistry Group; assistant, Ph.D. candidate

research on the path formation and structure of selected components of secondary atmospheric aerosol (LC-ESI-MS, GC-MS)

11.2012 – 07.2014 Center for Molecular and Macromolecular Studies, PAS, Department of Organic Chemistry; synthetic chemist

induction of chirality in fullerene C₆₀ structure (analytical methods used: ¹H, ¹³C, ³⁴P NMR, MALDI-MS, HPLC)

Didactic activity

- Thesis advisor of Master's thesis Patrycja Grzesiak, MA; winter/summer semester 2016/2017; Cardinal Stefan Wyszyński University
- Thesis advisor of engineering thesis Agaty Kołodziejczyk, Ph.D.; winter/summer semester 2014/2015; Warsaw University of Technology
- Conducting exercises with students of the Cardinal Stefan Wyszyński University entitled "Kinetics of atmospheric oxygen decay in polluted natural waters" at the Laboratory of Physical Chemistry in 2015
- 05.2015 and 05.2026 participation in the Science Picnic of Polish Radio and the Copernicus Science Center

Breaks in the scientific career

09.2017-11.2018 maternity leave

Abstract

Atmospheric particulate matter (PM) is a key air pollutant. The solid and/or liquid particles suspended in the air form **an atmospheric aerosol**. The latter is a complex chemical mixture encompassing compounds of different molecular masses, structures and physicochemical properties. The diversity of the chemical composition of atmospheric aerosol is influenced by multifold factors, including sources of gaseous precursors, availability of atmospheric oxidants, and meteorological conditions. For a given aerosol fraction collected at a site (defined by the maximum size of particles contained in it and the same concentration depending on the place of sampling and the conditions prevailing in it), its chemical composition may vary at either a qualitative or quantitative level. Aerosol particles strongly impact air quality, living organisms, and the Earth's climate, which is strongly dependent on the chemical composition of particles. Air pollution and smog evolution have become an increasingly popular subject of the research, due to the poor recognition of the composition of atmospheric aerosol, including respirable fractions, as well as due to the increasing number of cases of respiratory and cardiovascular diseases and premature deaths related directly to progressive air pollution. Air cleanliness is affected by both primary processes in which atmospheric dust is emitted directly into the atmosphere, e.g. through volcano emissions, and secondary processes where the particles are formed through the chemical reactions. Gaseous precursors, including sulfur and nitrogen oxides emitted to the atmosphere as a result of human activity, also enter secondary processes. In many regions of the world, regulations regarding the air purity standards are not obeyed. For example, this applies to the concentration limits for particulate matter (fraction PM_{10} and $PM_{2.5}$).

Despite considerable knowledge about the sources of atmosphere pollution, as well as its adverse effects, due to the complexity of processes occurring in the atmosphere, many issues remain unsolved. The submitted thesis encompasses a series of studies aimed at a detailed chemical characterization of secondary organic aerosol arising from the isoprene multiphase oxidation and proposing the likely mechanisms leading to its formation in the atmosphere. More specifically, I concentrated here on the characterization of the polar fraction of the PM matter, which is chiefly surpassed by

organosulfates and nitroxy-organosulfates, mostly of undefined structures and origins. Owing to this knowledge, it would make it possible to better assess their potential effects on the environment and human health, while the knowledge of the mechanisms of atmospheric aerosol formation should allow us to extend the atmospheric models to better predict smog episodes, and perhaps also to prevent them. To achieve the goal, I applied a combined approach linking the capacity of the liquid chromatography, mass spectrometry and organic synthesis for getting more insights into the aqueous-phase reactions between sulfate radicals ($\text{SO}_4^{\cdot-}$) and isoprene (C_5H_8) as well as isoprene oxygenates, i.e., methyl vinyl ketone and methacrolein (α , β -unsaturated carbonyls; $\text{C}_4\text{H}_6\text{O}$), leading to a novel chemical class of atmospheric particulate matter components – monoalkyl esters of sulfuric(VI) acids, hereinafter referred to as **organosulfates (OSs)**.

The research was conducted in several projects. First one encompassed a series of laboratory experiments, which equivocally proved that despite poor solubility of isoprene in the atmospheric waters, sulfate radicals-induced reactions of isoprene and its oxygenated derivatives, i.e., methyl-vinyl ketone and methacrolein, become important sources of aerosol-bound organosulfates. The results obtained from laboratory-conducted experiments revealed the presence of several atmospherically-relevant organosulfates. A series of LC-MS analyses carried out for fine ambient aerosol collected from various field campaigns confirmed their presence in natural samples. The comparison of chromatographic and mass spectral data obtained from both ambient and laboratory-generated aerosol allowed for the firm structural elucidation of several atmospherically relevant organosulfates, including the stereoisomeric assignments.

Streszczenie

Pył zawieszony (*ang.* particulate matter, PM) jest jednym z kluczowych zanieczyszczeń powietrza. Pył w postaci cząstek stałej lub ciekłej materii zawieszony w powietrzu tworzy aerozol atmosferyczny, który z chemicznego punktu widzenia stanowi złożoną matrycę środowiskową, składającą się z substancji o różnych składach elementarnych, masach cząsteczkowych, strukturach i właściwościach fizykochemicznych. Na różnorodny i złożony skład chemiczny aerozolu atmosferycznego ma wpływ wiele czynników, w tym: zmienne źródła prekursorów, różnorodność typów i stężeń utleniaczy atmosferycznych, czy aktualnie warunki atmosferyczne. Dla tej samej frakcji aerozolu, mierzoną poprzez maksymalną ilość znajdujących się w niej cząstek PM o zdefiniowanym rozmiarze aerodynamicznym i takiego samego stężenia w zależności od miejsca poboru próbki i panujących w nim warunków, skład chemiczny tej frakcji będzie różny. Cząsteczki aerozolu wywierają silny wpływ na organizmy żywe, jakość powietrza oraz klimat planety i różny w zależności od ich składu chemicznego. Obecnie temat smogu i zanieczyszczenia powietrza staje coraz pilniejszym przedmiotem badań, szczególnie w Polsce, między innymi ze względu na ciągle słabo rozpoznany skład chemiczny aerozolu atmosferycznego, w tym jego frakcji respirabilnych, jak również ze względu na lawinowo rosnącą liczbę pacjentów z chorobami oddechowo-kръżeniowymi i neurologicznymi oraz niepokojąco brzmiącymi danymi epidemiologicznymi, które wiążą przedwczesne zgony pacjentów z postępującym zanieczyszczeniem powietrza na obszarach miejskich i podmiejskich. Na jakość powietrza wpływ mają zarówno procesy pierwotne, w których pyły atmosferyczne są emitowane bezpośrednio do atmosfery, np. wybuchy wulkanów, jak i procesy wtórne, gdzie składniki aerozolu tworzą się w atmosferze w wyniku złożonych reakcji chemicznych. Dane z bezpośrednich pomiarów terenowych w różnych obszarach świata pokazują, że wkład źródeł wtórnych aerozolu jest zdecydowanie dominujący. W procesach wtórnych biorą udział również prekursorzy gazowe, w tym emitowane do atmosfery w wyniku działalności człowieka tlenki siarki(VI) i azotu(II). W wielu rejonach świata, w tym Azji i Ameryki południowej, nie są przestrzegane regulacje

dotyczące norm czystości powietrza, w szczególności wytyczne dopuszczalnych poziomów stężeń pyłu zawieszonego (frakcje PM_{10} i $PM_{2.5}$).

Pomimo dużej ilości badań na temat przyczyn zanieczyszczenia atmosfery, a także jego skutków, ze względu na złożoność zachodzących w atmosferze procesów nadal wiele zagadnień pozostaje nierozwiązanych. Niniejsza praca doktorska obejmuje cykl spójnych badań mających na celu oznaczenia na poziomie molekularnym składu wtórnego aerozolu organicznego, powstającego z wyniku utleniania izoprenu w systemach multi fazowych oraz zaproponowanie mechanizmów prowadzących do jego tworzenia w atmosferze. Dzięki pozyskanej wiedzy możliwe będzie w przyszłości poznanie jego oddziaływania na środowisko i ludzkie zdrowie, zaś znajomość mechanizmów – pozwoli w rozszerzyć dostępne modele atmosferyczne w celu lepszego przewidywania epizodów smogowych, w tym również płynących z nich zagrożeń. Główny nacisk w pracy położono na połączone zastosowanie narzędzi chromatografii cieczowej, spektrometrii mas oraz syntezy organicznej w celu dokładnego opisu przebiegu reakcji chemicznych zachodzących w fazie wodnej między rodnikami siarczanowymi (SO_4^-) a izoprenem (C_5H_8), jak również utlenowanymi pochodnymi izoprenu, tj. ketonem metyloowo-winylowym i metakroleiną (α,β -nienasycone związki karbonylowe; C_4H_6O), prowadzącymi do nowych składników atmosferycznych cząstek stałych – siarczanów organicznych, tj. monoalkilowych estrów kwasu siarkowego(VI), zwanych dalej w pracy organosiaraczami.

Badania prowadziłam w ramach równoległych projektów naukowych. Pierwszym z nich była seria eksperymentów laboratoryjnych, które jednoznacznie dowiodły, że pomimo słabej rozpuszczalności izoprenu w wodach atmosferycznych, inicjowane rodnikami siarczanowymi reakcje izoprenu i jego utlenowanych pochodny, stają się ważnym źródłem wtórnego aerozolu. Wyniki uzyskane z przeprowadzonych eksperymentów potwierdziły tworzenie wielu organosiarczanów istotnych z punktu widzenia chemii atmosfery. Następnie przeprowadziłam serię analiz LC-MS próbek naturalnego aerozolu atmosferycznego, zebranych podczas kampanii terenowych, w których potwierdziłam obecność organosiarczanów otrzymanych w pracach laboratoryjnych. Porównanie danych chromatograficznych i widm masowych, w tym widm fragmentacyjnych MS/MS istotnych składników aerozolu, uzyskanych zarówno

dla aerozolu naturalnego, jak i wytwarzanego laboratoryjnie, pozwoliło na dokładne przypisanie struktur szeregu istotnych pod względem atmosferycznym organosiarczanów, w tym rozpoznaniu ich złożonego profilu stereoizomerycznego.

Content

Acknowledgments.....	v
Funding	vii
Scientific achievements	viii
Professional Experience.....	xii
Didactic activity	xiii
Abstract.....	xv
Streszczenie	xvii
Content	xx
List of Charts	xxiii
List of Figures	xxiii
List of Schemes	xxvi
List of Tables.....	xxvii
List of Abbreviations.....	xxviii
1 LITERATURE OVERVIEW.....	1
1.1 Atmospheric aerosol – introduction	1
1.2 Classification.....	1
1.3 Sources.....	5
1.3.1 Primary.....	6
1.3.2 Secondary.....	8
1.4 Impact of atmospheric aerosols on climate and health.....	11
1.5 Secondary organic aerosol (SOA) in the atmosphere	13
1.5.1 Biogenic volatile organic compounds	14
1.5.1.1 Evolution of biogenic volatile organic compounds.....	16
1.5.1.2 Tropospheric oxidants	17
1.5.2 Main gas-phase oxidation pathways	20
1.5.3 Gas to particle partitioning theory.....	23
1.5.4 Particle – phase reactions of SOA.....	26
1.5.5 Non-oxidative processes	26
1.5.6 Oxidative processes.....	27
1.5.7 Selected SOA precursors in reactions with atmospheric oxidants.....	28
1.5.8 Isoprene-derived SOA markers formation	30
1.5.9 Organosulfates.....	33
1.6 Mass spectrometry as an analytical method for the aerosol characterization and quantitation.	35
1.6.1 Ionization techniques applied in the aerosol studies	35
1.6.2 Low- and high resolution mass spectrometry	45
1.6.3 Tandem mass spectrometry	45

1.6.4	Separation techniques	47
1.6.4.1	Gas chromatography technique	48
1.6.4.2	Liquid chromatography technique	49
1.6.4.3	Additional detectors in hyphenated LC-MS systems	50
2	AIM OF THE STUDY.....	53
3	EXPERIMENTAL SECTION.....	55
3.1	Chemicals.....	55
3.2	PM_{2.5} fine ambient aerosol samples.....	55
3.2.1	Filed sites	56
3.2.2	Sample preparation	59
3.2.2.1	Fine ambient PM _{2.5} aerosol used as a reference material in structural characterization of MW 212 OSs originating from isoprene.....	59
3.2.2.2	Fine ambient PM _{2.5} aerosol used as a reference material in radical oxidation of isoprene in the presence of ¹⁶ O ₂ and its ¹⁸ O ₂ isotopes.....	60
3.2.2.3	Ambient PM _{2.5} aerosol sample during LC-MS method optimization.....	60
3.2.2.4	Fine ambient PM _{2.5} aerosol used as a reference material in radical oxidation of methyl vinyl ketone and methacrolein	60
3.3	Samples of atmospheric waters	60
3.3.1	Field description and sample collection.....	60
3.3.2	Atmospheric waters sample preparation.....	61
3.3.2.1	Rain sample.....	61
3.3.2.2	Snow samples	61
3.3.2.3	Hail samples.....	62
3.4	Smog-chamber isoprene SOA.....	62
3.4.1	Experiment process.....	62
3.4.2	Sample preparation	64
3.5	Aqueous-phase reactions with auto-oxidation of S(IV) catalyzed by manganese (II) ions – MW 212 organosulfates characteristic.....	64
3.5.1	Homogenous oxidative degradation of isoprene, 3-methyl and 4-methyl-2(5H)-furanones.....	64
3.5.2	Heterogenous oxidative degradation of isoprene in the presence of atmospheric air.....	65
3.5.3	Heterogenous oxidative degradation of isoprene in the presence of isotopically-labeled oxygen ¹⁸ O ₂	65
3.6	Radical oxidation of methyl-vinyl ketone and methacrolein	66
4	METHODS.....	67
4.1	General remarks	67
4.1.1	Chromatographic separation.....	67
4.1.2	Operational parameters for the mass spectrometer.....	68
4.2	Homogenous oxidative degradation of isoprene, 3-methyl and 4-methyl-2(5H)-furanones	68
4.2.1	Chromatography	68
4.2.2	Operational parameters for the mass spectrometer.....	68

4.3	Heterogenous oxidative degradation of isoprene in the presence of atmospheric air and ¹⁸O₂ isotope	69
4.3.1	Chromatography	69
4.3.2	Operational parameters for the mass spectrometer	69
4.4	Radical oxidation of methyl-vinyl ketone and methacrolein	69
4.4.1	Chromatography	69
4.4.2	Operational parameters for the mass spectrometer	69
4.5	Analysis of organosulfates in atmospheric waters	69
4.5.1	Chromatography	69
4.5.2	Operational parameters for the mass spectrometer	70
5	RESULTS AND DISCUSSION	71
5.1	Structural characterization of isoprene-derived organosulfates with the MW 212 in PM_{2.5} ambient fine aerosol	71
5.1.1	Chemical characterization for the MW 212 OS isomers	77
5.1.1.1	The synthesis of sulfate esters of 3,4-dihydroxy-3-methyl-tetrahydro-2-furanone and 3,4-dihydroxy-4-methyl-tetrahydro-2-furanone	80
5.1.2	Quantum-chemical calculations	84
5.1.3	Improved and complementary chromatographic analysis for the MW 212 OS with use of RP-C18 and HILIC methods	89
5.1.4	Heterogeneous formation of the 212 organosulfate <i>via</i> aqueous-phase oxidative degradation of isoprene – mechanism investigation	96
5.1.5	Tentative Proposal for the Formation Mechanism for the MW 212 OSs under atmospheric conditions	100
5.1.6	Conclusions	104
5.2	Radical oxidation of methyl vinyl ketone and methacrolein in aqueous droplets: characterization of organosulfates and atmospheric implications	105
5.2.1	Reaction progress monitoring using UV-Vis	106
5.2.2	Characteristics of MVK photooxidation reaction products in the aqueous phase	107
5.2.2.1	SOA-derived organosulfate with the MW 154	109
5.2.2.2	SOA- derived organosulfate with the MW 156	109
5.2.2.3	SOA- derived organosulfate with the MW 168	109
5.2.2.4	SOA- derived organosulfate with the MW 184	109
5.2.2.5	Organosulfate with the MW 200	112
5.2.3	Chemical signatures of MACR photooxidation reaction products in the aqueous-phase mimicking experiments	113
5.2.3.1	Organosulfate with the MW 154	113
5.2.3.2	Organosulfate with the MW 184	114
5.2.3.3	Organosulfate with MW 200	114
5.2.4	Summary	115
5.3	Secondary Organic Aerosol markers in atmospheric waters	117
5.3.1	Organosulfates MW 184, MW 212, MW 214 and MW 216 in atmospheric precipitates	118
5.3.2	Conclusions	122
6	SUMMARY	124

List of Charts

Chart 1-1 Estimations of global share of volatile organic compounds carried out for year 2000 ²⁵	9
Chart 5-1 The isoprene decay profiles during its aqueous-phase degradation in the presence of <i>in situ</i> -generated sulfate radicals recorded with the UV-Vis spectroscopy (x-axis shows the wavelength units of the light in nanometers).	96
Chart 5-2 The relative abundance for selected organosulfates detected in the atmospheric waters samples collected in Poland during different seasons and locations: (A) summer rural rain sample collected in Woziwoda; B) autumn urban rain sample collected in Warsaw; C) late summer hailstone sample collected in Warsaw; D) and E) urban snow samples collected in Warsaw; F) winter rural snow sample collected in Puszcza Borecka; G) urban graupel sample collected in Skawina during late winter; H-J) PM _{2.5} fine ambient aerosol samples collected in Puszcza Borecka. The legend: OS nominal mass followed by retention time of structural isomer×100.....	122

List of Figures

Figure 1.1 Schematic representation of aerosols size distribution together with their major sources and removal processes. Based on Whitby. ¹¹	3
Figure 1.2 Sources and formation of primary and secondary aerosol along with processes they undergo in the atmosphere.	6
Figure 1.3 Direct and indirect impacts of atmospheric aerosols on the health and climate.	12
Figure 1.4 Pictures taken during smog episodes in Warsaw on 18.12.2018 (on the left; photography author: lukszczepanski).	13
Figure 1.5 An example of blue haze phenomena over the Great Smokey Mountains (source: visitmysmokies.com).	15
Figure 1.6 The main processes of isoprene oxidation in the atmosphere leading to the isoprene SOA formation; based on Carlton and co-workers work ¹²⁶	32
Figure 1.7 The bar graphs show the concentrations recorded in different locations around the world, distinguishing between the individual precursors. The biomass burning OSs are also included in the anthropogenic precursors. Total concentrations of OSs are placed in parentheses next to the location names. The color of the dots at specific locations corresponds to the determined concentrations of OSs as well. ¹³⁹	34
Figure 1.8 Schematic representation of the ionization phenomenon in an electrospray source, in the positive ion mode. Based on the graphic of Andreas Dahlin.	42

Figure 1.9 Schematic representation of key operation modes of tandem mass spectrometry: 1) product ion scan 2) precursor ion scan 3) neutral loss scan 4) selected reaction monitoring. CID – collision induced dissociation.....	47
Figure 1.10 The Acquity Ultra High Performance Liquid Chromatograph coupled to a Synapt G2-S High Definition Mass Spectrometer (Waters) used in my aerosol research; Mass Spectrometry Group, Institute of Organic Chemistry Polish Academy of Science.	51
Figure 3.1 Schematic representation of the ambient fine aerosol sample preparation for UHPLC-MS/MS analysis.....	56
Figure 3.2 Ambient aerosol sampling site in K-pusztá, Hungary. <i>Picture of the station building was uploaded from https://projects.nilu.no web site.</i>	57
Figure 3.3 The Centreville sampling site in Alabama, USA. <i>Picture of Centreville panorama was uploaded from https://datausa.io web site.</i>	58
Figure 3.4 Puszcza Borecka sampling site at Diabla Góra, Masuria Province, Poland. <i>Picture of the station building comes from private sources.</i>	59
Figure 3.5 Location of sampling sites where atmospheric precipitates were collected. D) Woźniwoda, Bory Tucholskie, <i>picture comes from private sources</i> ; E) Warsaw, capital city of Poland, <i>picture: Panorama Warszawy z mostu Siekierkowskiego, 2020, author: Qbolewicz</i> , F) Skawina, a city in a close vicinity to Cracow, <i>pictures' author Norber Rzepisko</i>	61
Figure 3.6 The Outdoor Smog Chamber on the roof of the UNC Gillings School of Global Public Health, Chapel Hill, NC. Picture uploaded by Kenneth G. Sexton ¹⁸¹ on ResearchGate.....	62
Figure 3.7 Schematic representation of One Atmosphere smog chamber, UNC Gillings School of Global Public Health, Chapel Hill, NC. ¹⁸²	63
Figure 5.1 LC/ESI-HRMS extracted ion chromatograms recorded at the <i>m/z</i> 211 channel for the following aerosol extracts and synthesized standards samples 1: (A) K-pusztá PM _{2.5} , (B) Diabla Góra PM _{2.5} , (C) Centreville PM _{2.5} , (D) smog chamber-generated isoprene SOA, (E) aqueous-phase mimics of isoprene SOA, (F) aqueous-phase mimics of 3-methyl-2(5H)-furanone SOA, and (G) aqueous-phase mimics of 4-methyl-2(5H)-furanone SOA. Chromatographic separation was performed using C-18 chromatography (Acquity HSS T3 1.8 μm column; 2.1 x 100 mm; Waters).	73
Figure 5.2 The chemical structures of the MW 212 organosulfates were assigned to sulfate esters of 3,4-dihydroxy-3-methyl-tetrahydro-2-furanone (structures A-D) and 3,4-dihydroxy-4-methyl-tetrahydro-2-furanone (structures E-H), respectively. Only one enantiomer of each compound is shown.	77
Figure 5.3 Negative ion electrospray product ion mass spectra of the target <i>m/z</i> 211 ions obtained for four resolved peaks in the extracted ion chromatogram of the K-pusztá PM _{2.5} sample (Fig. 5.1 A). CID collected with energy CE 25 eV.....	79
Figure 5.4 Negative ion electrospray product ion mass spectra of the target <i>m/z</i> 211 ions for: 1) aqueous-phase isoprene SOA samples: peaks with retention times at (A) 1.03 min. (B) 1.28 min (C) 1.41 min. and (D) 1.51 min. and 2) smog chamber isoprene SOA	

samples: peaks with retention times at (A) 1.06 min. (B) 1.30 min. (C) 1.43 min. and (D) 1.55 min. CID collected with energy CE 15 eV.	79
Figure 5.5 Overlapped LC/ESI-HRMS extracted ion chromatograms at the m/z 211 channel for the synthesized sulfate esters of 3,4-dihydroxy-3-methyl-tetrahydro-2-furanone (dashed line, peaks 3, 4, 5) and 3,4-dihydroxy-4-methyl-tetrahydro-2-furanone (solid line, peaks 1, 2, 6). Retention times for subsequent peaks (1-6): 1.07, 1.31, 1.33, 1.42, 1.48 and 1.57 min.	80
Figure 5.6 The MS ² data acquired for 4-methyl-2(5H)-furanone SOA for peaks with retention times at (A) 1.07 min. (B) 1.31 min. and (C) 1.57 min, respectively. CID were collected at the collision energy (CE) of 25 eV.	81
Figure 5.7 The MS ² data recorded for 3-methyl-2(5H)-furanone SOA for peaks with retention times at (A) 1.33 min., (B) 1.42 min. and (C) 1.44 min. CID were collected at the collision energy of 15 eV.	82
Figure 5.8 The RP-C18 separation power of organosulfate isomers with the MW 212 depending on the sample solvent deployed (chromatography (Acquity HSS T3 1.8 μ m column; 2.1 x 100 mm; Waters). ¹¹⁶	89
Figure 5.9 Comparison of differences in the RP-C-18 chromatographic separation of the MW 212 organosulfate isomers in fine ambient PM _{2.5} aerosol samples (sampling location: Diabla Góra; sampling time: 12h; sampling regime: day-time sampling during sunny summer time) depending on the sample solvent used. Column used: Acquity HSS T3 1.8 μ m column; 2.1 x 100 mm; Waters. ¹¹⁶	90
Figure 5.10 Proposed structures of organosulfate isomers with the MW 212 and corresponding chromatographic peaks.	92
Figure 5.11 Negative ion electrospray product ion mass spectra recorded for the m/z 211 isomers collected for peaks 2 and 7 (Scheme 5.4). CID collected with CE energy of 20 eV.	93
Figure 5.12 Negative ion electrospray product ion mass spectra recorded for the m/z 211 isomers collected for peaks 1,3 and 5 (Scheme 5.4). CID collected with CE energy of 15 eV.	94
Figure 5.13 Negative ion electrospray product ion mass recorded for the m/z 211 isomers collected for peaks 2 and 7 (Scheme 5.4). CID collected with CE energy of 15 eV.	95
Figure 5.14 Representative LC/MS extracted ion chromatograms for organosulfates produced <i>via</i> the aqueous-phase SO ₄ radicals-driven reactions of isoprene in the presence of: A) ¹⁶ O ₂ (m/z 211 channel; upper chromatogram) and B) ¹⁸ O ₂ (m/z 221 channel; bottom chromatogram). The data obtained using non-optimized RP-C18 chromatography.	97
Figure 5.15 Product ion mass spectra acquired for m/z 211 (left panel) and 221(right panel) resulted from the aqueous-phase SO ₄ radicals-induced reactions of isoprene in the presence of oxygen-16 (left panel) and oxygen-18 isotope (right panel), respectively: peaks at the RT 0.98 min. (A) and 1.01 (A'); 1.16 (B) and 1.21 (B'); 1.28 (C) and 1.31 (C'); 1.36 (D) and 1.37 (D'). In the case of the first eluting peak at the RT 1.01 min. overlapping of two structures occurred and sufficient separation of the spectra was not obtained.	98

Figure 5.16 Decay of UV absorption bands recorded for A) methyl vinyl ketone (λ_{\max} 210 nm) and B) methacrolein (λ_{\max} 220 nm) during the reaction in the aqueous phase with sulfate radicals. The insets show the maxima of the absorption bands as a function of time. 106

Figure 5.17 Extracted ion chromatograms along with negative ion electrospray product ion spectra recorded for A) m/z 183 ion in the fine ambient $PM_{2.5}$ aerosol sample; B) m/z 183 ion in the MVK aqueous photo-oxidation sample (the product ion spectrum for the RT 0.92 min isomer shown in Fig 3); C) m/z 199 ion in the ambient $PM_{2.5}$ aerosol sample; D) m/z 199 ion in the MVK aqueous photo-oxidation sample.³⁸ 110

Figure 5.18 The negative ion electrospray product ion mass spectrum recorded for the m/z 183 diagnostic ion from the MVK aqueous photo-oxidation experiment reveals a characteristic m/z 183 \rightarrow m/z 97 transition. 111

Figure 5.19 Extracted ion current chromatograms acquired for: m/z 183 from aqueous-photo oxidation of MACR 2) m/z 199 present in $PM_{2.5}$ aerosol and C) m/z 199 resulting as a product of MACR photo-oxidation, along with product ion spectra for the mentioned ions.³⁸ 113

Figure 5.20 LC/MS extracted ion chromatograms for a target m/z 183 ion in $PM_{2.5}$ fine ambient aerosol, hailstone and rain sample. 118

Figure 5.21 Negative electrospray product ion mass spectra for the m/z 183 ion present in a rain sample (A) and $PM_{2.5}$ fine ambient aerosol (B). 119

Figure 5.22 Extracted ion chromatograms for ions m/z 211 (left side) and m/z 214 (right side) in $PM_{2.5}$ fine ambient aerosol, hailstone and rain samples. 120

Figure 5.23 LC/MS extracted ion chromatograms for the m/z 215 ion in $PM_{2.5}$ ambient fine aerosol, hailstone and rain samples. 120

Figure 5.24 Negative electrospray product ion mass spectra of the m/z 215 ions sequentially eluting at RT 0.77 min. (upper) and 0.88 min. (bottom), respectively in A: $PM_{2.5}$ ambient fine aerosol (injection volume 2 μ l), B: hailstone (injection volume 5 μ l), C: rain (injection volume 10 μ l). Spectra were recorded with CE 20 eV. 121

List of Schemes

Scheme 1.1 Schematic representation of NO to NO conversion processes and O₃ formation (A) in the absence of VOCs and (B) with the presence of VOCs⁶² 18

Scheme 1.2 Processes of biogenic volatile organic compounds degradation in the atmosphere as a result of the formation of alkyl radicals or substituted alkyl radicals under the atmospheric oxidants. 22

Scheme 1.3 Schematic representation of alkene ozonolysis with the emphasis on two main pathways: the hydroperoxide channel and the stable Criegee channel. Based on Kroll's work.¹ 23

Scheme 5.1 Plausible fragmentation pathways for the m/z 211 ionic products, assigned to positional isomeric sulfate esters of A) 3,4-dihydroxy-4-methyl-tetrahydro-2-furanone,

and B) 3,4-dihydroxy-3-methyl-tetrahydro-2-furanone, based on the combined LC/MS/MS, MS ³ and accurate mass MS ² data.....	83
Scheme 5.2 Ion trap LC/MS ² and MS ³ product ion spectra of <i>m/z</i> 211 and <i>m/z</i> 193 obtained for the peak eluting with the RT 1.05 min. (left panels) and RT 1.53 min. (right panels) from <i>K</i> -puszta fine ambient PM _{2.5} aerosol sample (Fig. 5.1 A). Details of the experiment were described elsewhere. ¹⁸⁹	84
Scheme 5.3 Calculated activation energy barriers for eight MW 212 OS diastereoisomers for the water elimination reaction and bisulfate ion formation. The transition state electron energies and the ZPE correction were calculated at a B3LYP/6-311+g(2d,p) level of theory. The lowest energy values are highlighted in green color. ³⁶	86
Scheme 5.4 Chromatographic separation of the MW 212 organosulfate isomers using an RP-C-18 chromatography (upper trace) and the HILIC method (bottom trace). The scheme overlaps two fragmentation reaction channels at <i>m/z</i> 211/211 and <i>m/z</i> 211/97, respectively for each method.	91
Scheme 5.5 Proposed fragmentation pathways for the oxygen-18-labeled organosulfates (the MW 222 Da) bearing five incorporated oxygen-18 isotopes (marked with red color). 100	
Scheme 5.6 Tentative mechanism of the MW 212 OSs formation from the heterogeneous oxidation 2-methyltetrol-related OSs, involving heterogeneous oxidation of a terminal hydroxyl group to a carboxylic acid group, followed by lactonization. ³⁶	101
Scheme 5.7 The plausible formation mechanism of the MW 212 OS from isoprene in the aqueous solution is indispensably combined with the S(IV)-autooxidation process. A key step in this approach is an addition of the sulfate radical-anions onto the C=C bond. ³⁶ 103	
Scheme 5.8 Proposed fragmentation pathways of the MW 184 organosulfate originating from MVK aqueous photo-oxidation mimicking experiments: B1) early-eluting isomer with retention time 0.92 min. and B2) late-eluting isomer with a retention time of 0.96 min. ³⁸ 111	
Scheme 5.9 A tentative reaction mechanism explaining the formation of the MW 184 organosulfate from aqueous photo-oxidation of MVK. (with * was noted atmospherically- available red-ox systems, e.g., HSO ₃ ⁻ /SO ₃ ²⁻ -> HSO ₄ ⁻ /SO ₄ ²⁻ ³⁸	112
Scheme 5.10 Proposed fragmentation channels for forming MACR-derived organosulfates A) the MW 184 and B) the MW 200 formed <i>via</i> aqueous photo-oxidation reactions. ³⁸	114

List of Tables

Table 1-I Estimations of global emissions for selected biogenic volatile organic compounds.....	16
Table 1-II Calculated lifetimes of selected biogenic volatile organic compounds in reactions with OH radicals, NO ₃ radicals and O ₃	19

Table 1-III Schemes of accretion reactions that can take place in the particulate phase, resulting in the secondary organic aerosol formation.	27
Table 1-IV The most significant organic aerosol precursors and their marker compounds in the PM phase.	29
Table 1-V Commonly used ionization methods in <i>off-line</i> mass spectrometry of the atmospheric aerosol along with their brief outline.	36
Table 1-VI CI-MS techniques used in direct analysis of organic trace measurements in aerosols. Based on Noziere (2015) ⁵	41
Table 5-I The comparison of the main peaks areas for <i>m/z</i> 211 present in the ambient fine aerosol samples (K-puszta, Hungary; Diabla Gora, Poland; Centreville, USA), aqueous-phase isoprene SOA, and smog-chamber isoprene SOA, and ratios between the sum of the <i>m/z</i> 211 peak areas versus that of the <i>m/z</i> 215 2-methyltetrol sulfates. The data are based on the chromatographic separation on a C-18 column (Acquity HSS T3 1.8 μ m column; 2.1 x 100 mm; Waters).	74
Table 5-II The comparison of the main peaks areas for <i>m/z</i> 211 determined for the three ambient fine aerosol samples: (A) K-puszta, Hungary; (B) Diabla Gora, Poland; (C) Centreville, the U.S., and for the mimicking experiment samples: (D) aqueous-phase isoprene SOA and (E) smog-chamber isoprene SOA, and ratios between the sum of the <i>m/z</i> 211 peak areas versus that of the <i>m/z</i> 215 2-methyltetrol sulfates. The chromatographic separation was performed with use of the C-18 stationary phase column (Acquity HSS T3 1.8 μ m column; 2.1 x 100 mm; Waters).	76
Table 5-III Tentative structural assignments of the compounds A – H shown in Scheme 5.3 for peaks appearing on real LC/ESI-HRMS chromatograms shown in Fig. 5.5.	88
Table 5-IV Organosulfates identified as reaction products in aqueous MVK processing in the presence of sulfate radicals. ³⁸	108
Table 5-V Organosulfates identified as reaction products in aqueous MACR processing in the presence of sulfate radicals. ³⁸	116

List of Abbreviations

2MT	<i>2-methyltetrol</i>
APCI	<i>atmospheric pressure chemical ionization</i>
APPI	<i>atmospheric pressure photoionization</i>
aqSOA	<i>aqueous secondary organic aerosol</i>
BC	<i>black carbon</i>
BVOCs	<i>biogenic volatile organic compounds</i>
CI	<i>chemical ionization</i>
CID	<i>collision-induced-dissociation</i>

CIT	<i>California Institute of Technology</i>
CNN	<i>cloud condensation nuclei</i>
Da	<i>Dalton, mass unit</i>
DAD	<i>photodiode array detector</i>
DESI	<i>desorption electrospray ionization</i>
DMS	<i>dimethyl sulfide</i>
EC	<i>elemental carbon</i>
EI	<i>electron ionization</i>
EIC	<i>extracted ion chromatogram</i>
ESI	<i>electrospray ionization</i>
FWHM	<i>full width at half maximum</i>
GC	<i>gas chromatography</i>
HILIC	<i>hydrophilic interaction liquid chromatography</i>
HMML	<i>hydroxymethyl-methyl-lactone</i>
HOMs	<i>highly oxidized multifunctional organic compounds</i>
HPLC	<i>high performance liquid chromatography</i>
HRMS	<i>high resolution mass spectra</i>
IC	<i>inorganic carbon</i>
IEPOX	<i>isoprene epoxydiols</i>
LC	<i>liquid chromatography</i>
LRMS	<i>low resolution mass spectra</i>
MAC or MACR	<i>Methacrolein</i>
MAE	<i>methacrylic acid epoxide</i>
MALDI	<i>matrix-assisted laser desorption ionization</i>
MPAN	<i>methacryloyl peroxyxynitrate</i>
MS	<i>mass spectrometry</i>
MS/MS	<i>tandem mass spectrometry</i>
MVK	<i>methyl vinyl ketone</i>
MW	<i>molecular weight</i>
NCI	<i>negative mode ionization</i>

NL	<i>normalization level</i>
NMOCs	<i>non-methane volatile organic compounds</i>
NO_x	<i>nitrogen oxides</i>
OC	<i>organic carbon</i>
OS/OSs	<i>organosulfate/organosulfates</i>
OVOCs	<i>oxygenated volatile organic compounds</i>
PAHs	<i>polycyclic aromatic hydrocarbons</i>
PBAP	<i>primary biogenic aerosol particles</i>
PDMS	<i>Polydimethylsiloxanes</i>
PM	<i>particulate matter</i>
PM_{0.1}	<i>ultrafine particles, particles with diameters below 0.1 μm</i>
PM₁	<i>submicron particles, particles with diameters up to 1 μm</i>
PM₁₀	<i>coarse particles, particles with diameters up to 10 μm</i>
PM_{2.5}	<i>fine particles, particles with diameters up to 2.5 μm</i>
PT	<i>proton transfer</i>
QqQ	<i>triple quadrupole</i>
R[·]	<i>radical</i>
RO[·]	<i>alkoxy radical</i>
RO₂[·]	<i>peroxy radical</i>
RP	<i>reversed-phase chromatographic system</i>
RP-C18	<i>reversed-phase chromatography with C-18 chains</i>
RT	<i>retention time</i>
SCI	<i>stabilized Criegee intermediate</i>
SIA	<i>secondary inorganic aerosol</i>
SOA	<i>secondary organic aerosol</i>
SO_x	<i>sulfur oxides</i>
SPME	<i>solid phase microextraction</i>

xxx

SSA	<i>sea-salt spray aerosol</i>
TC	<i>total carbon</i>
TD	<i>thermal desorption</i>
ToF	<i>time of flight</i>
TSP	<i>total suspended particles</i>
UHPLC/UPLC	<i>ultra-high performance liquid chromatography</i>
UHPLC-ESI-MS	<i>electrospray mass spectrometer interfaced to ultra-high performance liquid chromatograph</i>
VOC	<i>volatile organic compounds</i>

1 Literature overview

1.1 Atmospheric aerosol – introduction

Atmospheric aerosol is the suspension of liquid and/or solid particles with diameters ranging from a few nanometers up to 100 micrometers in the air. When such particles are emitted directly to the atmosphere they are called *primary aerosol*, while when result from the chemical reactions on volatile organic compounds (VOCs) followed by the gas-to-particle conversion of product formed, they account for *secondary aerosol* (or *secondary organic aerosol*, SOA). Aerosol particles vary in sizes, shapes and what is significant from a chemical point of view – in the chemical properties. While in the air, pristine particles undergo further processing such as functionalization, oligomerization and fragmentation¹⁻³ which is regarded as the aerosol aging and which shape their chemical composition^{4,5}, physico-chemical properties⁶⁻⁸ and health effects^{9,10}.

1.2 Classification

Aerosols may be classified in terms of their sizes, chemical composition, geographical location and vertical position in the atmosphere. However, the classification mainly relies on a range of their sizes. Particles with diameters up to 2.5 μm are referred to as *fine particulate matter (PM)*, while with diameters far greater than 2.5 μm (usually more than 10 μm) as – *coarse PM*. Depending on the size of the particles they differ in physicochemical properties, sources and processes they undergo in the atmosphere. The size is also a key factor when it comes to the impact of particulate matter on the health owing to different ways of accumulation in living organisms.

We can distinguish the following particulate matter fractions:

- TSP – Total Suspended Particles
- PM₁₀ – particles with diameters up to 10 μm
- PM_{2.5-10} or PM_c – particles with diameters in between 2.5 to 10 μm , coarse particles
- PM_{2.5} – fine particles, particles with diameters up to 2.5 μm ,
- PM₁ – submicron particles, particles with diameters up to 1 μm

- PM_{0.1} – ultrafine particles, particles with diameters below 0.1 μm

Coarse particles are emitted to the atmosphere from natural and anthropogenic sources mainly through mechanical processes. In case of the natural materials being the source for particles larger than 2.5 μm we can mention the Earth crust, mineral dust and sea salt spray. Anthropogenic sources for coarse particles is dust from the roads (e.g., tires debris) and from the direct industrial and/or agricultural emissions. Due to their large sizes their atmospheric lifetimes are short (minutes to hours) and they are removed from the air by the sedimentation. Owing to their sizes, coarse particles affect the upper and lower respiratory tract and they also may irritate the ocular surface.

Fine particles we can differentiate due to a mode of their origin:

- Nucleation mode – particles with diameters smaller than 10 nm, *ultrafine* particles (UFP), generated *via* homogeneous nucleation in the atmosphere and as a result of combustion processes. The chemistry of these particles is poorly recognized because of their small size and mass. Also a very short lifetime (up to minutes) hinders their study.
- Aitken mode – *fine* particles (FP), particles with diameters in between 10 to 100 nm, generated in coagulation and/or condensation processes of particles in nucleation mode, with a short lifetime (minutes to hours).
- Accumulation mode – PM₁-PM_{0.1}, *fine* particles (FP), diameters in between 0,1-1 μm, they are formed mainly due to the coagulation of nucleation mode particles and Aitken's particles and the condensation onto already existing particles in the presence of inorganics such as sulfates, nitrates, ammonia and small amounts of organic material. Also incomplete processes such as combustion of wood or oil can be a source of these particles. Their size is too small to be effectively removed by gravitational forces from the atmosphere, which cause a long life time of this particles (days to weeks) and enable them to easily accumulate until they will be removed by wet deposition.

Ultrafine and fine particles because of their small sizes can reach the alveoli regions and from there the blood, which they can dissipate to organs, such as liver, brain, placenta and others.

Considering the number of particles, ultrafine and Aitken's mode particles are the most numerous representatives of particles in the atmosphere, but taking into account size and mass the accumulation mode particles constitute a percentage higher share of total aerosol mass (Fig. 1.1).

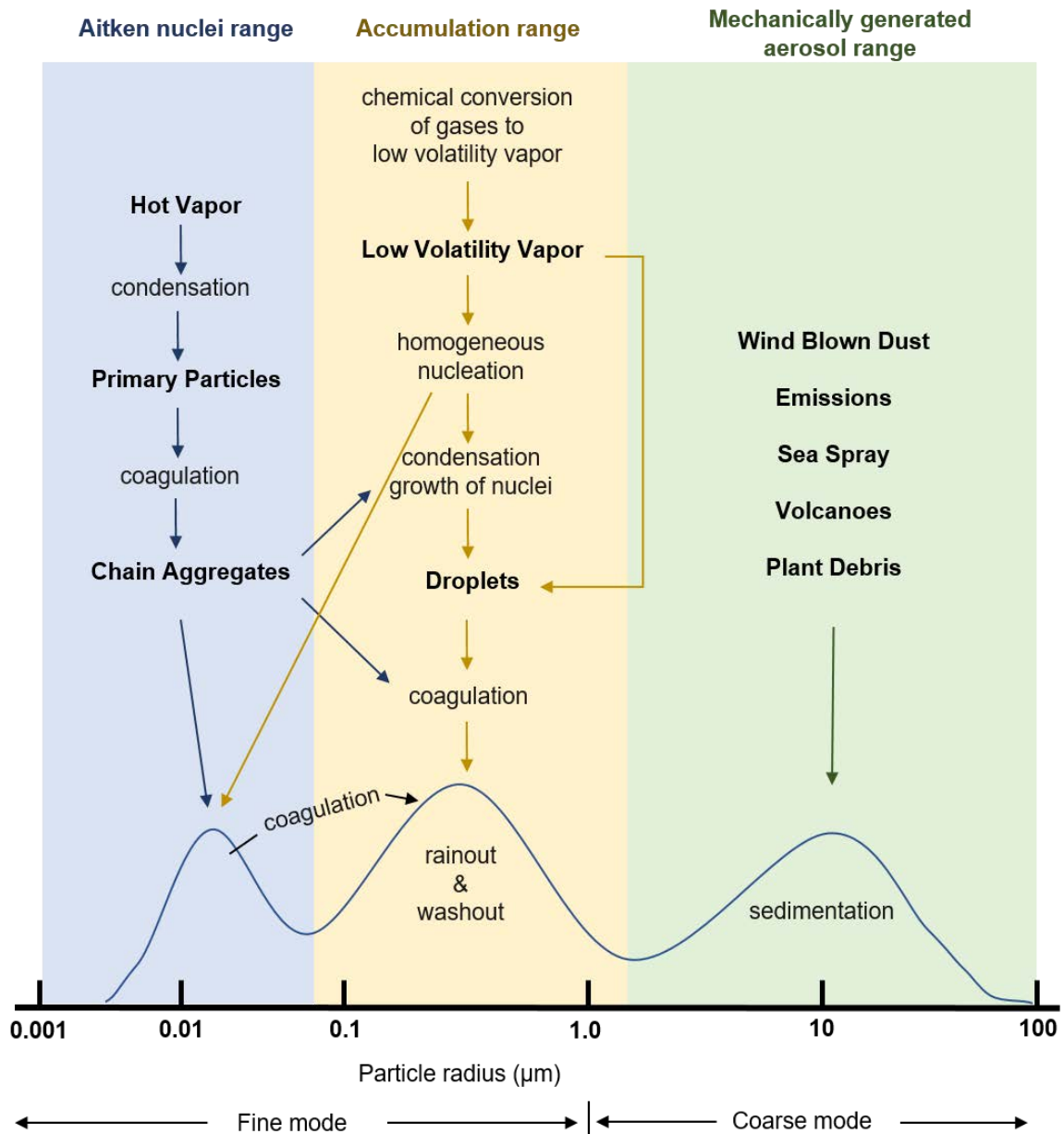


Figure 1.1 Schematic representation of aerosols size distribution together with their major sources and removal processes. Based on Whitby.¹¹

Another way of classification refers to the chemical composition of particulate matter, which depends on many factors, i.e., the location, weather conditions or seasons:

- Crustal material
- Sea-salt spray aerosol (SSA)
- Elemental carbon (EC) or black carbon (BC)
- Organic carbon (OC)
- Primary biogenic aerosol particles (PBAP)
- Secondary organic aerosol (SOA)
- Secondary inorganic aerosol (SIA)
- Trace elements

The chemical composition of the particles is also strongly related to the type of their source (see chapter 1.3). In general, it is very hard to elucidate the chemical composition of aerosol particles, because it changes in space and time. Among crucial components of inorganic aerosol, we can mention sulfates, nitrates and ammonium ions. Sulfate and ammonium ions, as well as organic and elemental carbon, are characteristic for fine particles ($PM_{1, PM_{2.5}}$). In case of coarse fractions ($PM_{2.5-10}$) the mineral dust, the dominant source of which is weathering of rocks and/or soils, and biogenic aerosol is more common. Nitrate ions and trace elements can be observed both in fine and coarse fractions. Sea-salt spray aerosol sizes refers to accumulation and coarse modes, rarely they can be observed in nucleation mode^{12,13}. One more type of particulate matter is the primary biological aerosol particles (PBAP), which the terrestrial biosphere is a source for. It encompasses biological organisms, alive and dead, and dispersal units, such as bacterial strains, fungi, viruses, spores etc. and its solid fragments or excretions, i.e. microbial fragments, plant debris, animal tissues and excrements¹⁴. Sizes of PBAP vary and are between a few nanometers and hundreds of micrometers¹⁵⁻¹⁷. Because of their small sizes PBAP particles can have a long residence time in the atmosphere, even several days. However these with large sizes (i.e., plant pollens, diameter above 10 μm) are in the air very briefly and more likely are rapidly deposited. While in the winter season, these particles constitute a negligible percentage of all suspended dust particles, whereas during vegetation they can constitute up to 5% of suspended aerosol mass¹⁸. The carbon-containing compounds, known as *the carbonaceous matter*, are one of the most important constituents of aerosols. They can originate from both primary and secondary sources and have either anthropogenic or natural background. The total mass of carbon matter in suspended dust is most often referred to as *total carbon* (TC), and among this main

fraction we distinguish the *organic carbon* (OC), *inorganic carbon* (IC) and black carbon (BC, also known as molecular carbon (EC) or soot) fractions. The organic carbon fraction is related to organic compounds such as alkanes, alkenes, polycyclic aromatic hydrocarbon, functionalized (i.e., oxygenated) hydrocarbons, and bio-aerosols, while the inorganic carbon fraction is mainly constrained to carbonates. Black carbon fraction corresponds to products resulting from the incomplete combustion processes of fossil fuels and/or biomass burning. Particles containing carbon atoms in their structure can both absorb and reflect solar radiation. The energy absorption is specific to the black carbon constituents, while the phenomenon of radiation scattering is observed in the case of organic carbon compounds.

1.3 Sources

There are two types of atmospheric aerosol sources – *primary*, when particles are emitted **directly** to the atmosphere, and *secondary*, when they are formed in the atmosphere as a result of **chemical reactions** between a given VOC and the atmospheric oxidant(s) such as nitrate radicals, ozone, hydroxyl radicals or sulfate radicals, with the forthcoming gas-to-particles conversion (Fig. 1.2). These processes start in the gas phase whereupon their products may further react and condense onto the surface of the pre-existing particles to render the particle growth. However, these transformations may also occur in the particle bulk and/or in droplets of atmospheric waters¹⁹⁻²². Each type of the source can be of natural or anthropogenic origins. Depending on the source and local atmospheric conditions, aerosol will differ in the chemical composition, mass concentration and health effects.

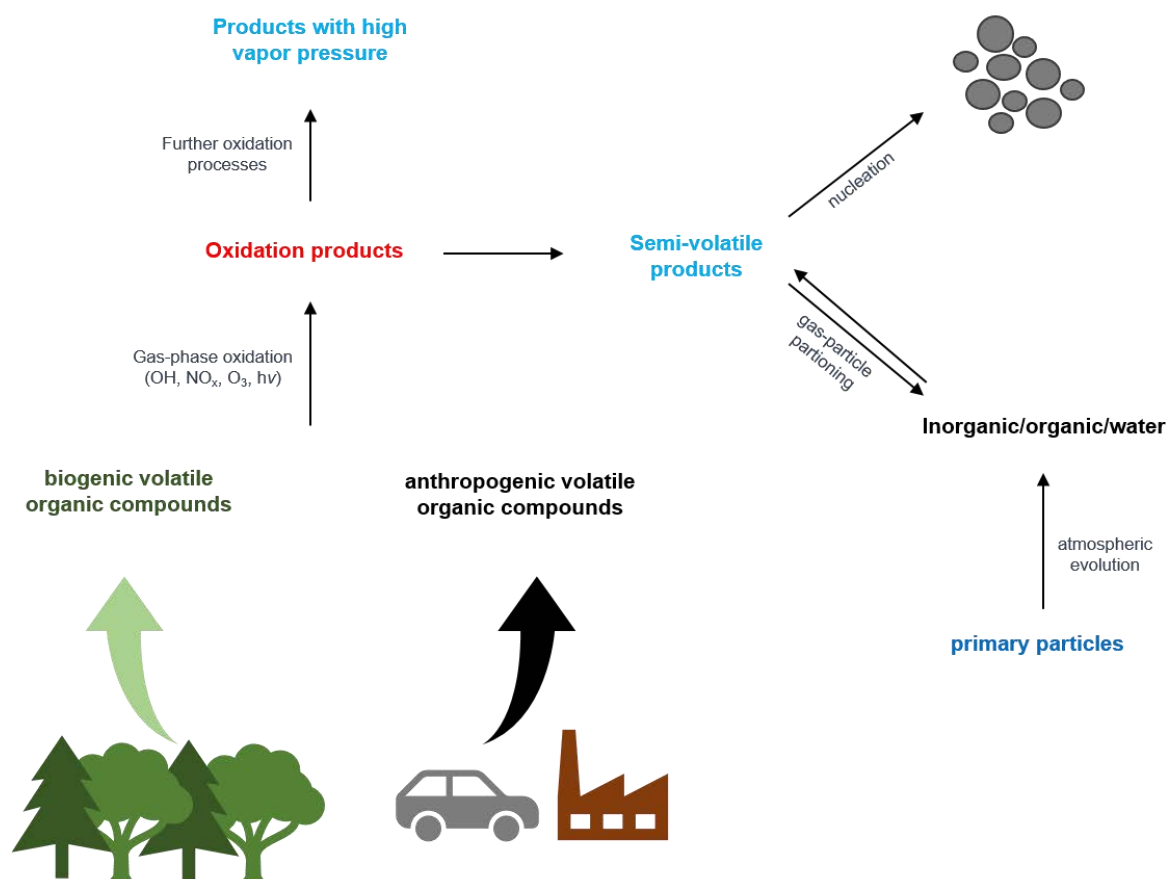


Figure 1.2 Sources and formation of primary and secondary aerosol along with processes they undergo in the atmosphere.

1.3.1 Primary

Primary sources of natural aerosol are bound to the particle emissions from ocean activity, vegetation, volcano eruptions, rock weathering, biomass burning (wildfires). Regardless of the source, the mechanism remains the same: particles enter the atmosphere directly from the source. The aerosol emitted from the ocean, called *marine* or *sea-salt spray aerosol* (SSSA) enters the lower atmosphere as highly concentrated solutions of inorganic salts with the additional content of biological material. The SSSA plays an important role in the scattering of solar radiation and acts as a cloud condensation nuclei (CNN). It is formed by bursting bubbles at the air-sea interface. Released particles vary in sizes from nano- to micrometers and their chemical profile depends upon the composition of oceanic water and ambient air.. In the beginning, the fresh sea spray droplets have the chemical composition like seawater with alkaline pH but it can change with the time when chemical processes occur. A part of particles simply drops off to the

water immediately, but those who will reach the equilibrium state form the fresh sea salt aerosol, and enriched with organic matter, inorganic salts, iodine or bacteria and other organisms can form aged form of sea salt aerosol. Under typical conditions of ambient relative humidity SSSA is a very concentrated solution of water-soluble inorganic salts, such as NaCl, CaSO₄, MgSO₄, MgCl₂ and KCl. In the bulk and/or onto the surface of SSSA many heterogeneous and multiphase chemical reactions can boost which make the aged SSSA more acidic and sulfate-enriched.

Direct emission also occurs when the wind hits the surface of the continent, causing soil residues to be transferred, which is the atmospheric source of the following elements: silicon, iron, magnesium, calcium, potassium and aluminum. This type of aerosol is called *mineral dust*. The composition of the latter in the atmosphere is strongly determined by the location of the emission source and local weather conditions. Preferred location for this aerosol is associated with large spaces, where there is limited vegetation and minimum geological obstacles to the wind. Deserts fulfill this criteria. In favorable conditions the dust can travel over thousands of kilometers and stay in the atmosphere for up to 22 days.

During volcanic eruption, millions of tons of mineral dust enriched with silicates and metallic oxides gets into the atmosphere. In addition, large amounts of sulfur dioxide and hydrogen sulfide accompany these emissions, which are one of relevant drivers to secondary atmospheric aerosols (SOA) (see next paragraph). Ash particles can have different resident times in the atmosphere, depending on the size of particles, chiefly from hours to weeks.

Biomass burning (intentional or off-controlled) leads to the release organic and/or inorganic particulates in high quantities. These particles occupy mainly an accumulation mode and have sizes not greater than 2 μm. Aerosols formed by burning processes include soot, organic species (e.g. sugar anhydrides, such as levoglucosan, nitrated phenols, polyaromatic hydrocarbons) and inorganic material (e.g., carbonates) in high concentrations. Worldwide, these processes constitute one of the major pollution source of the atmosphere since biomass burning is used massively as a source of the energy (e.g., residential heating) or the means of the low cost biowaste treatment. Wild fires add to these processes however, in contrast to controlled biomass burning usually occur at higher

temperatures which affect the chemical composition of particles released. Owing to the global warming, in recent years wild fires were happening more and more frequently in numerous places (e.g., Australia, California and in April 2020 in Poland – Biebrza Natural Reserve).

Anthropogenic primary aerosols enter the atmosphere due to incomplete combustions of fossil/biofuels and fires. As a result, the combustion of organic compounds delivers elementary carbon particles to the atmosphere with sizes not exceeding 2 μm . However, the latter through the coagulation, nucleation, condensation, and vaporization processes can afford novel particles²³, with sizes ranging from 0.02 to 90 μm ²⁴. Besides EC particles, through fossil fuels combustion also organic carbon is emitted, either as a primary particle and a result of reactions with gaseous precursors. This organic particulate matter consists of a mixture of many classes of chemical species, among them carboxylic or dicarboxylic acids, which makes the aerosol polar and hence water-soluble, and polycyclic aromatic hydrocarbons (PAHs), which pose a real threat owing to their confirmed cancerogenic and teratogenic propensities. A significant source of anthropogenic primary particles is also a waste and biomass burning. Through this route an abundant soot emissions occur along with other organics and/or gases, such as PAHs, dioxines, carbon oxides, nitrogen oxides and sulfur dioxide.

Other anthropogenic sources include: industry, road transport, agricultural activity and heating. These types of sources mostly supply the atmosphere with carbonaceous elemental carbon, sulfate, nitrate, ammonium.

1.3.2 Secondary

When aerosol particles arise from secondary sources it usually means chemical reactions (oxidation) of volatile organic compounds (VOC) with the subsequent gas-to-particle conversion of gaseous oxidation products, mainly OH-, COOH-, sulfur- and nitrogen-containing in the atmosphere through the nucleation and/or condensation. These chemicals can condense onto already existing particles, without multiplying the number of particles, or to form new condensed particles by nucleation (e.g., through dimer and/or oligomer formation). The formation of secondary aerosols are enhanced in the presence of atmospheric air pollutants, such as sulfur dioxides (SO_2), nitrogen oxides ($\text{NO}_x =$

NO+NO₂) and ammonia (NH₃), which is linked to the acid (or base)-catalyzed reactions. The thorough determination of the nature of secondary aerosol sources is very difficult due to the multitude of possible processes.

Volatile organic compounds – key precursors or SOA, can originate either from natural (biogenic) or anthropogenic sources. Biogenic VOCs (denoted as BVOCs) include compounds emitted by plants directly into the atmosphere due to plant vegetation and/or biotic (or abiotic) stresses. They are usually low-molecular weight species bearing at least one C = C bond in their structures. It is estimated that the overall BVOCs emissions surpasses these originating from man-made activities ²⁵.

BVOC global emissions

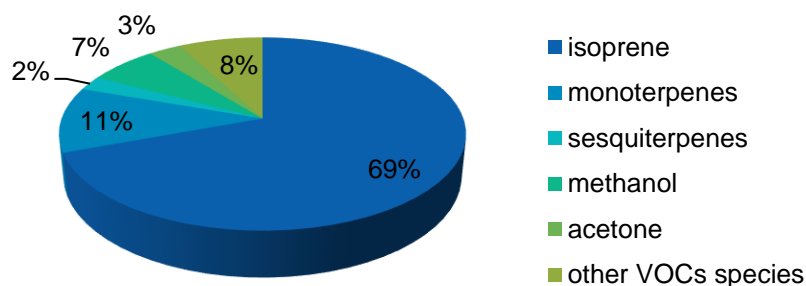


Chart 1-1 Estimations of global share of volatile organic compounds carried out for year 2000 ²⁵.

As it is shown in Chart 1.1 the most important non-methane SOA precursor is isoprene (2-methyl-1,3-butadiene, C₅H₈), which is emitted from a wide range of deciduous plants (e.g., mosses, oaks, ferns) as a by-product of photorespiration processes ²⁶. Its emissions rate is estimated as approx. 535 Tg/year ²⁵ and it is strongly light- and temperature-dependent. Due to the fact that the emission of isoprene increases significantly with temperature, it is considered to be a kind of protective shield for plants at very high temperatures (above 40 °C)²⁷. Isoprene overnight emissions are negligible, while the largest amounts of this hydrocarbon are produced during the sunny summer days, even up to 25 µg/(g dry-leaf-weight)/hour²⁸. Moreover, isoprene protects plants against potential damage when the leaves are exposed to ozone ²⁹.

The chemical structure of isoprene, which has two double bonds, makes it an extremely reactive molecule. When emitted into the atmosphere, it reacts very quickly with the present oxidants, resulting with oxygenated products, *i.e.* methacrolein and methyl vinyl ketone. The contribution of isoprene to the SOA budget was long undermined, only in 2004 the work of Magda Claeys and co-workers³⁰ opened up a global discussion on the role of isoprene and its oxygenates in the formation of secondary organic aerosol in the atmosphere. Considerable efforts, both in the field^{31,32} and laboratory³³⁻³⁸ have confirmed that isoprene and its derivatives are one of the major SOA precursors.

Another family of unsaturated biogenic hydrocarbons emitted from the Earth's ecosystem to the atmosphere are monoterpenes (C₁₀H₁₆), which chemically are built up by two isoprene units. They have linear or cyclic structure, and in the case of terpenoids also additional hydroxyl, carbonyl, carboxyl, ketone or aldehyde functional groups. Terpenes emissions are associated with various plant secretions - essential oils, coniferous resin, and are not as strongly temperature- and light-dependent as isoprene. The annual emission of monoterpenes is estimated at 162 Tg²⁵. On a global scale tropical forests have the largest share in the emission of BVOCs due to the ideal conditions for plant growth (temperature, humidity) and their density.

The emission rate of volatile organic compounds into the atmosphere from natural sources is more than seven times greater than from anthropogenic sources³⁹. In addition, these compounds play a key role in atmospheric chemistry, because once they get there, they undergo the oxidation processes, forming an important class of secondary organic aerosols (SOA).

In the case of sulfur containing gas natural sources are volcanic eruptions, during which sulfur dioxide (SO₂) is released to the atmosphere, and biogenic, for example a phytoplankton which produces dimethyl sulfide (DMS). Regardless of natural emissions, the main source of sulfur oxides are fuel combustion processes, which are of anthropogenic origin. Apart from SO₂ and DMS, other naturally emitted sulfur gases are hydrogen sulfide (H₂S), carbon disulfide (CS₂) and carbonyl sulfide (COS). The latter is important due to the long time residence, which is about 44 days, and together with DMS in the presence of free radicals in the atmosphere is oxidized to SO₂, just as H₂S. In turn,

SO₂ oxidized to SO₃, which in reaction with water forms sulfuric(VI) acid (H₂SO₄). This strong acid can get neutralized by ammonia, which comes from natural sources to a lesser extent, because of agriculture, animals and their excrement, as well as agriculture and the associated consumption of huge amounts of nitrogen fertilizers are considered to be the main emission source. The nitrogen oxides (NO_x) originates from the oxidation of N₂ simply present in air, and other natural sources such as soil emissions, biomass burning processes, denitrification at the ocean surface. Nitrogen and nitrous oxide (NO) are dominant nitro- gasses in the atmosphere, however other nitrogen-containing gasses are significant species in atmospheric chemistry. Ammonia can neutralize sulfur acid, as it was stated earlier, and nitric acid as the only one basic gas.

1.4 Impact of atmospheric aerosols on climate and health

Aerosol particles are ubiquitous in the atmosphere, and thus constitute an integral part of the Earth's climate system. As a result, they affect the atmosphere in every part, both locally and globally (Fig. 1.3). Their lifetime in the atmosphere may vary from minutes to weeks and during this period they influence the climate by absorbing and/or reflecting the solar radiation, thus exerting the cooling and/or warming effects, depending on the chemical character of particles and their mass concentrations. They impact the Earth's energy budget, affect clouds and the water budget, which translates into precipitations reducing efficiency. Finally, they can get removed from the atmosphere by dry or wet deposition ⁴⁰. The former means a simple deposition on the Earth's surface, while the latter happens when particles are incorporated into hydrometeors, i.e., rain, fog, hail, snow etc.^{19,41,42}.

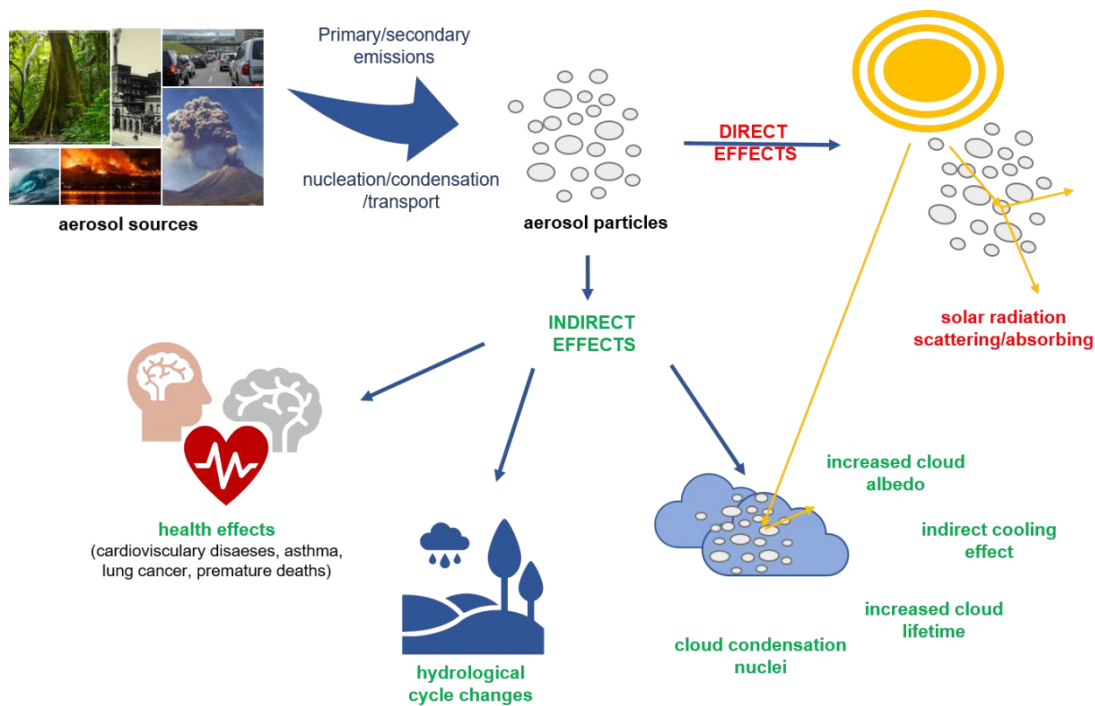


Figure 1.3 Direct and indirect impacts of atmospheric aerosols on the health and climate.

The problem of air pollution associated with increasingly frequent smog episodes directly translates into health problems of residents¹⁰. Currently, the concentration levels of particulate matter are constantly monitored in both European countries by the European Environmental Agency and the United States of America by the Environmental Protection Agency. In addition to government agencies, many applications have been created that allow you to constantly check the air around your place of residence and in the case of PM concentrations exceeding standards in winter often by several hundred percent, it is recommended that city dwellers stay at home or use public transport without ticket fees.

In Poland, especially in cities such as Cracow or Warsaw (Figure 1.4), where smog can persist for several days in windless periods, residents are more severely affected by the effects of poor air quality. It is dangerous especially for infants and young children and the elderly. The harmful effects of PM depend largely on the size of the particles, those with diameters of about 10 μm mainly irritate the conjunctiva, nasal mucosa or throat. However, respirable fractions enter the pulmonary follicles and from there can move freely with blood to all organs. The finest dusts are able to cross the blood-brain

barrier. It is estimated that in Europe, up to 573 000 people die prematurely every year only due to PM_{2.5} exposure ⁴³.

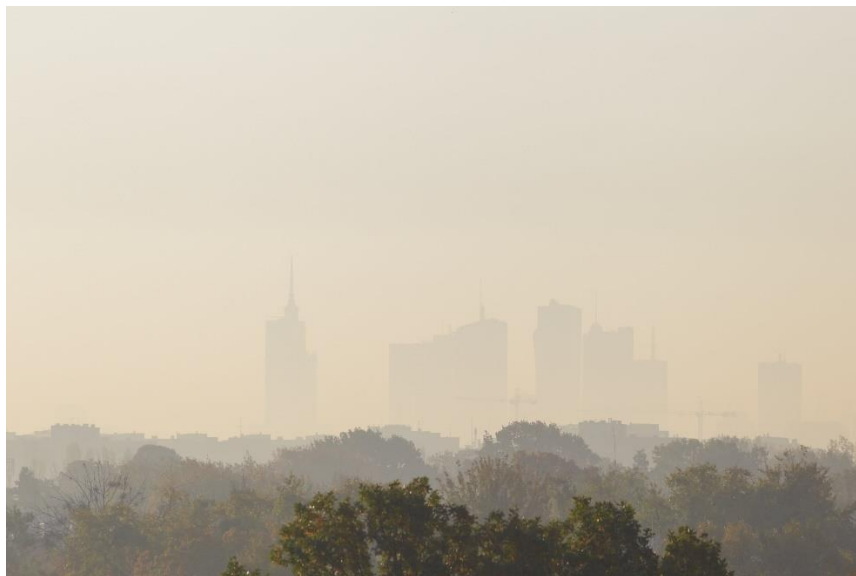


Figure 1.4 Pictures taken during smog episodes in Warsaw on 18.12.2018 (on the left; *photography author: lukszczepanski*).

Due to the complexity and diversity of atmospheric particles, only about 10 – 15% of the atmospheric aerosol constituents has been identified, and the challenge remains to determine their chemical composition, along with their acute health effects. In addition, a multitude of potential factors affecting the formation and transformation of aerosols in the atmosphere requires research in a multifaceted and multidisciplinary manner. Currently, the issue of the Earth's climate changes, the reasons for these processes that we can already observe, and those that we are trying to predict in the near future, is one of the most important issues faced by the scientific community all over the world.

1.5 Secondary organic aerosol (SOA) in the atmosphere

Secondary organic aerosol is formed by chemical reactions of volatile organic compounds (VOCs) emitted by plants (i.e., biogenic) or by anthropogenic sources (e.g. transport), with oxidants present in the atmosphere. After VOCs enter the atmosphere they can undergo removal processes such as dry/wet deposition, photochemical processes, or they can undergo chemical transformations with hydroxyl radicals, nitrate radicals, ozone, chlorine or bromine atoms ⁴⁴⁻⁴⁶. As a result of these processes, usually highly oxidized molecules (HOMs) with the profoundly reduced volatility are formed,

which than can be either accumulated in the gas phase, if their vapor pressure is high, or condense on already pre-existing particles ^{47,48}, forming secondary species. Due to the complexity of atmospheric reactions, a variety of factors affecting the SOA formation, including types and mass concentrations of the organic and/or gaseous precursors as well as local atmospheric conditions, the recognition of the mechanisms leading to SOA is a very demanding research task ^{5,47,49}.

1.5.1 Biogenic volatile organic compounds

The first hypothesis that the atmospheric aerosol has a solid interlink with biogenic (plant) emissions was raised by Went in the early 60s ⁵⁰. Dr. Went observed the enhanced *blue haze* formation (Fig. 1.5) over forested and vegetatively active during sunny summer days. He excluded four possible suggestions for the nature of *blue haze*, concluding that only particles with a diameter of up to 1 μm are able to scatter the light with a wavelength corresponding to blue rays. Given how much energy would be needed to form such small particles by fragmenting larger ones, the only pathway for submicron particle formation is through the condensation or agglomeration of particles already present in the atmosphere. During the next five years Went and Rasmussen carried out an extensive research, taking air samples at various vegetation periods and in several different locations in the United States, using a mobile laboratory with a gas chromatograph installed ⁵¹. Following the research on VOC emissions, they found that while anthropogenic emissions are predominant in urban agglomerations, compounds emitted by plants in rural areas are the main organic components of the organic aerosol fraction.

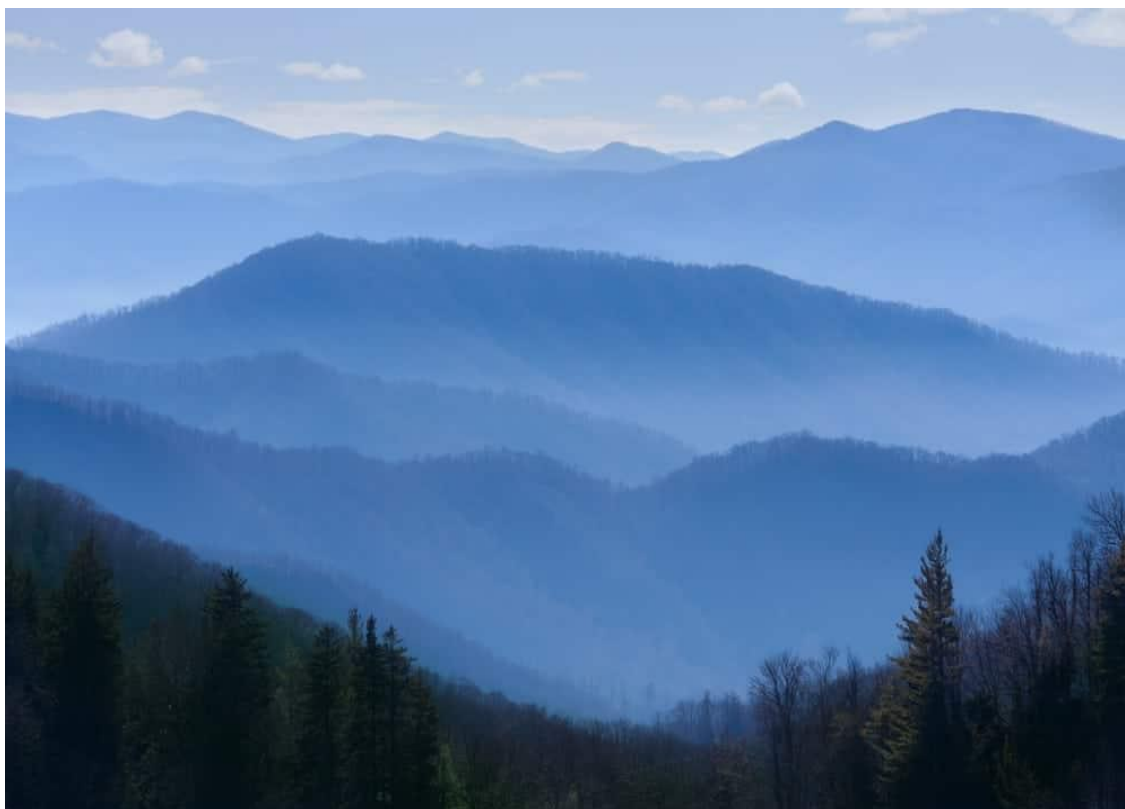


Figure 1.5 An example of *blue haze* phenomena over the Great Smokey Mountains (source: visitmysmokies.com).

Groups of compounds characteristic of biogenic emissions include various types of acyclic olefins (e.g., isoprene), or triolefins (e.g., myrcene, ocimene), bicyclic olefins (e.g., 3-carene, α -pinene, β -pinene, sabinene), cyclic diolefins (e.g., D-limonene), sesquiterpenes (e.g., β -caryophyllene), and a wide range of oxygenated species, including alcohols (e.g., methanol, 2-methyl-3-but-2-ol, linalool). The recent estimates indicate that emissions of biogenic volatile organic compounds into the atmosphere reaches about 1000 Tg/year, with isoprene having the largest share among BVOC, with its annual emission to the atmosphere of 535 Tg²⁵. For compounds of the monoterpenes ($C_{10}H_{16}$) and sesquiterpenes ($C_{15}H_{24}$) class, their annual emissions are estimated at around 15% of total BVOC emissions. The estimated atmospheric loads of selected BVOCs in a year scale are summarized in Table 1.1.

Table 1-I Estimations of global emissions for selected biogenic volatile organic compounds.

Compound	Emissions (Tg/year) ^a
Isoprene	535
α -Pinene	66.1
β -Pinene	18.9
D-Limonene	11.4
Sabinene	9.0
Δ^3 -Carene	7.1
Camphene	4.0

a 25

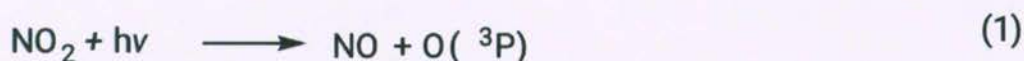
1.5.1.1 Evolution of biogenic volatile organic compounds

Three main stages can be distinguished in the formation of secondary organic aerosol components. In the first step, a given VOC precursor is oxidized in the gas phase under the influence of atmospheric oxidants. As a result, an array of oxygenated volatile organic compounds (OVOCs) are formed, with functional groups such as carbonyl, hydroxyl, carboxylic, peroxyde, nitrate, ester, peroxy-carboxy, hydroperoxy^{1,52,53}. OVOCs can be also fragmented into smaller oxidized particles, with lower molecular weights and the higher vapor pressure, with tendency to undergo further oxidation processes in the gas phase. Providing that the residence time in the atmosphere is long enough, final oxidation products of VOC species should be H₂O and CO₂ molecules only. Products with the reduced volatility compared to their precursors, have increased water solubility, and thus their tendency to partition is increased. The next stage is the partitioning of the semi-volatile products between the gas phase and the particulate phase. Finally, in the third step, SOA in the condense phase may undergo further processes leading to the formation of other SOA compounds with increasing O:C ratios. There are some structural and chemical patterns for the organic molecule to be an efficient SOA precursor⁵⁴. Usually such a compound shows an adequate degree of volatility, and is atmospherically abundant and chemically reactive. Therefore, low molecular weight

alkanes and alkenes containing less than 6 carbon atoms do not meet these criteria, e.g., methane, which is on the most abundant trace organic component in the atmosphere. The exception is isoprene (C₅H₈), which significant participation in the formation of SOA has been confirmed in numerous laboratory and/or field studies^{30,34,49,55-57}. The general trend shows that the yield of SOA increases with a number of carbon atoms and functional groups, as well as with additional methylene groups in the structure. The addition of polar functional groups (e.g., hydroxyl, peroxy, carboxyl or nitrate) can lower vapor pressure of the oxidized molecule even over two orders of magnitude⁵⁸. Other factors that affect SOA formation include the ambient temperature and an intensity of the sunlight: higher they are, the increasing SOA mass concentrations are observed. One of the crucial factors implying formation paths of SOA is the concentration of nitrogen oxides. Depending on whether the reactions take place under high or low NO_x conditions, VOCs reacting with oxidants can be altered, as well as various intermediate steps on these pathways.^{59,60} Eventually, the relative humidity and the other SOA constituents also influence formation processes of secondary particulate matter.⁶¹

1.5.1.2 Tropospheric oxidants

In the first step of gas-phase processes occurring in the atmosphere, BVOCs may undergo photolysis (at a wavelength $\lambda > 290$ nm) or an oxidation reaction in the presence of hydroxyl radicals, nitrate radicals or ozone.^{8,47,62} In marine or coastal areas, these gaseous precursors can also react with chlorine or bromine atoms, i.e. radicals.^{46,63} Most atmospheric ozone is found in the stratosphere, where it absorbs solar radiation with the UV wavelength in the range of 240-290 nm, and also significantly reduces the amount of UV-B radiation ($\lambda = 290 \div 320$ nm). The ozone concentration in the troposphere is much lower – it can diffuse from the stratosphere or it can be formed as a result of chemical transformations of other compounds. Precursors of the ozone formation are non-methane volatile organic compounds (NMOCs), carbon monoxide and methane, however, the most important source of ozone in the lower atmosphere is NO₂ photolysis:

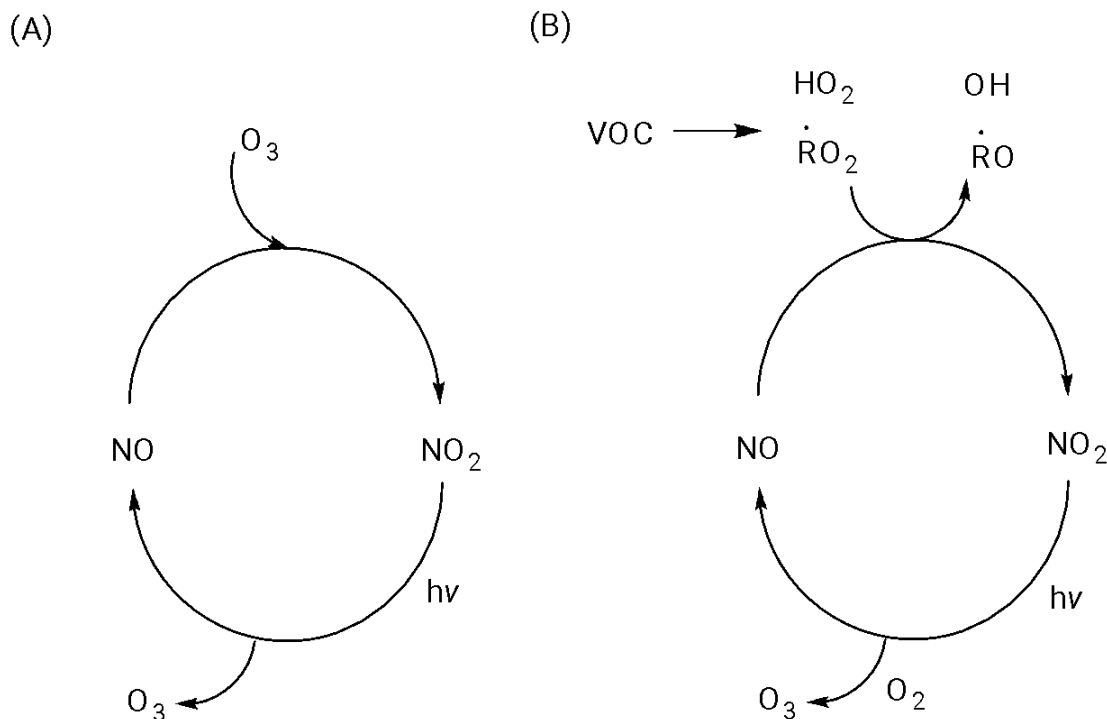


Generated O₃ immediately react with NO to form NO₂:



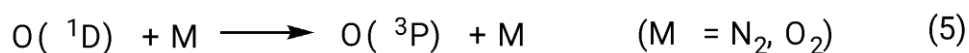
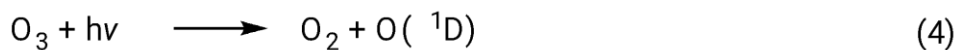


Reactions (1) – (3) built-up a photo equilibrium between all three species (Scheme 1.1 A). However, in the presence of VOCs alkylperoxy and peroxy radicals are formed and they react with NO to form NO₂ (Scheme 1.1B)



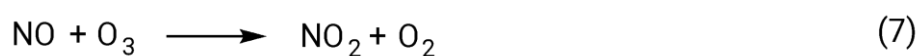
Scheme 1.1 Schematic representation of NO to NO conversion processes and O₃ formation (A) in the absence of VOCs and (B) with the presence of VOCs ⁶²

The presence of O₃ in the atmosphere also has a significant impact on the formation of hydroxyl radicals, which almost all emitted to the atmosphere volatile compounds react with. In a wavelength range of 290 and 350 nm, ozone photolysis produces oxygen in ¹D state, reaction (4), followed by deactivation to the ground state ³P, reaction (5), or after reaction with water vapor is a source of hydroxyl radicals, reaction (6).



The production of hydroxyl radicals arising from the ozone photolysis is the major process that provides these radicals in the troposphere. Other sources, independent of the daylight regime, are the reaction of O₃ with alkenes, or reactions of NO₃ radicals with alkenes or aldehydes.⁶⁴

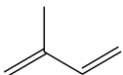
Nitrate radicals are the third most important tropospheric oxidants. As a result of the consecutive reactions of NO and NO₂ with O₃, reactions (7) and (8), the NO₃ radical is formed. It is also important, whether the reactions occur during the day or at night – during the night nitrate oxides are converted to nitrogen dioxide⁵³. With the access of light NO₃ almost immediately undergoes photolysis.

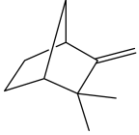
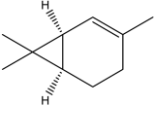
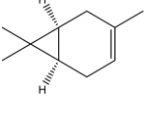
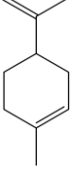
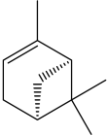
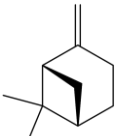



It was observed that in the case of low-molecular compounds, the SOA yield increases inversely proportional to the NO_x concentration,^{48,56,65} while in the case of high-molecular compounds the situation is opposite and the SOA yield increases as the NO_x concentration increases.⁵⁹

Calculated lifetimes of biogenic VOCs show high reactivity in reactions with mentioned above main tropospheric oxidants (Table 1.2). Times of minutes or hours combined with high dependence on other components of air masses, time of day, meteorological conditions and geographical location, also show how difficult it is to study the transformation of these compounds.⁶⁶

Table 1-II Calculated lifetimes of selected biogenic volatile organic compounds in reactions with OH radicals, NO₃ radicals and O₃.

BVOC	Structure	Representative lifetimes ^a due to reaction with:		
		OH ^b	O ₃ ^c	NO ₃ ^d
Isoprene		1.4 h	1.3 day	1.6 h

Camphene		2.6 h	18 day	1.7 h
2-Carene		1.7 h	1.7 h	4 min.
3-Carene		1.6 h	11 h	7 min.
Limonene		49 min.	2.0 h	5 min.
α -Pinene		2.6 h	4.6 h	11 min.
β -Pinene		1.8 h	1.1 day	27 min.
Sabinene		1.2 h	4.8 h	7 min.

^a From Atkinson ⁶⁶

^b assumed OH radical concentration used in calculations: 2.0×10^6 molecule cm^{-3} , 12 h daytime average

^c assumed O_3 concentration used in calculations: 7.0×10^{11} molecule cm^{-3} , 24 h daytime average

^d assumed NO_3 radical concentration used in calculations: 2.5×10^8 molecule cm^{-3} , 12 h daytime average

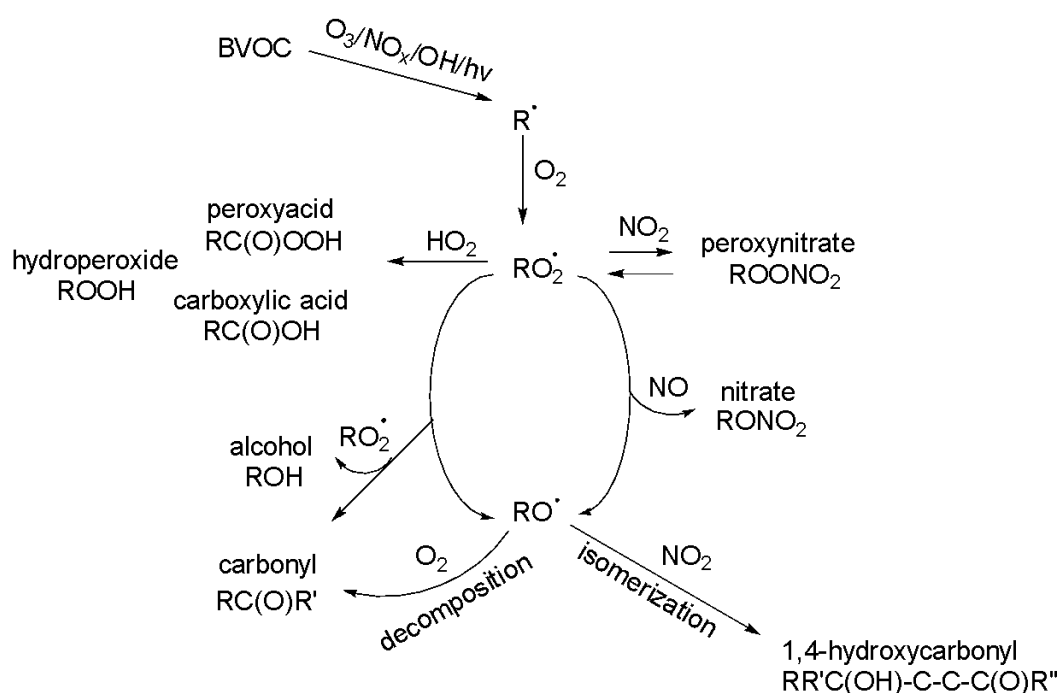
1.5.2 Main gas-phase oxidation pathways

The reaction pathways of volatile organic compounds, including these of biogenic origin, occurring in the gas phase have been thoroughly studied in the last two decades ^{1,52,62,66-71}. Depending on the type of oxidant, the effect on the VOC compound varies. In contrast to addition reactions, if proton detachment occurs, this will not translate into the

precursor volatility. The addition of a hydroxyl or nitrate radical to a double bond in alkanes results in a similar effect on the compound's vapor pressure, however, the difference between these radicals is visible in subsequent reaction stages. The nitrate radical may degenerate into the NO₂ radical, which in turn may affect the increase in volatility⁷².

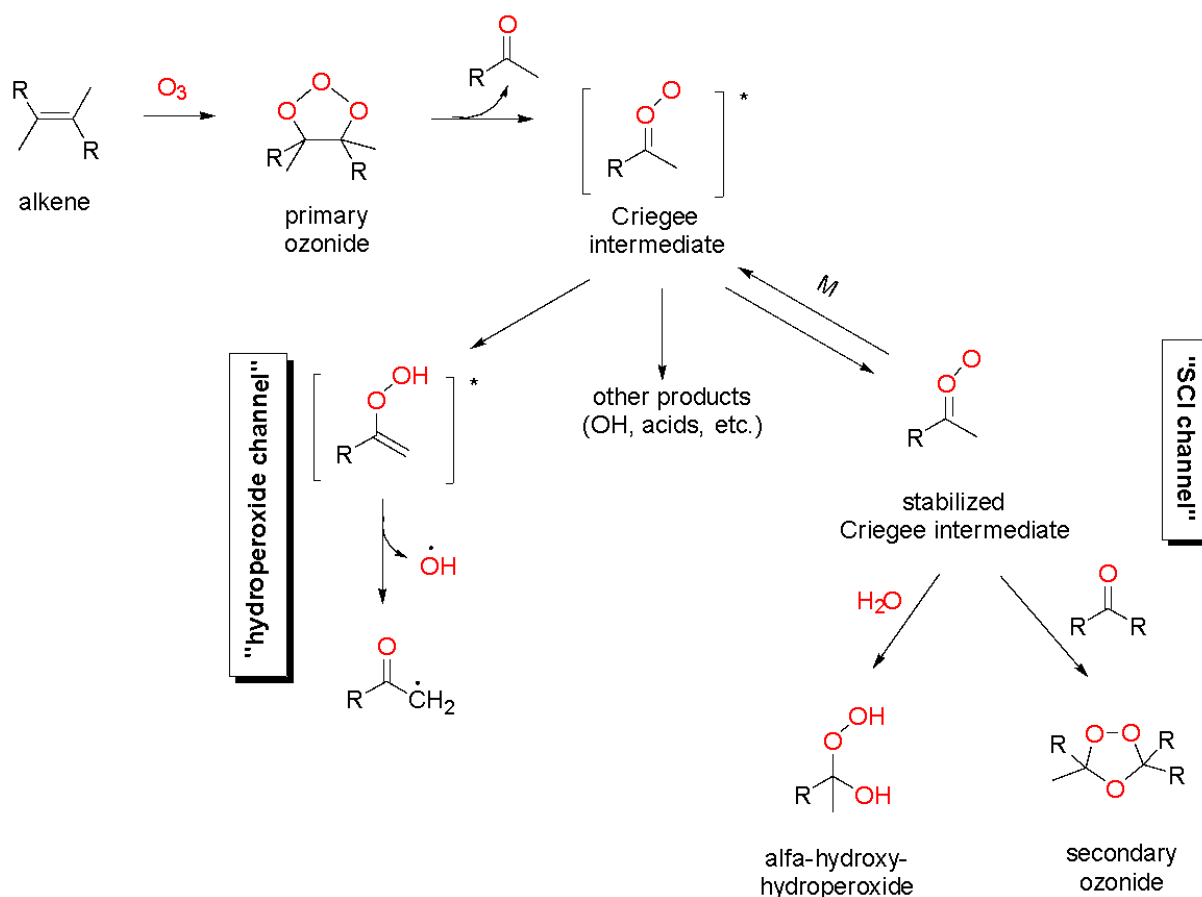
In the first initial step, alkyl or substituted alkyl radical is formed after oxidant attack or after light absorption, with subsequent formation of peroxy- and alkoxy radicals. In general, this reaction step can take place in two different ways: 1) as a result of NO₃ radical, OH radical or O₃ addition to C=C unsaturated bond and 2) after H-abstraction from C-H or O-H bonds by Cl atoms, NO₃ radicals, OH radicals. O₃ can only react by addition to a C=C double bond; the mechanism of this type of addition will be discussed in the next sections of the chapter. In the case of NO₃ and OH radicals, addition to C=C bonds dominate over the abstraction of the hydrogen atom. In that event hydroxy- and nitrooxy-substituted alkyl radicals are formed. For nitrooxy- and hydroxyl radicals H-atom abstraction reactions are of lesser importance, except for compounds containing an aldehyde group and a C = C bond, as in the case of methacrolein. Hydrogen atom loss occurs from C-H bonds in classes of compounds such as alkanes, esters, ethers, alcohols and carbonyl compounds. Resulting of this type of reaction, alkyl or alkyl substituted radicals are formed. A representation of the possible reaction paths of alkyl radicals or substituted alkyl radicals (R[•]) following the initiating step is shown in the Scheme 1.5.2. Subsequent reactions proceed to form an organic peroxy (RO₂[•]) or alkoxy (RO[•]) radical.

Cl radicals are produced *via* photolysis and they can react with BVOCs similar to OH and NO₃ radicals - by detachment of hydrogen atom from C-H bond or by addition to C=C double bond, results with peroxy and chloroperoxy radicals. Although the abundance of chlorine radicals is significantly lower than OH radicals (by 1 to 3 orders of magnitude), because of its high reactivity and high reaction rates it is considered as a primary oxidant^{73,74} especially in *high*- NO_x conditions.^{63,75} Sources of reactive forms of halogens in the atmosphere are not well recognized, and therefore their contribution to SOA is probably underestimated. The latest research shows that oxidation reactions initiated with a chlorine radical lead to the formation of SOA components.⁷⁶



Scheme 1.2 Processes of biogenic volatile organic compounds degradation in the atmosphere as a result of the formation of alkyl radicals or substituted alkyl radicals under the atmospheric oxidants.

The addition of ozone to the carbon-carbon double bond, or VOCs containing an unsaturated bond system in its structure, leads to the formation of an intermediate ozonide (1,2,3-trioxolane), according to a mechanism proposed by Criegee and co-workers.⁷⁷ In the first step of 1,3-dipolar addition primary ozonide is formed, with subsequent decomposition into carbonyl compound and carbonyl oxide (Criegee intermediate) in step two. At this point Criegee intermediate, which is energetically excited, can decompose in two main pathways. The first route is called the hydroperoxide channel and results with formation of OH and an alkyl radical. In the second pathway, the stabilized Criegee intermediate (SCI), the excited Criegee Intermediate is stabilized by quenching and can react with water to form α -hydroxyperoxides or with carbonyl compound to form secondary ozonide (Scheme 1.3). Ozonolysis of biogenic alkenes is an important source of OH radicals, regardless of the time of a day.^{64,78,79}



Scheme 1.3 Schematic representation of alkene ozonolysis with the emphasis on two main pathways: the hydroperoxide channel and the stable Criegee channel. Based on Kroll's work. ¹

1.5.3 Gas to particle partitioning theory

When speaking of secondary organic aerosol, we mean a complex mixture of semi-volatile products of transformations of volatile organic compounds in the gas phase, followed by a subsequent transfer of the resulting compounds into the particle phase by nucleation and/or coagulation (Fig. 1.1). In other words, first we have oxidized VOCs products in a gas phase, and then some of the offspring with a low vapor pressure condensed onto pre-existing particles, which lead to secondary organic-carbon products. Considering that oxidation products and condensation products can simultaneously partition between two phases, we should know how this process occurs to determine the yields of secondary organic aerosol. Without determine on what means a partition process took place (i.e., adsorption, absorption or both), the temperature-dependent partition

coefficient K_p parameter that determines adsorption of vapor components on the aerosol particles is used (equation 9)⁸⁰:

$$K_p = \left(\frac{F}{TSP}\right)/A \quad (9)$$

where K_p is partition coefficient ($\text{m}^3/\mu\text{g}$), and F and A are respectively the concentration values of the species in the aerosol phase and the gas phase (ng/m^3) and TSP is total suspended particulate material ($\mu\text{g}/\text{m}^3$).

We can transform the equation (9) to the form (10):

$$\frac{F}{A} = K_p \times TSP \quad (10)$$

to obtain a relationship which shows that the ratio of the concentration of the species in the gas phase to the concentration in the molecular phase is directly proportional to the product of the partition coefficient and the concentration of the total aerosol mass. One of the most important formulations of partitioning theory between gas and particulate phase, in which he took into account adsorption and absorbent inserts, was given by Pankow.⁸¹ According to this theory if the partitioning would be only the adsorptive process we could express the partition coefficient as (11):

$$K_{p,i} = \frac{N_s a_{tsp} T e^{(Q_1 - Q_v)/RT}}{1600 p_L^0} \quad (11)$$

where:

N_s is the surface concentration of sorption sites sorption sites (sites/cm^2)

a_{tsp} is specific surface area (m^2/g) for the atmospheric particulate material

T is the temperature (K)

R is the gas constant

Q_1 is the enthalpy of desorption from the surface (kJ/mol)

Q_v is the enthalpy of vaporization (kJ/mol) of the liquid (sub-cooled, if necessary)

p_L^0 the compound's vapor pressure (torr) as a pure liquid (subcooled if necessary) at given temperature

On the other hand, when the process is dominated by the absorptive partitioning and species concentration is expressed by concentration of species in a particulate phase, the partition coefficient K_p can be expressed as the ratio of molecules in the particulate phase [ng/μg] to the molecules in the gas phase [ng/m³] (12):

$$K_{p,i} = \left(\frac{F_{i,om}}{TSP}\right)/A_i = \frac{760RTf_{om}}{10^6MW_{om}\zeta p_{L,i}^0} \quad (12)$$

where:

$F_{i,om}$ [ng/m³]: concentration of i -compound in the absorbing organic material phase

TSP [μg/m³]: total suspended PM concentration

A_i [ng/m³]: gas phase concentration of i -compound

R : the ideal gas constant (8.25E-5 m³ atm/mol K)

T [K]: temperature

f_{om} : the weight fraction of the TSP that is the absorbing organic matter phase

MW_{om} [g/mol]: the mean molecular weight of the absorbing organic matter

ζ_i : the activity coefficient of species i in the particle phase

$p_{L,i}^0$ [torr]: the compound's vapor pressure as a pure liquid (subcooled if necessary) at given temperature

Taking into account both the mechanisms, adsorption and adsorption, we obtain the equation (13):

$$K_{p,i} = \frac{1}{p_L^0} \left[\frac{N_s a_{tsp} T e^{(Q_1 - Q_v)/RT}}{1600} + \frac{760RTf_{om}}{10^6 MW_{om} \zeta} \right] \quad (13)$$

Primarily adsorptive processes will be favored with increasing a_{tsp} surface area and $e^{(Q_1 - Q_v)/RT}$, and the primarily absorptive ones with increasing f_{om} and decreasing both

activity coefficient ζ and the mean molecular weight of the absorbing organic matter MW_{om} .

Over the past few decades, at least several indirect methods were developed to express the SOA yield, such as determination of the elemental and organic carbon ratio⁸², chemical mass balance method (CMB), in which the total carbon mass is related to functional groups and molecular composition⁸³ or the fractional aerosol yield understood as a fraction of reactive organic gas converted to aerosol^{84,85}.

1.5.4 Particle – phase reactions of SOA

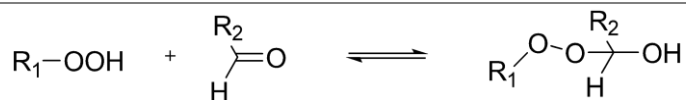
The first oxidation products of volatile organic compounds in the atmosphere may undergo further processes in the condensed phase, resulting in their volatility and chemical properties change. The lowering of the volatility of particle-bound SOA components has a direct effect on the phase partitioning.^{1,52} Reactions in the condensed phase that take place in a time shorter than the average lifetime of the particles present in the troposphere (up to a week) are especially important. The two main types of processes that we can distinguish relate to the oxidation state of the carbon atoms in the molecule, i.e., they are oxidative and non-oxidative processes.

1.5.5 Non-oxidative processes

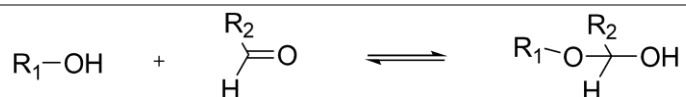
Processes, such as secondary oxidation reactions, cyclization or formation of oligomers - simply the formation of high-molecular weight species with low or significantly low vapor pressures, also known as *accretion reactions*, are considered as an important source of secondary organic aerosol.^{34,86-89} The resulting secondary products typically exhibit covalent bond character, although non-covalent species have also been observed.^{90,91} Exemplary types of reactions that may occur in the particulate phase are summarized in Table 1-III. It was observed that the presence of acidic seeds had a significant effect on increasing the efficiency of SOA formation, especially in case of precursors with high volatility, such as isoprene.⁹²

Table 1-III Schemes of accretion reactions that can take place in the particulate phase, resulting in the secondary organic aerosol formation.

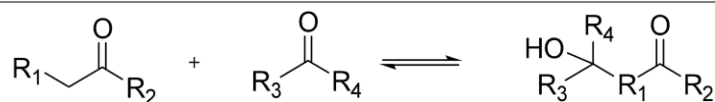
Formation of peroxyhemiacetal :



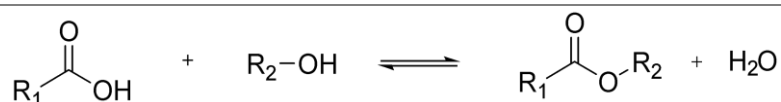
Formation of hemiacetal:



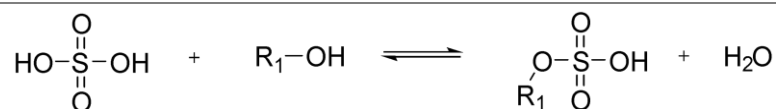
Formation of aldol reaction product:



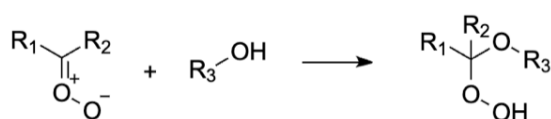
Formation of ester or acid anhydride product:



Formation of sulfate monoester:



Formation of Criegee intermediate adduct:



1.5.6 Oxidative processes

Chemical oxidative processes that aerosol particles undergo in particulate-phase are known as *aerosol aging*⁹³ and they can occur through heterogeneous uptake of atmospheric oxidants, analogous to these in the gas phase (OH, NO₃, NO₂, O₃), or as a

result of oxidation in the liquid phase.⁹⁴ Changes in the chemical and physical properties of particles resulting from the fragmentation of existing structures by breaking carbon-carbon bonds, lead to the modification of the original structures by adding polar groups in it or transformation of functional groups. Fragmentation and functionalization processes increase the O:C ratio, but in the case of fragmentation we obtain higher volatility, and with functionalization, the opposite.^{95,96} One of the most important differences between the oxidation processes taking place in the gas phase and those in the particle phase is the residence time of organic compounds in the atmosphere, which in the first case is only a few hours, while in the second it can take up to about a week, simply due to mass-transfer limitations.^{97,98} This significantly affects a number of possible processes that organic compounds can succumb, and at the same time it makes it difficult to recreate the aging processes in the molecular phase in the laboratory.

1.5.7 Selected SOA precursors in reactions with atmospheric oxidants

In recent years, aerosol aging processes occurring in the aqueous phase have been more and more intensively studied due to the potentially important role of oxidation of VOCs particle precursors^{36-38,99,100} and because of potential significance in cloud processing.^{101,102}

Among the variety of possible biogenic SOA precursors to the most important one we include non-methane compounds containing one or more isoprene units in their backbone, therefore compounds fulfilling the so-called isoprene rule – hemiterpene (C₅H₈), monoterpenes (C₁₀H₁₆), sesquiterpenes (C₁₅H₂₄) and oxygenated derivatives of these classes of compounds. The qualitative and quantitative examination of the SOA components allows the source apportionment and to verify the possible mechanisms of their formation and aging in the atmosphere. The compounds of particular interest are the molecular tracers of SOA, i.e. compounds identified in significant amounts as products of transformation of specific gaseous precursors, although not always one tracer is formed from one precursor.^{5,103} We define “tracer” as a stable product under atmospheric conditions, for which the path from the source to sink is well known. Since meeting the criteria for a tracer¹⁰⁴ is not an easy task, the term "marker" referring to potency or identity is used more often. Despite intensive research in the area of molecular characterization of marker compounds (see examples of marker compounds, their

precursors and references in Table 1-IV), there is still a limited amount of data. The main difficulties with molecular recognition and identification of the components and markers of the secondary organic aerosol mainly concerns the complex matrices of the collected samples, short residence time of markers in the atmosphere, as well as the many possible degradation paths. For example aqueous-phase reactions are currently considered one of the important pathways for the degradation and transformation of SOA in the atmosphere, but are still poorly understood.

Table 1-IV The most significant organic aerosol precursors and their marker compounds in the PM phase.

organic precursor	marker compound	reference
hemiterpenes		
<i>isoprene</i>	2-methylthreitol	30,105
	2-methylerythritol	105
	(2 <i>S</i> , 3 <i>R</i>)-, (2 <i>R</i> , 3 <i>S</i>)-, (2 <i>S</i> , 3 <i>S</i>)-, (2 <i>R</i> , 3 <i>R</i>)-2-methyltetrols	106,107
	2-methyltetrol organosulfates	108
	2-methylglyceric acid	105
	2-methylglyceric acid oligoesters, sulfates, nitrates	60,92,109-111
	methyl vinyl ketone, methacrolein sulfonates	38,109
	<i>cis</i> - and <i>trans</i> -3-methyl-3,4-dihydroxytetrahydrofuran	112,113
	isoprene epoxydiols (IEPOX)	114
	methacrylic acid epoxide (MAE)	115
	3,4-dihydroxy-3-methyltetrahydrofuranone	36,116,117

	3,4-dihydroxy-3-methyltetrahydrofuranone	
	isoprene nitrate	118
monoterpenes		
<i>α,β-pinene</i>	3-hydroxyglutaric acid, 3-methyl-1,2,3-butanetricarboxylic acid	86,110
	<i>cis</i> -pinic acid	119
	hydroxy-pinonic acid	120,121
	hydroxy-pinonaldehyde	120,121
	terpenylic/terebic acid	105,121,122
	diaterpenylic acid acetate	123
	diaterpenylic acid	122,123
sesquiterpenes		
<i>β-caryophyllene</i>	β-caryophyllene aldehyde, β-nocaryophyllene aldehyde	124
	β-caryophyllonic acid, β-nocaryophyllonic acid, β-caryophyllinic acid, 3,3-dimethyl-2-(3-oxobutyl)- cyclobutanecarboxylic acid, 2-(2-carboxyethyl)-3,3-dimethylcyclo- butanecarboxylic acid	125

1.5.8 Isoprene-derived SOA markers formation

It is estimated that isoprene contributes up to 4.6 Tg year⁻¹ to SOA mass.⁵² Therefore the interest in the SOA components formation mechanisms, for which isoprene

serves as the precursor, is completely understandable. The general outline of isoprene oxidation processes in the atmosphere along with the main products resulting from them are presented in Fig. 1.6.

In the case of isoprene, hydroxyl radicals play the most important role in the oxidation processes resulting in isoprene hydroxy-peroxy radicals. In the next stages, depending on the concentration of nitrogen oxides, 1st generation products are formed, *i.e.* methyl vinyl ketone and methacrolein.^{49,126} Vapor pressure of 1st oxidation products is too high to enable the condensation process, however, when subjected to subsequent processes, they lead to the formation of semi-volatile products capable of partition into the condensed phase. The first compounds detected in SOA samples associated with isoprene were 2-methyltetrols (2-methylthreitol and 2-methylerythritol).³⁰ These compounds are formed under low nitrogen oxides concentration, as a result of subsequent reactions with hydroxy-peroxy radicals. Concentration of nitrogen oxides has a great impact on isoprene gas-phase chemistry. Under low concentrations of nitrogen oxides and the presence of hydroxy- and hydroxy-peroxy radicals, isoprene forms intermediate epoxydiols (IEPOX).¹²⁷⁻¹²⁹ High concentrations of nitrogen oxides open up other possible pathways for SOA formation starting from the methacrolein formation, through low volatility nitrates methacryloyl peroxyxynitrate (MPAN), with subsequent formation of hydroxymethyl-methyl-lactone (HMML)¹³⁰ and methacrylic acid epoxide (MAE).¹¹⁵ The epoxides formed in the gas phase undergo further multiphase reactions on the surface of the condensed phase, leading to the formation of isoprene markers, such as previously mentioned 2-methyltetrols, C5-alkenetriols and their sulfate esters (for low NO_x conditions) or 2-methylglyceric acid (for high NO_x pathway).

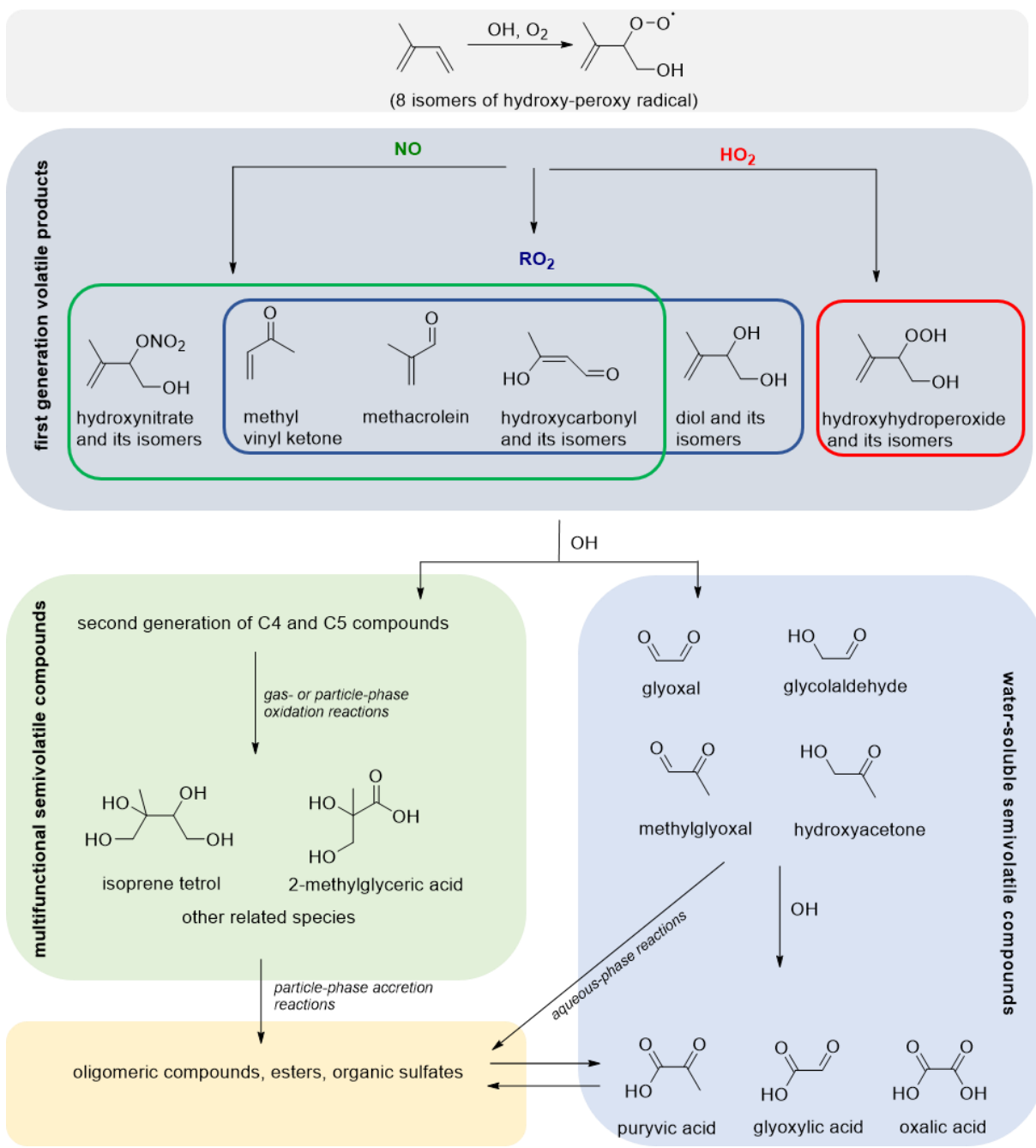


Figure 1.6 The main processes of isoprene oxidation in the atmosphere leading to the isoprene SOA formation; based on Carlton and co-workers work¹²⁶

1.5.9 Organosulfates

Sulfate esters, commonly referred to as organosulfates (R-OSO₃H), which are monoesters of sulfuric(VI) acid, are one of the most interesting SOA markers intensively examined during the last decade. It is estimated that isoprene-derived organosulfates constitute up to 42% of the total sulfate aerosol, and their content in the organic fraction of the aerosol is approx. 3.5%.¹³¹ Until recently, a main source of organosulfates (OSs) in the atmosphere was considered to be a chain of multiphase reactions of organic compounds with inorganic sulfate ions, mostly originated from anthropogenic sources, such as acid rain production or intensive coal burning. However, recent research shows that organosulfates can also originate from a variety of other sources, including SO₂-based chemistry in the gas phase^{132,133} in the aqueous phase^{38,134} or through heterogeneous processes, in which gas- and particle-phases are involved.¹³⁵⁻¹³⁷ The current state of research allows to distinguish 6 mechanisms of organosulfates formation, exactly:

- Epoxide intermediate mechanism (IEPOX, MAE)
- Esterification of sulfuric acid mechanism
- Nucleophilic substitution reactions (S_N) of alcohols with sulfuric acid
- Heterogeneous chemistry of SO₂
- Radical reactions in aqueous-phase through the addition of the sulfate radical to unsaturated double bond or through the radical-radical reactions of sulfate alkyl radicals
- Formation of monoterpene-derived highly oxidized OSs through the uptake of highly oxidized multifunctional organic compounds (HOMs) and reaction with bisulfate anions

Although OSs are believed to be markers of secondary atmospheric aerosol aging, little is known about their further fate in the atmosphere. Due to their low volatility, they mostly occur in the particle phase and can undergo hydrolysis reactions or react with oxidants present in the gas phase at the phase interface. The sulfate group in the structure

makes these particles surface active compounds, *i.e.* they lower the surface tension at the liquid-gas interface, in the case of IEPOX-OSs up to 15%¹³⁸. This translates onto hygroscopic properties and affects the processes of cloud condensation nuclei (CCN) formation increasing droplet formation in clouds from aerosols.

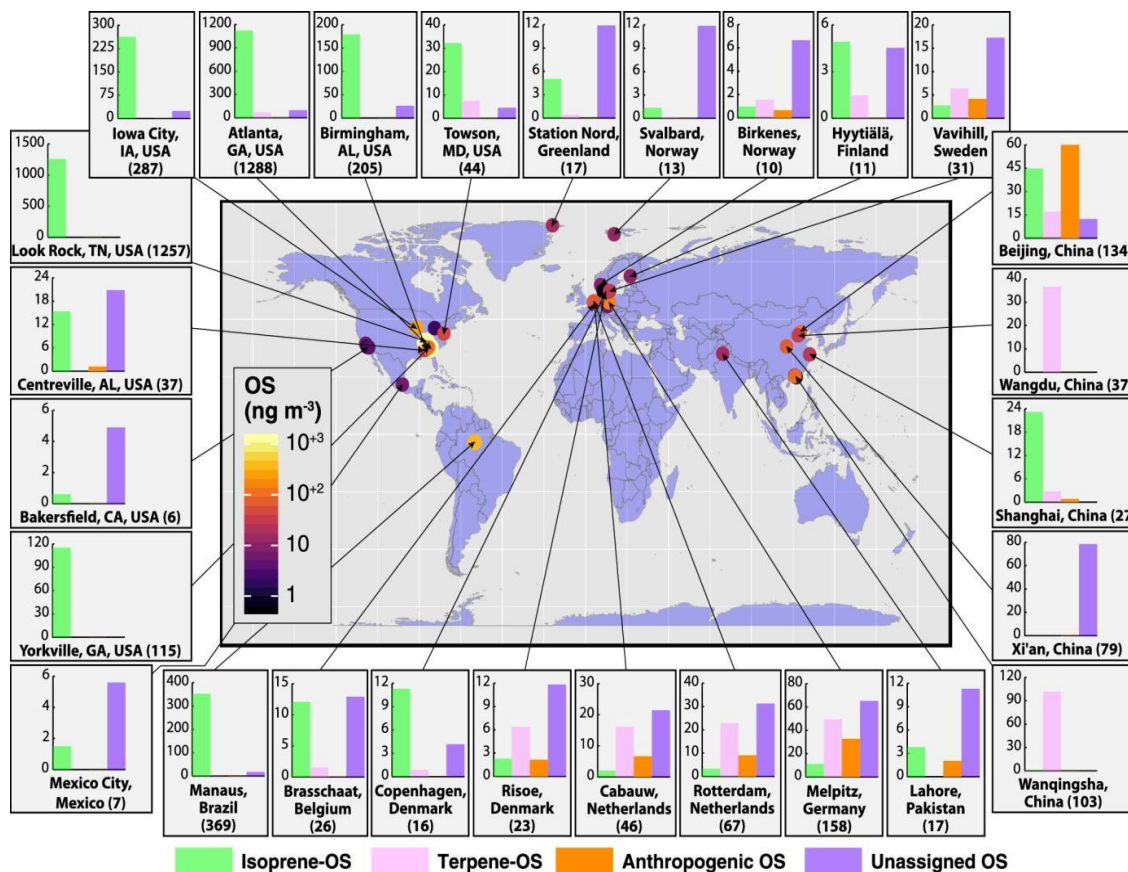


Figure 1.7 The bar graphs show the concentrations recorded in different locations around the world, distinguishing between the individual precursors. The biomass burning OSs are also included in the anthropogenic precursors. Total concentrations of OSs are placed in parentheses next to the location names. The color of the dots at specific locations corresponds to the determined concentrations of OSs as well.¹³⁹

1.6 Mass spectrometry as an analytical method for the aerosol characterization and quantitation.

Taking into account the chemical complexity of atmospheric aerosol, the determination of their composition (both quantitative and qualitative) is a challenge and thus requires analytical precise tools. Mass spectrometry, a technique by which we measure a mass-to-charge ratio of ions (m/z), is definitely one of them. In the last three decades, the development of mass spectrometry, as well as the possibility of its coupling with the separation techniques, i.e., gas- (GC) and liquid (LC) chromatography or electrophoresis, has made it a leading method used to characterize the organic aerosol fractions.¹⁴⁰⁻¹⁴⁴ Regardless of a mass spectrometer used, each measurement always consists of three steps: sample ionization (with an ion source), ion separation (with a mass analyzer) and signal recording (with a detector that converts the ion beam into an electric signal).

1.6.1 Ionization techniques applied in the aerosol studies

Depending on the aerosol sample and its properties, there is a wide range of ionization methods used in the environmental mass spectrometry. We can distinguish ionization methods in high vacuum, medium vacuum and atmospheric pressure, as well as desorption methods.¹⁴⁵ Table 1-V summarizes the main ionization techniques commonly used with their brief characteristics. In the aerosol research, the most frequently techniques used are: electron ionization (EI), chemical ionization (CI), electrospray ionization (ESI), atmospheric pressure chemical ionization, photospray ionization and matrix-assisted laser desorption ionization (MALDI).^{5,142} It worth noting that soft ionization methods, including CI, ESI, APPI, APCI are the most favorable ones due to the fact that key steps towards SOA are based on the oxidation chemistry, which evidently results in the formation of polar aerosol components, such as organosulfates.^{19,21,36,38,116}

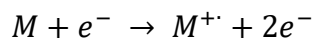
Table 1-V Commonly used ionization methods in *off-line* mass spectrometry of the atmospheric aerosol along with their brief outline.

Measurements conditions	Type of ionization	Process description	Applications
High vacuum	Electron Ionization (EI)	the analyte in the gas phase is bombarded with an electron beam of energy ranging from several to several dozen electron volts; the energy of the passing energy is transferred to the molecule of a compound, and as a result the electron may be detached from the HOMO orbital with the radical cation formation	highly volatile compounds with low or medium polarity
Medium vacuum	Chemical Ionization (CI)	electron ionization of the reagent gas leads to the formation of primary ions, which then react, and thus ionize the analyte, also ionization in the negative ion mode is possible owing to electron capture processes	highly volatile compounds with low or medium polarity, in the negative ion mode: halogens, compounds containing nitro groups
Atmospheric Pressure	Electrospray Ionization (ESI)	ions from the liquid phase are transferred to the gas phase due to a high electrical field on nebulized droplets; in a first step charged spray eluting from a capillary forms a Taylor cone, in the next repetitive evaporation and desolvation processes occurs; finally ions solvated in a gas phase are formed in a medium pressure region of a mass spectrometer	non-volatile polar compounds in a wide range of mass

	Atmospheric Pressure Chemical Ionization (APCI)	the principle of operation is close to chemical ionization, but under atmospheric pressure; with use of ionization electrode and corona discharge phenomenon, in the initial phase nebulizer gas molecules are ionized, which react with the solvent molecules and then analyte molecules	non-volatile medium-sized compounds of moderate polarity and poor polarity
	Atmospheric Pressure Photoionization (APPI)	ionization is initializing by the reaction of an analyte (M)/dopant(D) molecule with photons (generated by xenon UV-lamp) and formation of corresponding molecular ion radicals (M^+ or D^+); analyte radical ions usually reacts with solvent molecules giving MH^+ ions; dopant radical ions can ionize analyte molecules giving molecular ions which can react in the same manner as molecules ionized directly by photons	non-volatile medium-sized compounds of moderate and poor polarity bearing chromophoric residues
Desorption methods	Matrix-Assisted Laser Desorption (MALDI)	dissolved analyte mixed with an appropriate matrix is applied to a metal plate, evaporated to dryness and, after being placed in the ionization chamber, irradiated with laser pulses, which results in the formation of neutral particles and ions	large molecules of different polarity, often used for the analysis of proteins, peptides, oligonucleotides, large organic molecules such as dendrimers or polymers
	Desorption Electrospray (DESI)	the substance to be analyzed is knocked out of the sample surface by charged solvent droplets;	a very universal method for molecules with higher masses

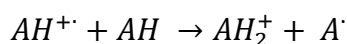
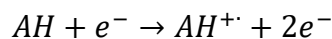
ionization occurs under ambient pressure; positive (MW > 1000 Da), suited both
and negative ionization modes are possible for non-polar and highly
functionalized compounds

Electron impact ionization is by far the oldest ionization technique in which a volatile and chemically stable compound is bombarded with an electron beam. As a result of this process, cation radicals are formed:



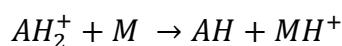
Spectra recorded with the same energy value of 70 eV for specific compounds are reproducible and collected in mass spectra libraries.* This is a great advantage, when it comes to identifying individual compounds. However, relatively high ionization energy values have some disadvantages. First, they often ionize all organic compounds present in the sample. Moreover, for compounds with low ionization energies, we may not observe the molecular ion ($M^{+\cdot}$) of the compound of interest at all, but a whole range of fragmentation ions that are already formed in the ion source. Although fragmentation ions provide valuable structural information, for complex samples, they do not allow unambiguous assignment of specific peaks to fragments of structures of individual compounds. For complex mixtures, such as ambient aerosol, it would be very difficult to assign appropriate signals to specific structures. Therefore, of the EI ionization is often combined with a prior gas chromatography.^{30,34,146-148}

In addition to the classical operation of the EI source, chemical ionization (CI) due to the fact that it follows a different mechanism than EI, is also used to avoid a high degree of fragmentation of the tested analyte. The reagent gas (AH) is introduced into the ionizing chamber and ionized with the stream of electrons. Ions capable of reacting with molecules of the substance analyzed, according to the scheme below for a positive ion mode, are formed:

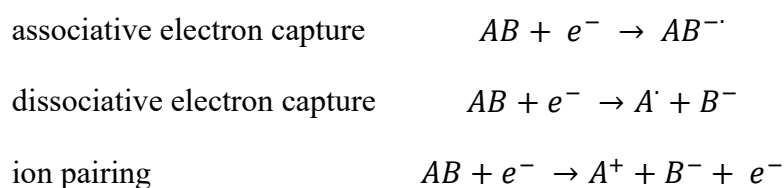


In the next step, a protonated ion of the reagent gas ionizes the analyte molecules (M):

* NIST and Wiley (<https://www.sisweb.com/software/ms/wiley.htm>) libraries are two of the most overwhelmingly applied in laboratory routine use



A landmark feature of the CI process is the ability to select an appropriate reagent gas, which may be specific for the class of compounds analyzed. In fact, the term chemical ionization defines several different possible processes. In the case of direct methods, the most frequently used process is a proton transfer, in which the proton is transferred from the hydronium ion to the molecule of the analyzed organic substance in the gas phase. Also this type of ionization was the first one allowing negative ion mode ionization (NCI), involving the electron capture reactions or ion pair formation:



The NCI method is widely used in the analysis of compounds containing halogens in their structure, as well as aromatics. And as such, the NCI was probed in the determination of polycyclic aromatic hydrocarbons¹⁴⁹ or their nitrated-derivatives^{Li, 2018 #580} in atmospheric aerosol samples.

Chemical ionization is often used in direct MS analysis of aerosols.^{150,151} Examples of frequently deployed direct CI-MS techniques are presented in Table 1-VI. As with EI, this technique is often preceded by gas chromatography. The GC-EI/CI-MS method for compounds containing acidic or hydroxyl moieties requires an additional step in sample preparation in the form of a derivatization process, e.g., trimethylsilylation^{152,153} or alkylation.^{154,155} Nevertheless, this method gave very good results in SOA species identification, as for example in the case of α -pinene acidic photooxidation products¹¹⁰ or isoprene photooxidation products 2-methyl glyceric acid oligomers,⁶⁰ as well as quantification of polar SOA components bearing hydroxyl and/or carboxyl groups.^{146,156}

Table 1-VI CI-MS techniques used in direct analysis of organic trace measurements in aerosols. Based on Noziere (2015) ⁵.

Acronym ^a	Reagent	Analyte	Diagnostic ions
PTR-MS	H ₃ O ⁺	alkenes, alcohols, carbonyls, aromatics, acetonitrile	[A + H] ⁺
CIT-CIMS	CF ₃ O ⁻	organic hydroxyperoxides, carboxylic acids, multifunctional organic compounds	[CF ₃ O + A] ⁻ [A + F] ⁻
NI-PT-CIMS	CH ₃ C(O)O ⁻	carboxylic acids	[A - H] ⁻
TD-CIMS	I ⁻	peroxyacyl nitrates	[A - NO ₃] ⁻
CI-MS	C ₂ H ₅ OHH ⁺	ammonia, amines	[A - C ₂ H ₅ OHH] ⁺

^aacronym: PT –proton transfer, CIT – California Institute of Technology, NI – negative ion, TD – thermal desorption

Following soft ionization techniques used in aerosol science there are methods operating under atmospheric pressure. The latter are currently one of the most intensively used ionization sources in mass spectrometry. When combined with tandem mass spectrometry (see chapter 1.6.3) and prior separation with liquid chromatography use (see chapter 1.6.4) it has been applied with great success in determination and quantification of organic compounds in aerosol samples ^{36,91,111,116,117,157-159}.

The principle of electrospray operation is to spray the dissolved sample of the analyte in a polar solvent eluting from the capillary to which an electric voltage is applied (up to 5 kV). In addition, the capillary is flushed with a gas that supports to fuse (Figure 1.8). As a result, a mist composed of many charged droplets is formed, and due to evaporation of the solvent, their sizes are reduced until the surface tension of the droplets is not able to balance the repulsive force of the homonymous charges accumulated on the drop surface. The droplet breaks up onto small offspring. This phenomenon is called the Coulomb explosion.

When the droplet reaches a size of *ca.* 10 nm, two consecutive ionization mechanisms are possible to occur, depending on the nature of the analyzed particle:

- 1) for compounds of moderate polarity, small and medium-sized, i.e., up to *ca.* 1000 Da, the electric field at the droplet surface is high enough to release ions into the gas phase. This mechanism is known as **ion emission from the droplet**.
- 2) compounds of high polarity and large sizes, such as proteins, form multi-charged and highly solvated ions. As a result of multiple evaporation, single multi-charged ions are formed. This mechanism is called **dry evaporation**.

When measurements are carried out in the positive ion mode, we mainly obtain protonated $[M + H]^+$ and sodiated ions $[M + Na]^+$, while in the negative ion mode deprotonated molecules are dominant $[M - H]^-$.

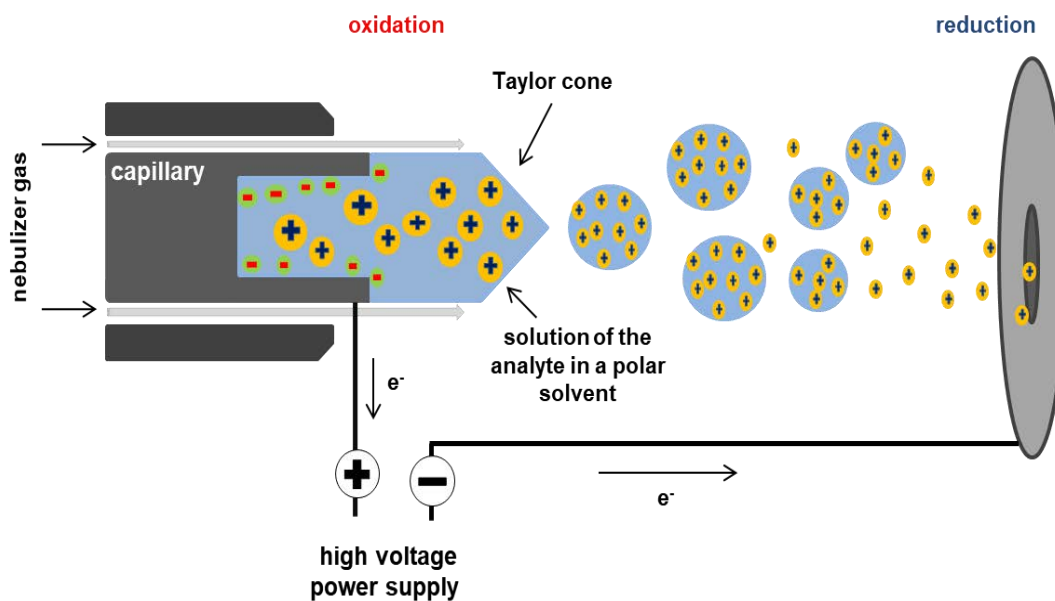


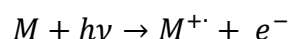
Figure 1.8 Schematic representation of the ionization phenomenon in an electrospray source, in the positive ion mode. Based on the graphic of Andreas Dahlin.[†]

[†] https://www.flickr.com/photos/visualize_your_science/21589986840/

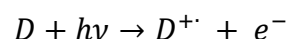
For LC-MS measurements where formic acid or acetic acid is used as mobile phase modifier, adducts with anions of these acids ($[M + \text{HCOO}]^-$ and $[M + \text{CH}_3\text{COO}]^-$) are observed. This type of ionization is also often used in the desorption electrospray (DESI) method,¹⁶⁰ in which the analyte is detached from the sample surface by the solvent spray. One of its biggest advantages is the fact that ionization takes place under ambient conditions and it can be done directly on the surface of the sample. Another increasingly widely used method is nano-DESI, which is a technique for extracting and ionizing liquids under atmospheric pressure. Analyte desorption takes place between the two capillaries and the sample surface. A high voltage is applied between the first solvent transport capillary and the mass spectrometer inlet, causing the formation of a self-priming nano spray. Importantly, this method can control the desorption, ionization and transport processes. In the case of atmospheric aerosol research, DESI and nano-DESI techniques allow analyzing the organic aerosol deposited on the filter surface without the need to prepare it in advance, thus it is preferable for very sensitive material in its native environment.¹⁶¹⁻¹⁶⁴

Atmospheric pressure chemical ionization (APCI) combines the principle of chemical ionization, except that it is carried out under atmospheric pressure. This method is less gentle than electrospray, often fragmentation of compounds occurs in the source. This is due to the higher energy values applied during the ion formation. The ionization process is started by applying a high voltage to an ionizing electrode in the form of a pointed needle. In the first step the nebulizer gas molecules in the source are ionized as a result of the phenomenon of corona discharges, forming the primary ions (mainly N_2^+ in positive ion mode). Gas-phase cation/anion radicals react with the vaporized solvent molecules and subsequently these reagent ions transfer their charge to the neutral molecules of the analyte to form stable ions in a final step of the process. Depending on the polarization mode, in which we want to carry out the ionization, the voltage applied to the ionizing capillary should be positive or negative. This method is successfully used as a complementary method to ESI for moderate and low polarity compounds, with poor volatility. In aerosol science this type of ionization is frequently used for on-line measurements of α -pinene oxidation products.^{165,166} On the other hand, as an off-line technique van Eijck and collaborators used APCI-MS in aim to characterize the oxidation products of β -caryophyllene in chamber experiments.¹²⁵

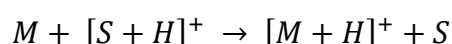
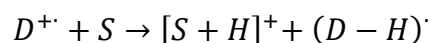
The last soft ionization technique is atmospheric pressure photoionization (APPI), in which the source of energy needed for ionization is an UV lamp and the ionizing agents are simply photons. The first ionization step is in the region illuminated by a krypton or xenon lamp that emits the light with a wavelength of 254 nm and an energy of *ca.* 10 eV. The energy value is selected so that the ionization potential is sufficient to ionize a fairly wide range of organic compounds, but low enough to prevent solvent molecules ionization. In the direct method the molecule of analyte (M) is ionized with formation of molecular ion:



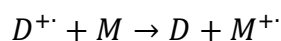
But often in this method, dopant has to be used (D), which under the selected conditions, is ionized as first with the formation of a radical cation:



Then, dopant cation radicals can ionize the solvent molecule, which depends on its proton affinity. If the affinity for the proton of the analyte is higher than that of the solvent particles, they can be ionized by solvent protonated molecules, according to the proton transfer mechanism:



If the dopant ionization energy is higher than the analyte one, the charge from the radical cation will be transferred to the particle of the analyte molecule:



APPI allows for ionization of low or non-polar compounds. Hanold and collaborators examined atmospheric pressure photospray interfaced to LC and showed that APPI MS provides robust results in the bezno[α]pyrene detection, with strong $[M + H]^{+\cdot}$ signal at m/z 253, while in the case of ESI source analyte molecule was barely ionized.¹⁶⁷ An important group of compounds for which APPI gives very good results are polyaromatic hydrocarbons (PAH's), especially for the oxidized or nitrogenated forms.¹⁶⁸

1.6.2 Low- and high resolution mass spectrometry

Depending on the resolution power of the spectrometer, mass spectra can be recorded in a low or high resolution mode. Low resolution (LR) measurements have accuracy of the mass unit, while in the case of high resolution (HR) we measure an exact mass with the accuracy of approximately 1 mDa. The former type enables us to distinguish an ion of m/z 99 from an ion of m/z 100, while in the latter, we are able to determine the exact mass, and thus the chemical formula of a compound. To be able to record the HR spectrum, a mass spectrometer with a resolving power FWHM (Full Width at Half Maximum) of at least 10 000 is required. The most popular mass analyzers allowing high resolution measurements are Time-of-Flight -analyzer (ToF) from 10,000 FWHM for ToF with a single ion reflectron to 50,000 for a system containing two ion reflectrons. This type of analyzer provides high sensitivity, accuracy and fast scanning times. On the other hand, Orbitrap analyzers permit the measurements with a great resolution power (up to 300 000 FWHM) without loss of sensitivity.

1.6.3 Tandem mass spectrometry

Tandem mass spectrometry (MS/MS) refers to mass spectrometry with more than one mass analyzer. In routine use, however, tandem mass spectrometry is often confined to the application of the same analyzers, e.g., quadrupole, giving rise to a triple quadrupole (QqQ) system. The combination of different types of analyzers, e.g., quadrupole-ToF or quadrupole-Orbitrap leads to the *hybrid spectrometry*. The use of such a system allows for studying fragmentation processes, which in turn enable in-depth structural analysis of a compound. Narrowing further description to the QqQ analyzer, which was deployed in my research, the following sequence of events may take place:

- selection of an precursor ion in the first quadrupole
- fragmentation of selected ions in the second quadrupole, which serves as a collision chamber
- detection of the product ions in the third quadrupole.

Fragmentation processes can be enhanced by non-elastic collisions of ions with inert gasses, such as N₂, Ar or SF₆, which turn the kinetic energy of colliding species into

their internal energy ¹⁶⁹. This type of MS/MS scanning is called *collision-induced-dissociation (CID)*. In general, there are three ionic groups that leave the source after the ionization and depend on their stability and therefore duration of lifetimes. The first group are stable ions, which have lifetimes sufficiently long (10^{-6} s) to reach a detector without changes in their charge/structure; the second group encompasses a short-lifetime and unstable ions that leave the ion source in the form of fragments. However for the CID purposes are the third ionic group which covers the ions stable enough to reach a first analyzer and at the same time have an excess of energy allowing fragmentation to occur. The most useful scan modes for MS/MS experiments are summarized in Figure 1.9.

Tandem mass spectrometry has a wide range of applications for the characterization of atmospheric aerosol,⁵ ranging from the structural elucidation of unknown SOA component(s)^{36,91,102,170,171} to tracking reactions in the gas phase or studying the kinetics and thermodynamics of chemical reactions.¹⁶² A detailed analysis of fragmentation channels for selected SOA compounds often allows for distinguishing their isomeric forms, which arise from isobaric aerosol precursors, e.g., α -pinene and Δ^3 carene, and thus is used to study the SOA sources and formation mechanisms.^{110,116,153}

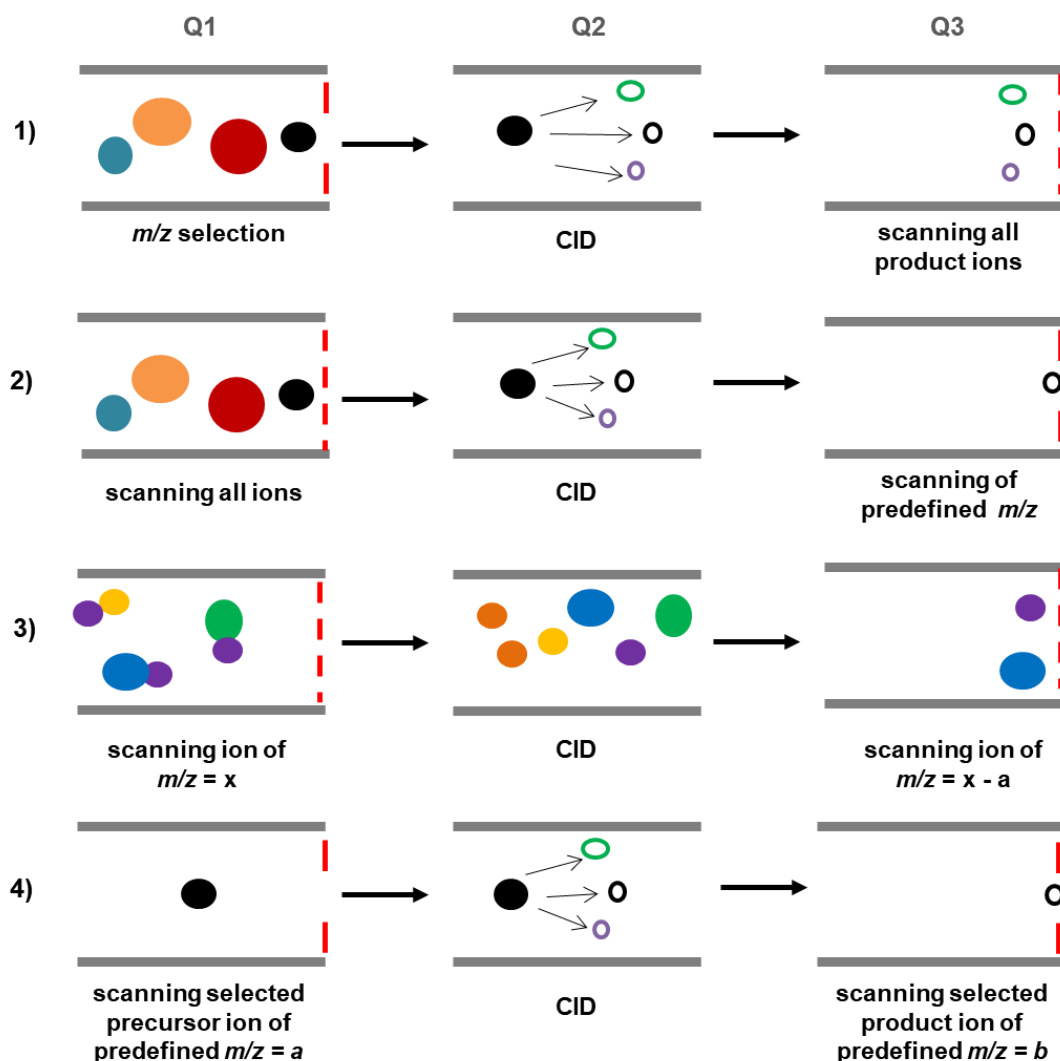


Figure 1.9 Schematic representation of key operation modes of tandem mass spectrometry: 1) product ion scan 2) precursor ion scan 3) neutral loss scan 4) selected reaction monitoring. CID – collision induced dissociation.

1.6.4 Separation techniques

In modern analytics, hyphenated methods are widely used in many scientific areas, including atmospheric chemistry. The identification of organic components of complex matrices, such as aerosol samples, with MS detection requires prior separation with gas- (gas chromatography, GC) or/and liquid chromatography (high performance chromatography, HPLC or ultra-high performance chromatography, UPLC). The literature survey from the last two decades clearly reveals that ESI-MS has been readily coupled with HPLC or UHPLC, while EI and/or CI-MS with GC.^{5,141} The selection of an appropriate column and operation conditions for the chromatographic separation allows

for isolation of a single compounds of interest from a complex SOA mixture composed of thousands of organic and/or inorganic components. When choosing the appropriate separation technique, and then the proper chromatographic column and separation conditions, one should take into account the physicochemical properties of the analyte such as: vapor pressure, boiling point, polarity and solubility in various solvents.

1.6.4.1 Gas chromatography technique

In chromatography, a substance analyzed is separated through its different affinity between the mobile and stationary phases. In case of the gas chromatography the mobile phase is a gas, most often helium or hydrogen, and the stationary phase consists of polysiloxanes or polyethylene glycols with various modifications. The properties of the GC columns differ in the degree of polarity of the filling, resistance to different pH range or stability of the package in a given temperature program. The samples analyzed by GC-MS can be in a gaseous state only. The sample may be introduced into the measurement in several different ways. The classical one is to inject a small volume of the sample dissolved in a volatile solvent. In the second one, the gaseous sample is taken from the solid or liquid supra-surface phase (i.e., headspace). The third way is solid phase microextraction (SPME) and its operation is based on the adsorption of volatile substances from the liquid or gas surface onto a thin polymeric adsorbent embedded onto a quartz fiber, such as polydimethylsiloxanes (PDMS) and its preconcentration. Both processes are governed by equilibria constants of the analyte between gas- and solid phases.¹⁷² Then this fiber is placed into the injector and volatile component(s) are desorbed. If the analyte shows too low volatility and/or high instability under the measurement conditions, the GC-MS analysis must be preceded with the derivatization . The most popular methods include sialylation (for alcohols, carboxylic acids, amines, thiols using i.e., bis-trimethylsilyl fluoroacetamide containing 1% trimethylchlorosilane in pyridine)¹⁷³, alkylation (i.e., carboxylic acids using diazomethane or trifluoro bromide in methanol)¹⁵⁴ or oximation (for carbonyl compounds with use of *O*-(2,3,4,5,6-pentafluorobenzyl)hydroxylamine hydrochloride).¹⁷⁴ GC-MS is the technique of choice in the analysis of alkanes, alkenes, aromatic compounds, benzene substituents, PAH's, as well as their oxygenated derivatives, and gives very good results in organic compounds

identification, especially when the separation is performed with use of multidimensional GC x GC-MS systems.¹⁷⁵

Despite its advantages, GC-MS as a separation technique suffers from several limitations. The major constraints concern the sample volatility, temperature degradation and the need to extract samples dissolved in water.

1.6.4.2 Liquid chromatography technique

For a long time, for the coupling of liquid chromatography with the mass spectrometer, a serious problem was the evaporation of the sample to introduce the ions in the gas phase into the spectrometer. When electrospray ion sources appeared in the market, HPLC-MS developed dynamically. Despite the higher cost than GC-MS systems, liquid chromatography gives a lot in return. First, it is possible to modify both the composition of the solid phase by selecting different column packages and their modification, as well as the properties of the mobile phase. The polarity of the latter can be altered and although the solvents used for HPLC-MS measurements are mostly polar, the content of the non-polar component of the mobile phase can reach even 70%. Depending on the selected column, measurements can be carried out in a wide pH range, selecting conditions appropriate to the analyte.

The chromatographic separation of the organic fraction of atmospheric aerosol is usually performed in a reversed-phase chromatographic system (RP) using C-18 nonpolar columns with a variety of chain modifications.^{157,176,177} However, in recent years, hydrophilic interaction liquid chromatography (HILIC) gained a lot of attention as it enables the separation of ionic compounds containing polar groups in their structures.^{116,117} In HILIC, a dedicated columns stationary phase is functionalized by polar material, i.e., amide or silica, while the mobile phase used consist of a low organic solvent content with buffered water/acetonitrile or water/methanol as a leading solvent. The combination of ion exchange, partitioning between the adsorbed aqueous layer together with interactions by hydrogen bonding permits the retention of a compound which, in the case of reverse-phase chromatography, elutes unretained. Undoubtedly, it is the greatest advantage of the HILIC chromatography. However, the capricious nature of this method, such as low stability and poor data reproducibility confines HILIC

applicability to the analysis of complex matrices. However, HILIC is to be taken as a complementary separation method to RP chromatography since together they allow the separation of highly polar compounds, such as SOA-bound organosulfates.¹¹⁶

1.6.4.3 Additional detectors in hyphenated LC-MS systems

The hyphenated HPLC/UHPLC-MS systems are often accompanied by additional detection method based on the light absorbing detectors:

(a) in the UV region, mostly in one or two selected wavelengths, according to the absorption range of analyzed compounds and

(b) a photodiode array (DAD) detector, which measures the absorption in a whole range of wavelengths in real time.

The light absorbing detectors are especially useful in analyses of aerosol samples enriched with components bearing strong chromophore residues, such as black carbon^{178,179}

The basic UHPLC-UV-MS/MS system used in my research is shown below (Fig. 1.10).

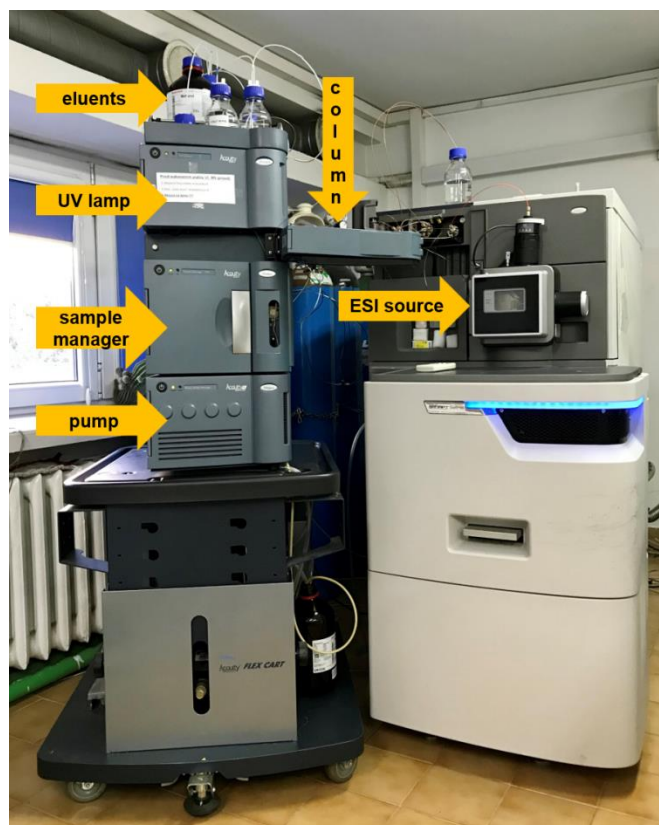


Figure 1.10 The Acquity Ultra High Performance Liquid Chromatograph coupled to a Synapt G2-S High Definition Mass Spectrometer (Waters) used in my aerosol research; Mass Spectrometry Group, Institute of Organic Chemistry Polish Academy of Science.

2 Aim of the study

The aim of this work was to identify and chemically characterize important markers of aerosol particles formed from *in-cloud* oxidation of isoprene (C_5H_8) and its first oxidation products and propose their possible formation routes.

To achieve these goals the electrospray mass spectrometry interfaced to ultra-high performance liquid chromatography (UHPLC-ESI-MS) technique was used along with the organic synthesis, isotope labeling experiments and quantum calculations.

The task was carried out in several intermediate stages:

- (1) application of UHPLC-ESI-MS technique for the structural elucidation of novel chemical components of atmospheric particulate matter – monoalkyl esters of sulfuric(VI) acids, referred to as organosulfates (OSs), in ambient aerosol samples
- (2) application of UHPLC-ESI-MS technique for detection of organosulfates in laboratory generated samples via multiple aqueous-phase reactions of isoprene (C_5H_8) as well as their oxygenates, i.e., methyl vinyl ketone and methacrolein (α , β -unsaturated carbonyls; C_4H_6O) in the presence of sulfate anion radicals or sulfate radicals
- (3) detailed interpretation of high-resolution negative ion electrospray ionization tandem mass spectra (-) ESI MS/MS
- (4) raising hypotheses on likely formation mechanisms of selected SOA-bound organosulfates

3 Experimental Section

3.1 Chemicals

Ultra-pure water ($18.2 \text{ M}\Omega\cdot\text{cm}^{-1}$ resistivity at $25 \text{ }^\circ\text{C}$) obtained from Milli-Q Advantage water purification system (Merck, Darmstadt, Germany) was used to perform all of the experiments in the aqueous phase, reconstitution of filter extracts and mobile phases preparation used in chromatographic separations. Methanol (HPLC grade) used for sample preparation and LC analyzes was purchased from Sigma-Aldrich (St. Louis, MO 63103, USA). As a phase modifier ammonium acetate (HPLC grade, Scharlab S.L., Spain) was used in all performed experiments.

All of the following chemicals were used in the experiments without prior purification: isoprene (Merck), sodium metabisulfite, $\text{Na}_2\text{S}_2\text{O}_5$ (pure, POCH, Gliwice, Poland), sodium sulfite anhydrous, Na_2SO_3 (analysis grade, Merck), 3-methyl-2(5*H*)-furanone and 4-methyl-2(5*H*)-furanone (TCI Europe, Zwijndrecht, Belgium), manganese (II) sulfate (VI) monohydrate ($\text{MnSO}_4 \times \text{H}_2\text{O}$; analysis grade, Sigma-Aldrich), potassium persulfate, $\text{K}_2\text{S}_2\text{O}_8$ (pure, POCH, Poland), methyl vinyl ketone (99 %; Sigma Aldrich), methacrolein (95%; Sigma Aldrich).

Additionally, isotopically-labeled $^{18}\text{O}_2$ (99%, Sigma Aldrich) was used in aqueous-phase isoprene SOA formation experiments to get insights into the mechanistic pictures.

3.2 PM_{2.5} fine ambient aerosol samples

The work flow from the ambient sample collection, through the sample preparation and analysis is shown in Figure 3.1. The detailed information is provided in followed up sections.

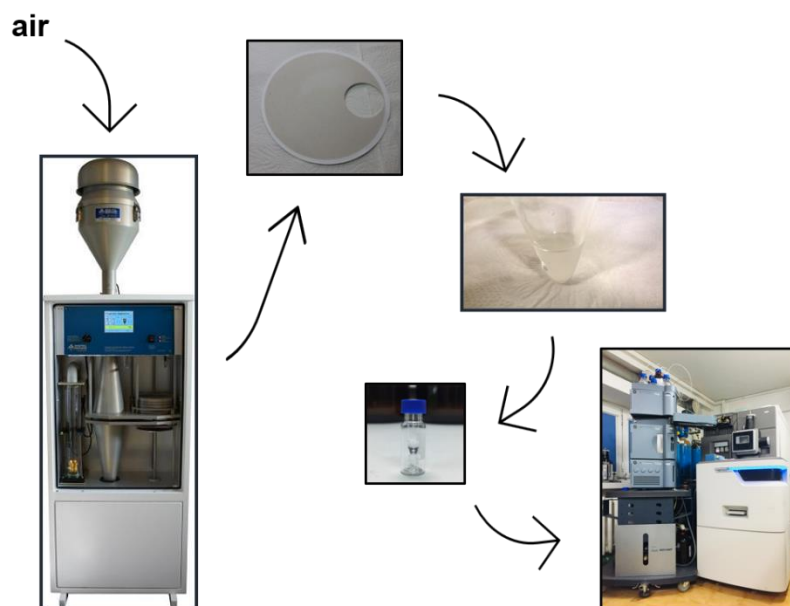


Figure 3.1 Schematic representation of the ambient fine aerosol sample preparation for UHPLC-MS/MS analysis.

3.2.1 Filed sites

Ambient $PM_{2.5}$ secondary organic aerosol samples used in my research originated both from the MARKER field campaigns carried out in Diabla Gora, Poland or were partially transferred as part of a scientific cooperation with Prof. Magda Claeys from the University of Antwerp and Prof. Willy Meenhout from the Ghent University (*K-puszt*a aerosol samples, Hungary) and Prof. Jason D. Surrat from the University of North Carolina at Chapel Hill (Centreville aerosol samples, AL, United States of America).

The first location is in *K-puszt*a, Hungary (46°58'N, 19°35'E). This is a rural site located on the Great Hungarian Plain, 80 km southeast of Budapest (Figure 3.2).



Figure 3.2 Ambient aerosol sampling site in K-pusztá, Hungary. *Picture of the station building was uploaded from <https://projects.nilu.no> web site.*

Samples were collected using a dichotomous sampler on pre-baked quartz-fiber filters purchased from Pall Corporation, Port Washington, NY, USA) The samples were stored in a freezer at $-25\text{ }^{\circ}\text{C}$. Samples were collected during the BIOSOL (Formation mechanisms, marker compounds, and source apportionment for biogenic atmospheric aerosols) campaign (22.05. - 29.06.2006 r).¹⁸⁰ In my research archived pooled $\text{PM}_{2.5}$ samples were deployed, which were gained through a close scientific collaboration Belgian partners (Prof. Magda Claeys and Prof. Willy Meenhaut).

The second location is a rural site in Centreville, AL, in the United States of America ($32^{\circ} 19' \text{ N}$, $86^{\circ} 54' \text{ W}$), 85 km south-southwest of Birmingham, AL, and 50 km south of Tuscaloosa, AL (Figure 3.3).

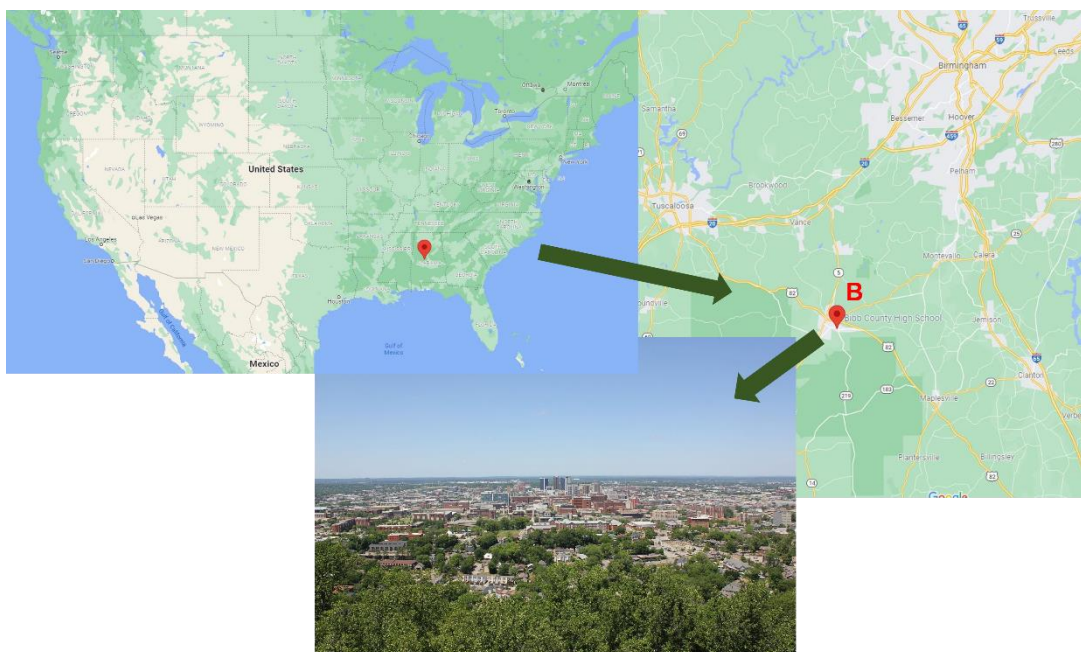


Figure 3.3 The Centreville sampling site in Alabama, USA. *Picture of Centreville panorama was uploaded from <https://datausa.io> web site.*

The samples analyzed in the study were collected during daytime on June 8, during the 2013 SOAS (Southern Oxidant and Aerosol Study) campaign. PM_{2.5} aerosol samples were collected using an air high-volume sampler (Tisch Environmental, air flow at 1 m³ min⁻¹) onto prebaked quartz-fiber filters with a diameter of 8 × 10 in (Tissquartz Filters, Pall Life Sciences). Filters were stored at - 20 °C and used for my study through the cooperation with Prof. Jason D. Surratt.

The third PM_{2.5} ambient aerosol sampling location, Diabla Gora, Poland (Figure 3.4), is a rural site in the Borecka forest of the Masuria Province (54°07'29.52"N; 22°02'17.08"E).



Figure 3.4 Puszca Borecka sampling site at Diabla Gora, Masuria Province, Poland. *Picture of the station building comes from private sources.*

This site is surrounded by lakes and mixed forest with a broad-leaf tree prevalence, being an important source for isoprene emissions. Moreover, the air in the region is considered as the least polluted in Poland, according to the continuous measurements of particulate matter concentrations performed in “*Puszca Borecka*” reference station for measuring clean air masses and monitoring air pollution. $PM_{2.5}$ samples were collected during the summer campaign in 2014 (26-31.07) in a 24h regime using a high-volume sampler (Digitel DHA-80, Switzerland) onto prebaked quartz-fiber filters (500 °C for 24h). After collection filters with aerosol loads were stored at - 20 °C in a laboratory deep freezer.

3.2.2 Sample preparation

3.2.2.1 Fine ambient $PM_{2.5}$ aerosol used as a reference material in structural characterization of MW 212 OSs originating from isoprene

From each quartz-fiber filter, two 1 cm² punches were taken and extracted 3 times for 15 min. with 10 mL of methanol using an ultrasonic bath. Extracts were combined and concentrated to *ca.* 1 mL under reduced pressure at 35 °C, using a rotary evaporator (Büchi Labortechnik AG), and filtered through a Teflon filter (0.2 µm). Prepared extracts were then evaporated to dryness under a gentle stream of nitrogen and reconstituted with 300 µL methanol/water (1:1 *v/v*) short before UHPLC/(-)ESI-MS analysis.

3.2.2.2 Fine ambient PM_{2.5} aerosol used as a reference material in radical oxidation of isoprene in the presence of ¹⁶O₂ and its ¹⁸O₂ isotopes

The procedure was the same as described above (subsection. 3.2.2.1).

3.2.2.3 Ambient PM_{2.5} aerosol sample during LC-MS method optimization

From two quartz-fiber filters after 24h exposure, 1 cm² punches were taken and extracted 3 times with 10 mL of methanol. Process was conducted using an Orbital shaker (Biosan, Poland). Combined and concentrated to *ca.* 1 mL (rotary evaporator, Büchi; 35 °C, reduced pressure) extracts were filtered through a 0.2 µm Teflon filter and evaporated to dryness under a gentle stream of nitrogen. Reconstitution with the use of 140 µL of methanol/water (1:1; v/v) was performed before UHPLC/(-)ESI-MS analysis. During the verification of the influence of the sample solvent on the chromatographic separation, the samples were reconstituted in pure water and/or pure methanol.

3.2.2.4 Fine ambient PM_{2.5} aerosol used as a reference material in radical oxidation of methyl vinyl ketone and methacrolein

From two quartz-fiber filters after 24h exposure, 1 cm² punches were taken and extracted 3 times with 10 mL of methanol. Process was conducted using an Orbital shaker (Biosan, Poland). Combined and concentrated to *ca.* 1 mL (rotary evaporator, Büchi; 35 °C, reduced pressure) extracts were filtered through a 0.2 µm Teflon filter and evaporated to dryness under a gentle stream of nitrogen. Reconstitution with the use of 140 µL of methanol/water (1:1; v/v) was performed before UHPLC/(-)ESI-MS analysis.

3.3 Samples of atmospheric waters

3.3.1 Field description and sample collection

Samples of rain, snow and hail were collected spontaneously, depending on the rainfall/snowfall/hailstorm episodes, respectively in severe locations (Scheme 3.5), in sterile polypropylene containers. The rain samples come from locations in Woziowda (53°40'N, 17°54'E) and Warsaw, capital city of Poland (52°13'47''N, 21°00'42''E). Woziowda is located in Bory Tucholskie, a densely forested area with a predominance of pine forest (mainly, Scots pines). Rain samples were collected during a downpour in summer. Warsaw represents the urban area and the rain samples from this location were

collected during the autumn rainfall. Warsaw was also a place where samples of hailstone during a storm in September 2016 and samples of fresh snow in February 2017 were collected. The last sample – a graupel collected in March 2017, comes from Skawina (49°58′30″N, 19°49′43″E), a city located near Krakow.

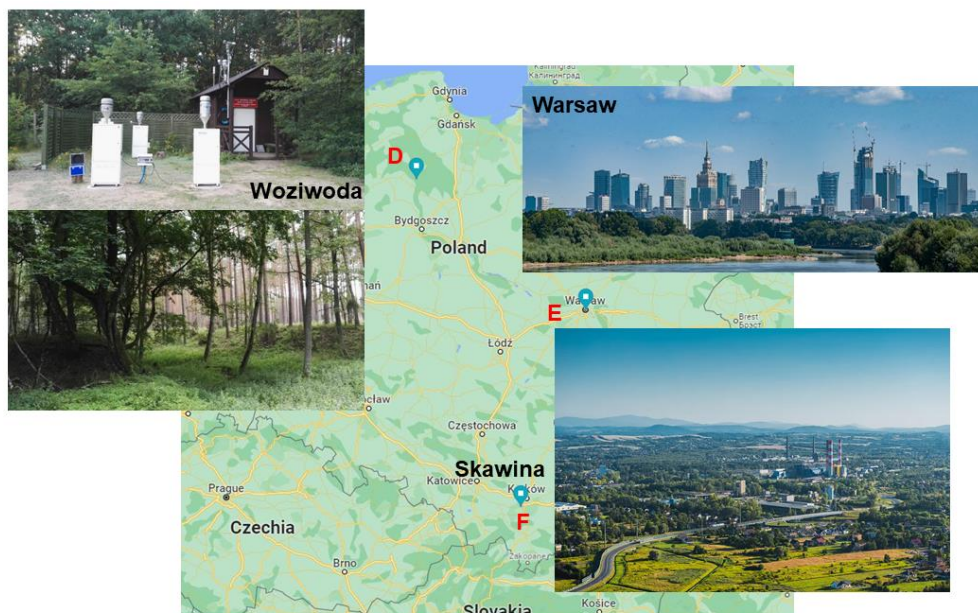


Figure 3.5 Location of sampling sites where atmospheric precipitates were collected. D) Woziwoda, Bory Tucholskie, *picture comes from private sources*; E) Warsaw, capital city of Poland, *picture: Panorama Warszawy z mostu Siekierkowskiego, 2020, author: Qbolewicz*, F) Skawina, a city in a close vicinity to Cracow, *pictures' author Norber Rzepisko*.

3.3.2 Atmospheric waters sample preparation

3.3.2.1 Rain sample

The raw rain samples after filtration through a 0.2 μm Teflon syringe filter were concentrated under the gentle stream of nitrogen (from ca. 2 mL to approx. 100 μL). As such, the sample was transferred to micro vials for further analysis.

3.3.2.2 Snow samples

After melting in a room temperature, the aqueous phase was subjected to the procedure described in the subsection 3.3.2.1.

3.3.2.3 Hail samples

To avoid contamination of the sample with the adsorbed organic and inorganic matter on the external layers of hail, grains outer layers were washed with ultrapure water and only the core (approx. 2 mm thick) was taken for further analysis. After melting, the samples were processed as stated in the subsection 3.3.2.1.

3.4 Smog-chamber isoprene SOA

3.4.1 Experiment process

Isoprene-derived SOA was generated through the photo-oxidation of 5 ppmv isoprene (Sigma-Aldrich, 99%) in the presence of $100 \mu\text{g m}^{-3}$ of acidified sulfate seed aerosols and 200 ppbv nitric oxide (NO, Airgas, 1% NO/N₂), under natural solar radiation. Experiments were conducted in an outdoor Teflon film chamber “One Atmosphere” (capacity of *ca.* 120 m³), located on the roof of the Gillings School of Global Public Health at the University of North Carolina at Chapel Hill.



Figure 3.6 The Outdoor Smog Chamber on the roof of the UNC Gillings School of Global Public Health, Chapel Hill, NC. Picture uploaded by Kenneth G. Sexton¹⁸¹ on ResearchGate.

The use of an outdoor smog chamber allows to carry out reactions that may take place in the atmosphere under natural sun irradiation, in a significantly simplified reaction environment. The "One Atmosphere" chamber (Figure 3.6) has been designed in such a way that it is possible to study both reactions taking place in the gas- and aerosol phase.

Under the surface of the chamber are research laboratories, where it is possible to directly analyze all the resulting constituents. A demonstration graphic showing the structure of the entire system can be found below (Figure 3.7).

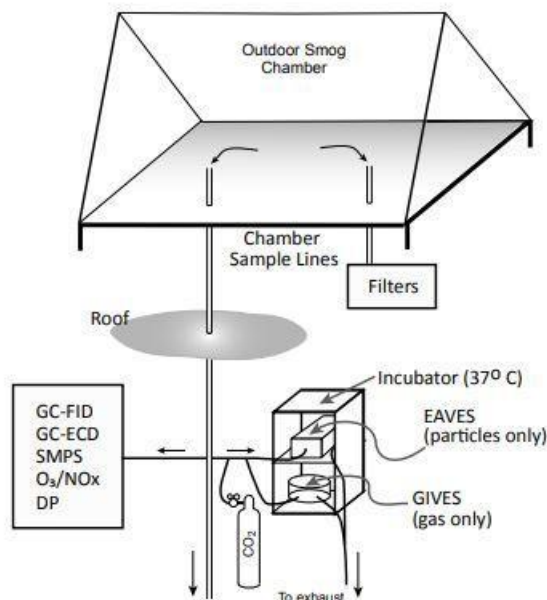


Figure 3.7 Schematic representation of One Atmosphere smog chamber, UNC Gillings School of Global Public Health, Chapel Hill, NC.¹⁸²

Experiments with isoprene-derived SOA were conducted during two days in 2014 (August 27 and September 30). Acidified sulfate seed aerosols were atomized into the chamber with a constant output atomizer (TSI, model 3076) with solution containing 0.06 M magnesium sulfate (VI) and 0.06 M sulfuric (VI) acid. At the concentration of aerosol seeds approx. $\sim 100 \mu\text{g m}^{-3}$, measured using a differential mobility analyzer (DMA, BMI model 2002) coupled to a mixing condensation particle counter (MCPC; BMI model 1710), NO and isoprene were injected into the chamber, to initiate OH radical-driven oxidation. The relative humidity was set between 50 and 60% during all experiments (measured with a dew point meter; Dew Prime I, EdgeTech, Marlborough, MA). Consumption of NO was controlled with the NO_x analyzer (ML9841 Series, American Ecotech, Warren, RI). As the concentration of NO decreased, the aerosol volume concentrations began to increase due to the formation of SOA from the isoprene oxidation.

The aerosol was collected onto three Teflon membrane filters (47 mm diameter, 1.0 μm pore size; Pall Life Science), at the concentration of $\sim 35 \mu\text{g m}^{-3}$, at a flow rate of 16–18 L min^{-1} for 1 h.

3.4.2 Sample preparation

The extraction proceeded as it was described earlier (subsection 3.3.1.3.), except for the amount of filter taken - in the case of the Teflon filter, the entire filter surface was used for extraction.

3.5 Aqueous-phase reactions with auto-oxidation of S(IV) catalyzed by manganese (II) ions – MW 212 organosulfates characteristic

Several experiments (subsections 3.5.1., 3.5.2., 3.5.3.) were carried out to determine the tentative structure(s) and the likely mechanism formation of the atmospherically-relevant organosulfates with MW 212 from isoprene, coupled with auto-oxidation of S(IV)-catalyzed by Mn(II) ions. The method was adapted from earlier studies.^{183,184}

3.5.1 Homogenous oxidative degradation of isoprene, 3-methyl and 4-methyl-2(5H)-furanones

The oxidation reactions were conducted following the same protocol for each of the organic precursors – isoprene, 3-methyl- and 4-methyl-2(5H)-furanones. Precursors stock solutions were prepared using MilliQ ultra-pure water. In order to prepare a stock solution of isoprene, the flask was calibrated each time before the experiment, considering the upper meniscus (total volume approx. 125 mL). Isoprene was injected directly into the flask filled with water and then placed in an ultrasonic bath for 10 mins. For 3-methyl- and 4-methyl-2(5H)-furanones, there was no need to use ultrasounds to prepare homogeneous aqueous solutions.

Reactions were carried out homogeneously in a well-stirred glass reactor closed with a Teflon cover, with a capacity of 0.25 L. Aqueous solution contained dissolved oxygen (2.5×10^{-5} M), Mn (II) ions (9.7×10^{-6} M $\text{MnSO}_4 \times \text{H}_2\text{O}$), and depending on the experiment an organic precursor with concentration: isoprene (9.6×10^{-5} M); 3-methyl- or 4-methyl-2(5H)furanone (1.3×10^{-4} M). The oxidation process was started by injecting into the glass reactor aqueous stock solution containing sodium sulfite

Na₂SO₃ and sodium metabisulfite Na₂S₂O₅, each prepared in a separate volumetric flask with an initial concentration of S(IV) ions in the reactor 7.8×10^{-4} M. The initial reactions were carried out at 25 °C, and their products were sampled for LC-MS analysis for 60 minutes.

3.5.2 Heterogenous oxidative degradation of isoprene in the presence of atmospheric air

The reaction was conducted in a glass reactor (volume 0.12 L) closed with a Teflon cover, in which oxygen electrode and balloon filled with atmospheric air were placed. The initial oxygen concentration in pure aqueous phase was 7.56 ppm. After opening the valve supplying air to the reactor and saturating the gas phase, the oxygen concentration in the aqueous phase increased to 16.59 ppm. The concentrations of the added reagents were as follow: Mn (II) ions (9.27×10^{-6} M MnSO₄ × H₂O), isoprene (1.66×10^{-4} M) and S(IV) ions 2.09×10^{-3} M). The progress of the reaction was monitored spectrophotometrically with high-resolution UV-vis spectrophotometer Jasco V-570 UV/VIS/NIR spectrophotometer, over the wavelength range of 200–300 nm.

For LC-MS analysis samples were taken directly from the reaction environment after 25, 60 and 90 min.

3.5.3 Heterogenous oxidative degradation of isoprene in the presence of isotopically-labeled oxygen ¹⁸O₂

The reaction was carried out analogously to the reaction described above (subsection 3.5.2.). Before proceeding the experiment, all the vessels used to prepare the solutions were deoxygenated under a stream of argon. The ultra-pure water used in the reaction and to prepare stock solutions was deoxygenated by bubbling argon through it. Stock solutions were made in the same way as discussed in subsection 3.5.2. The reaction system was equipped with an ¹⁸O₂ oxygen isotope-filled balloon. Samples for LC-MS analyzes were taken from the reaction medium after 4, 16, 30, 73 and 120 min.

3.6 Radical oxidation of methyl-vinyl ketone and methacrolein

In order to determine the products of radical reactions that may take place under atmospheric conditions, a series of experiments was carried out with the participation of two main products of isoprene oxidation - methacrolein and methyl vinyl ketone. The mentioned C₄-precursors were subjected to radical reactions in the aqueous phase in the presence of K₂S₂O₈, in which the homolytic cleavage was induced by natural UV-vis radiation. Concentrations of used chemicals were as follows: of MAC and MVK 0.19 mmol L⁻¹; inorganic potassium persulfate (K₂S₂O₈), 0.16 mmol L⁻¹. Reactions were proceeded under the sun irradiation in quartz cuvettes with volume of 1 mL. The sun exposition time was 200 min. during a summer day in May 2016. During the experiment a decay of organic reactant, the ambient air temperature, and the light intensity were controlled every 30 min. The temperature of ambient air measured at the site of the reaction ranged from 298 to 303 K, and the sunlight intensity measured with an ILT 1400A radiometer (International Light Technologies) varied from 26.8 to 33.1 mWcm². UV-vis spectra were recorded with a Jasco V-570 spectrophotometer within the range of 200-300 nm (band width 0.1 nm, data pitch: 0.5 nm, scanning speed: 400 nm min⁻¹). Milli-Q ultra-pure water served as a baseline reference. The reference spectra for MAC and MVK were acquired with the same concentration levels, i.e., 0.19 mmol L⁻¹, and measurement parameters as stated above. As reference samples, experiments without access to sunlight (dark experiments) were performed, following the same procedures as those for the sun exposed. All the stock solutions were prepared freshly before each experiment and stored wrapped in aluminum foil. The UV-vis and negative ion electrospray mass spectra of aliquots were recorded immediately after sampling. Samples used for the LC-MS analyses were diluted with methanol (1:1; v/v).

4 Methods

4.1 General remarks

The main analytical method used during my research was mass spectrometry coupled with liquid chromatography. Chromatographic separations were performed with an UHPLC ACQUITY UPLC I-Class chromatograph (Waters). Exact mass measurements and fragmentation experiments were performed with a high-resolution Maldi Synapt G2-S HDMS mass spectrometer (Waters, Milford, MA, USA), equipped with an electrospray ion source, and a q-TOF analyzer. The instrument worked in the negative ion mode in the sensitivity mode with the resolving power of the TOF analyzer 20 000 FWHM. An external calibration on sodium formate was used with a lock spray correction on the leucine-enkephalin spectrum that was generated by the lock spray source. The exact mass measurements for all peaks were performed within 3 mDa mass error. Instrument operation and data analysis were performed using the MassLynx 4.1 software package. During numerous analyzes of organosulfates in various natural samples, an important stage of the work was the optimization of the sample preparation process, the conditions of the chromatographic separation and the parameters of the mass spectrometer.

4.1.1 Chromatographic separation

Two chromatographic modes were employed: reversed-phase with C-18 column and HILIC method. In the RP-C₁₈ chromatography an Acquity HSS T3 1.8 μm column (2.1 x 100 mm; Waters) was used in gradient elution starting with 100% phase A (10 mM ammonium acetate) for first 1.7 min, with flow rate 0.35 mL/min. Next, gradient changed to phase B (methanol) with a flow rate 0.25 mL/min, reaching 100% in 4.7 min. and remained constant for 1 min. Column temperature during the analysis was set to 40 °C.

For HILIC chromatography, the Acquity BEH Amide 1.7 μm column (2.1 x 100 mm) (Waters) was used with the gradient elution with a flow rate 0.5 mL/min. Elution program was as follows: 100% of phase B (acetonitrile: water 95:5 (v/v) with 10 mmol ammonium acetate adjusted to pH 9 using NH₃ solution) for the first 3 mins, during next 3 mins switch to 40% of phase A (water with 10 mmol ammonium acetate adjusted to pH

9 using NH₃ solution) and kept for 1 min. For the last 5 mins 100% of phase B was set. Column temperature was set to 45 °C.

4.1.2 Operational parameters for the mass spectrometer

For the full scan experiments 0.1 s scan time was set, and for the MS/MS experiments 0.2 s. The optimized source parameters were as follows: capillary voltage –0.3 kV, cone voltage –15 V, desolvation gas flow 800 L/h with the temperature 350 °C, nebulizer gas pressure 5.5 bar, source temperature 120 °C. All presented MS/MS experiments data was recorded using collision energy 20 eV. The EIC window was ±0.0015.

4.2 Homogenous oxidative degradation of isoprene, 3-methyl and 4-methyl-2(5H)-furanones

4.2.1 Chromatography

Chromatography was performed using an ACQUITY UPLC HSS T3 column (1.8 µm, 2.1 × 100 mm; Waters). The mobile phases applied consisted of 20 mM ammonium acetate (A) and methanol (B). The gradient elution program was as follows: the concentration of eluent A was kept at 100% for the first 3 min with the flow rate of 0.35 mL min⁻¹. During the next 5 min, eluent B was increased to 100% with a flow rate of 0.25 mL min⁻¹ and kept at this level for 2 min. For the last 3 min, eluent B was decreased to 0% at a flow rate of 0.35 mL min⁻¹. The data processing and the instrument control were done using a MassLynx V4.1 software package (Waters).

4.2.2 Operational parameters for the mass spectrometer

The measurements were carried out in the negative ion mode with a sampling cone voltage of 20 V, a capillary voltage of 3 kV and a mass resolving power of 20 000. The exact mass measurements for all peaks were recorded within 3 mDa mass error. The full scan and MS/MS with collision-induced dissociation (CID) experiments were conducted with a scan time of 0.1 and 0.5 s, respectively. MS/MS CID spectra were recorded at collision energies 15, 20, or 25 eV, with argon as a collision gas.

4.3 Heterogenous oxidative degradation of isoprene in the presence of atmospheric air and ¹⁸O₂ isotope

4.3.1 Chromatography

Chromatographic conditions were analogous to 4.2.1.

4.3.2 Operational parameters for the mass spectrometer

Chromatographic conditions were analogous to 4.2.2.

4.4 Radical oxidation of methyl-vinyl ketone and methacrolein

4.4.1 Chromatography

Chromatographic separation was performed with RP-C₁₈ ACQUITY UPLC HSS T3 column (1.8 μm, 2.1 x 100 mm). The applied mobile phases consisted of (A) 20 mmol ammonium acetate and (B) methanol. The gradient elution program was as follows: 0-3 min. A was kept at 100%, during the next 5 min eluent B was increased to 100% and was kept at this level for 2 mins, then for the last 3 mins of analysis eluent B was decreased to 0%. A flow rate through the whole chromatographic process was 0.35 mL/min.

4.4.2 Operational parameters for the mass spectrometer

The measurements were carried out in the negative ion mode with a sampling cone voltage of 20 V, a capillary voltage of 3 kV and a FWHM mass resolving power of 20 000.

4.5 Analysis of organosulfates in atmospheric waters

4.5.1 Chromatography

The analysis of water precipitates were performed with ACQUITY UPLC HSS T3 column (1.8 μm, 2.1 x 100 mm, Waters), thermostated at 40 °C. Mobile phases consisted of (A) 10 mM ammonium acetate in water and (B) methanol. The gradient elution program started with 100% of phase A, with a flow rate at a 0.35 mL/min. After 2.3 min. gradient started to change linearly to 100% of phase B with the flow rate at 0.25 mL/min for 4.7 min. 100% B was kept for 1 minute and after this time decreased to 0%.

4.5.2 Operational parameters for the mass spectrometer

Experiments were carried out in negative ion mode with the sensitivity mode. A mass resolving power of a TOF analyzer was 20 000 FWHM.

5 Results and Discussion

General note

The following section discusses the research findings on the identification and/or chemical characterization of organosulfates related to secondary organic aerosols (SOA) conducted in 2014-2017 as part of my doctoral studies.

5.1 Structural characterization of isoprene-derived organosulfates with the MW 212 in PM_{2.5} ambient fine aerosol

The chapter describes my thorough research study on the chemical profile of polar organic sulfates (OSs) in fine aerosol particles collected from the suburban forested sites. The OSs with the molecular weight (MW) of 212 Da are formed during the isoprene reactive uptake by the atmospheric aqueous environment and cascade chain reactions with sulfate radical-anions. The study aimed to provide more structural evidence for the hypothesized lactone-containing structures of the MW 212 OSs from isoprene oxidation. The polar OS MW 212, which has an elemental composition of C₅H₈SO₇, is commonly found in ambient fine aerosol (PM_{2.5}) collected from various forested places.^{34,186,187} These species may be formed during the isoprene uptake by the atmospheric droplets and subsequent chain reactions with sulfate radicals on their surfaces. While previous studies have described OSs with the MW 212, their chemical entities and biogenic precursor (i.e. isoprene) have not been fully understood and proved. The research described below aims to firmly confirm structural assignment for the proposed MW 212 organosulfates.

To chemically characterize the MW 212 OS from the isoprene oxidation, I conducted a series of laboratory aqueous-phase experiments with isoprene, as well as smog chamber experiments. The latter were performed in collaboration with Gilling's School of Global Public Health at the University of North Carolina at Chapel Hill, the U.S. (group of Prof. Jason D. Surratt) using the "*One Atmosphere*" smog chamber facility located on the roof. For the chemical analyses, the liquid chromatography coupled to the negative ion electrospray high resolution mass spectrometry [LC/(-)ESI-HRMS] with

both a reversed-phase LC column (with a trifunctionally bound C-18 stationary phase was used to maintain polarity) and HILIC chromatography at a later stage of my research. The high-resolution mass spectrometry was used to determine the elemental composition for diagnostic ions, while tandem mass spectrometry (MS/MS) was deployed to retrieve a bunch of information on the presence of functional residue(s) and their likely position(s) in target structure(s). The proposed lactone-containing structures were supported by aqueous-phase synthesis of target compound(s) from 3-methyl-2(5H)-furanone and 4-methyl-2(5H)-furanone and reaction with the sulfate radicals.

Figure 5.1 displays selected LC/ESI-HRMS chromatographic data, specifically extracted ion chromatograms for m/z 211 (EIC), for ambient $PM_{2.5}$ samples collected from various locations affected by isoprene emissions. These samples were taken from either a laboratory or a smog chamber, and from SOA mimetics in the aqueous phase resulting from the reaction of a solution of isoprene, 3-methyl-2(5H)-furanone, and 4-methyl-2(5H)-furanone with sulfate radicals. The chromatographic data clearly shows that four main compounds (m/z 211) eluting between 1.05 and 1.57 min., detected in ambient $PM_{2.5}$ samples, were also generated from isoprene *via* aqueous chemistry involving sulfate radicals. It is evident that the ratios between four peaks differ. The relative peak abundances at RT 1.05 minutes (Fig. 5.1 A) and RT 1.08 min. (Fig. 5.1 B), as well as at RT 1.53 min. (Fig. 5.1 A) and RT 1.57 min. (Fig. 5.1 B), were higher in ambient $PM_{2.5}$ samples than in the aqueous phase SOA isoprene sample (RT 1.03 min. and RT 1.51 min., Fig. 5.1 E). In the case of a peak eluting at RT 1.43 min. I could observe the broadening of this peak in samples from ambient fine $PM_{2.5}$ aerosol and aqueous phase mimics of isoprene SOA (Fig. 5.1 A, B, C and E), but in the sample of smog chamber-generated isoprene SOA I could clearly note its splitting at the top (Fig. 5.1 D). The improved chromatographic separation used in further stages of my research revealed that the peak at RT 1.43 min. was split into two peaks. The ratios between the different isomers of m/z 211 clearly differ from those observed in the ambient samples of the $PM_{2.5}$ isoprene and SOA aqueous phase mimetics. The first eluting isomer (Fig. 5.1D) in smog chamber-generated isoprene SOA (RT 1.06 min) is the major one, as in aqueous phase mimics of isoprene SOA (Fig. 5.1 E) formation route for this isomer is not preferable, which in both cases contrast with the ratios in fine ambient $PM_{2.5}$ aerosol samples.

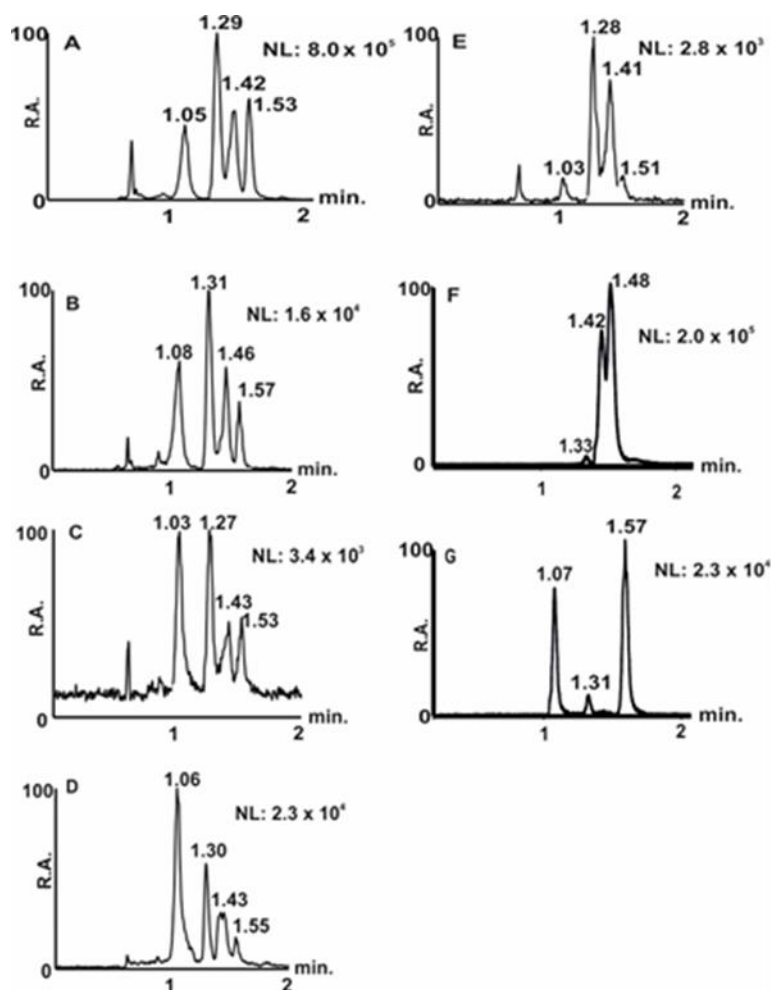


Figure 5.1 LC/ESI-HRMS extracted ion chromatograms recorded at the m/z 211 channel for the following aerosol extracts and synthesized standards samples I: (A) K -puszta $PM_{2.5}$, (B) Diabla Gora $PM_{2.5}$, (C) Centreville $PM_{2.5}$, (D) smog chamber-generated isoprene SOA, (E) aqueous-phase mimics of isoprene SOA, (F) aqueous-phase mimics of 3-methyl-2(5H)-furanone SOA, and (G) aqueous-phase mimics of 4-methyl-2(5H)-furanone SOA. Chromatographic separation was performed using C-18 chromatography (Aquity HSS T3 1.8 μ m column; 2.1 x 100 mm; Waters).

The relative abundances of the m/z 211 target compounds in selected samples of ambient $PM_{2.5}$ are comparable to these of one of the most common SOA isoprene markers, 2-methyltetrol sulfates, which are formed from C_5 -epoxydiols by particle-phase sulfation. Table 5-I shows the ratios between the sum of the m/z 211 peak areas and that of the m/z 215 2-methyltetrol sulfates.

Table 5-I The comparison of the main peaks areas for m/z 211 present in the ambient fine aerosol samples (K-pusztta, Hungary; Diabla Gora, Poland; Centreville, USA), aqueous-phase isoprene SOA, and smog-chamber isoprene SOA, and ratios between the sum of the m/z 211 peak areas versus that of the m/z 215 2-methyltetrol sulfates. The data are based on the chromatographic separation on a C-18 column (Acquity HSS T3 1.8 μm column; 2.1 x 100 mm; Waters).

Sample type	Peak no.	Retention time (min)	Peak area (%) ^a	$\Sigma(m/z$ 211)/ $\Sigma(m/z$ 215) ^b
K-pusztta PM _{2.5}	1	1,05	18,34	1,3
	2	1,29	37,06	
	3	1,40	24,27	
	4	1,52	20,33	
Diabla Gora PM ₁₀	1	1,07	28,25	0,47
	2	1,32	37,67	
	3	1,46	22,95	
	4	1,57	11,13	
Centreville PM _{2.5}	1	1,03	37,68	0,19
	2	1,27	3,18	
	3	1,42	17,19	
	4	1,53	13,35	
Aqueous-phase isoprene SOA	1	1,03	4,81	3,70
	2	1,27	49,24	
	3 ^c	1,41	45,95	
Smog chamber isoprene SOA	1	1,05	47,21	0,05
	2	1,30	23,47	
	3	1,45	23,59	
	4	1,55	5,74	

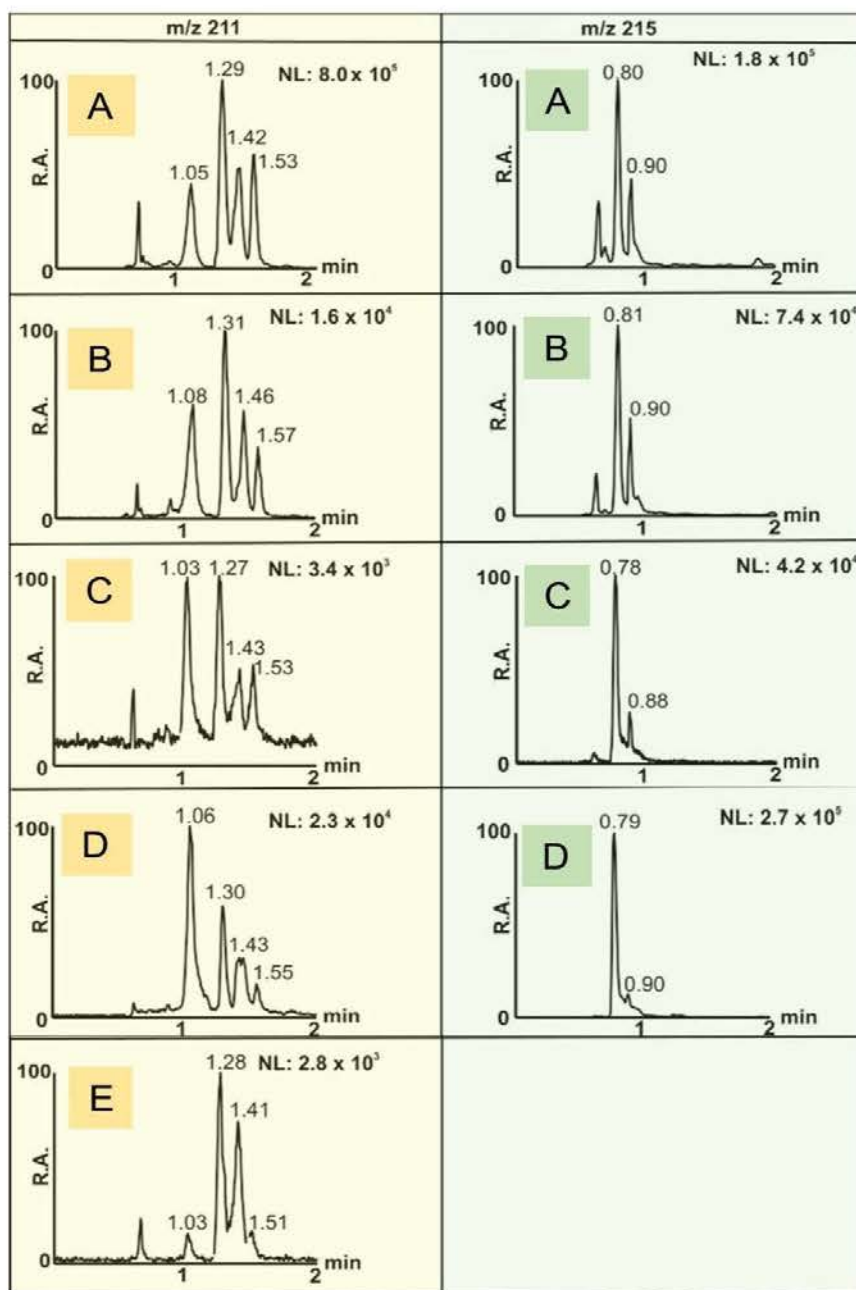
^a the relative composition in percentage of the total peak areas in the m/z 211 extracted ion chromatograms (EICs)

^b the ratios were determined from the m/z 211 and m/z 215 EICs (Table 5-II)

^c Peaks 3rd and 4th were integrated together due to the low peak resolution

The results obtained for the isoprene SOA smog chamber samples confirm that the relative abundances of the m/z 211 compounds, which elute between 1 and 1.6 min., are lower than these of the m/z 215 compounds. The result suggests that the formation of a target m/z 211 organic SOA species is of a secondary route under smog chamber conditions (Table 5-II).

Table 5-II The comparison of the main peaks areas for m/z 211 determined for the three ambient fine aerosol samples: (A) *K*-puszta, Hungary; (B) Diabla Gora, Poland; (C) Centreville, the U.S., and for the mimicking experiment samples: (D) aqueous-phase isoprene SOA and (E) smog-chamber isoprene SOA, and ratios between the sum of the m/z 211 peak areas versus that of the m/z 215 2-methyltetrol sulfates. The chromatographic separation was performed with use of the C-18 stationary phase column (Acquity HSS T3 1.8 μ m column; 2.1 x 100 mm; Waters).



5.1.1 Chemical characterization for the MW 212 OS isomers

Figure 5.2 depicts solved chemical structures of the target MW 212 OS, which are assigned to the sulfate esters of 3,4-dihydroxy-3-methyltetrahydro-2-furanone and 3,4-dihydroxy-4-methyl-tetrahydro-2-furanone. The compounds are divided into two groups of positional isomers: four diastereoisomers with the sulfate group located in the C-3 position (structures A, B, G, H) and four in the C-4 position (structures C, D, E, F). All of the listed compounds are chiral.

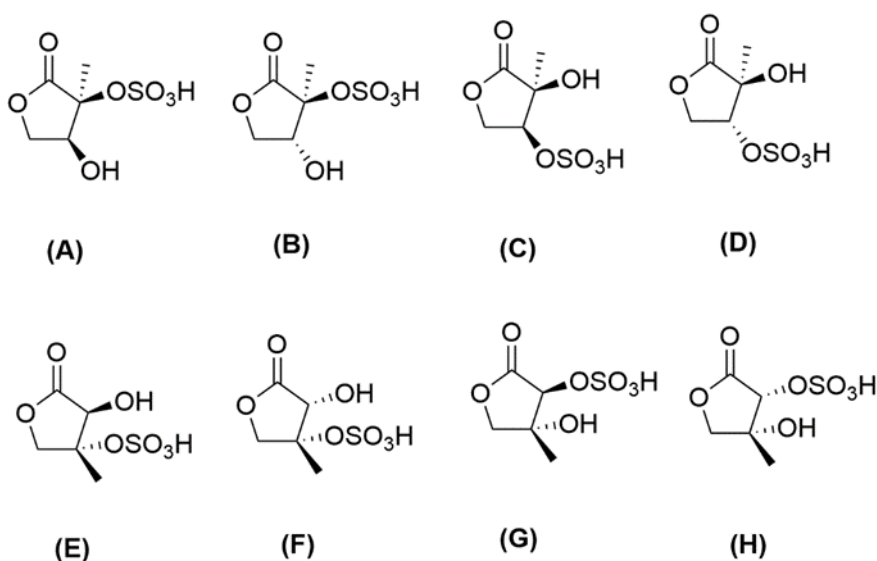


Figure 5.2 The chemical structures of the MW 212 organosulfates were assigned to sulfate esters of 3,4-dihydroxy-3-methyl-tetrahydro-2-furanone (structures A-D) and 3,4-dihydroxy-4-methyl-tetrahydro-2-furanone (structures E-H), respectively. Only one enantiomer of each compound is shown.

The high resolution ESI mass spectra recorded for the m/z 211 deprotonated ion reveal the $C_5H_7SO_7$ elemental composition for the MW 212 OS. The formula corresponds to two ring and/or double bond equivalents and supports the proposed lactone-containing structures.

In the next step, I recorded and analyzed product ion mass spectra (MS^2) for the m/z 211 ions appearing in each fine ambient $PM_{2.5}$ SOA sample. Figure 5.3 shows selected data for m/z 211 MS^2 obtained for four isomers (Fig. 5.1 A, RT 1.05, 1.29, 1.42, and 1.53 min) detected in a *K-puszt* $PM_{2.5}$ sample, which is considered a representative *pooled* sample. I also generated fragmentation spectra for SOA isoprene aqueous phase mimics and SOA isoprene smog chamber-generated samples, which are displayed in Figure 5.4.

The ion product spectra of m/z 211 of the four peaks contain a bisulfate ion at m/z 97, which is consistent with the presence of a sulfate group in a target structure(s). For peaks with retention times of 1.05, 1.29, and 1.53 min., respectively (Figure 5.3), the loss of an SO_3 unit (Δ mass = 80 Da) resulting in the m/z 131 fragment ion is observable. Such a fragmentation process is consistent with the MS^2 data for organosulfur compounds.^{5,188} The two of the mentioned peaks (i.e., RT 1.05 min. and 1.53., Figure 5.3) provided additionally informative ions: m/z 193 and 113 at RT 1.05 min. and m/z 193, 165, 121, 113, and 81 at RT 1.53 min. The ion at m/z 81 corresponds to HSO_3^- species, which is often observed for mass spectrometric behavior of organosulfates.^{37,108} The mass spectrometric data for the RT 1.05 and 1.53 min. peaks and for the RT 1.29 and 1.42 min. peaks are significantly different from each other, but the data is too limited to indicate a positional isomeric structure.

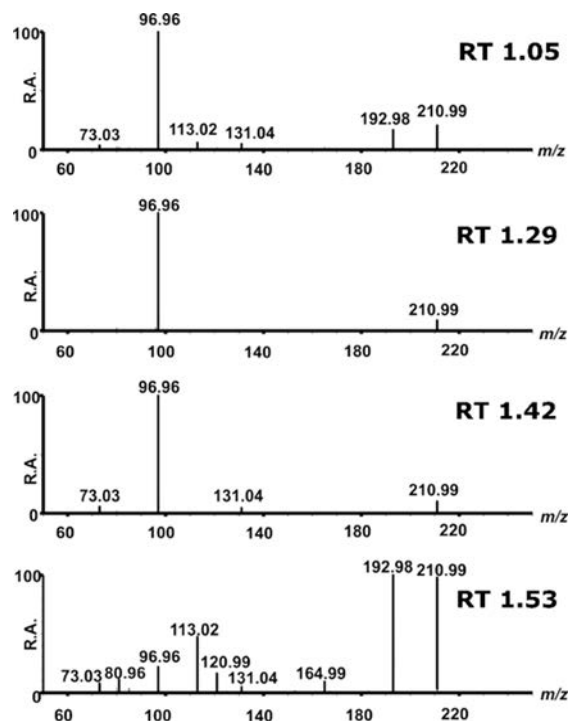


Figure 5.3 Negative ion electrospray product ion mass spectra of the target m/z 211 ions obtained for four resolved peaks in the extracted ion chromatogram of the K-puszcza $PM_{2.5}$ sample (Fig. 5.1 A). CID collected with energy CE 25 eV.

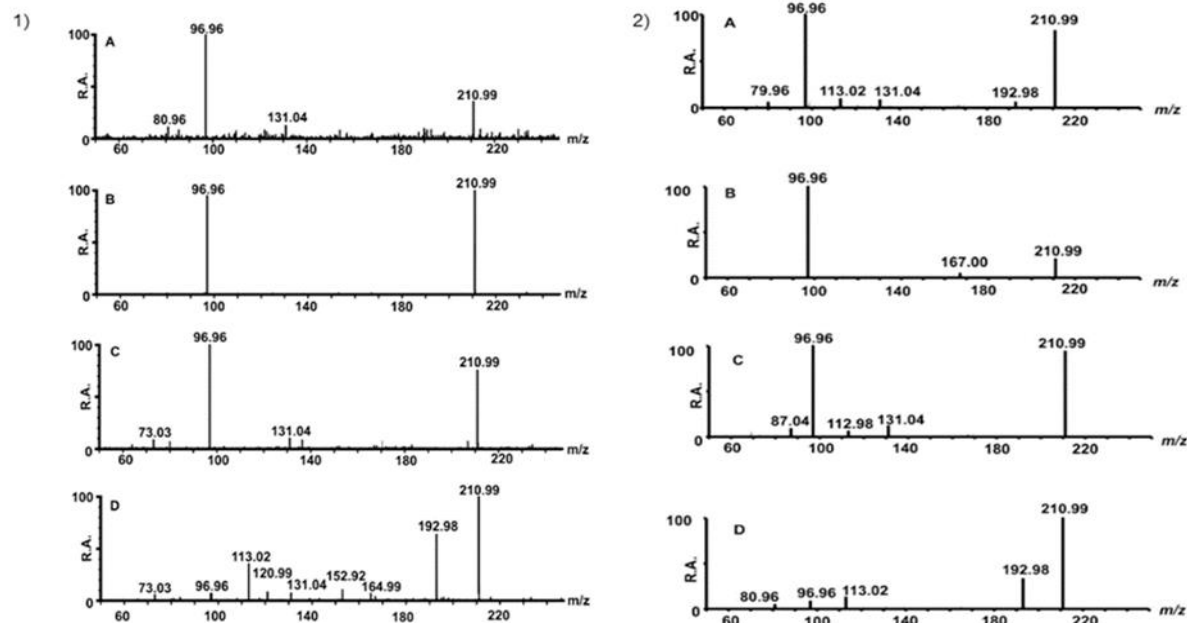


Figure 5.4 Negative ion electrospray product ion mass spectra of the target m/z 211 ions for: 1) aqueous-phase isoprene SOA samples: peaks with retention times at (A) 1.03 min. (B) 1.28 min (C) 1.41 min. and (D) 1.51 min. and 2) smog chamber isoprene SOA samples: peaks with retention times at (A) 1.06 min. (B) 1.30 min. (C) 1.43 min. and (D) 1.55 min. CID collected with energy CE 15 eV.

5.1.1.1 The synthesis of sulfate esters of 3,4-dihydroxy-3-methyl-tetrahydro-2-furanone and 3,4-dihydroxy-4-methyl-tetrahydro-2-furanone

In order to obtain the target MW 212 OSs and confirm their likely structure(s), at this stage of the research, I attempted to synthesize in aqueous solution sulfate esters of 3,4-dihydroxy-3-methyl-tetrahydro-2-furanone and 3,4-dihydroxy-4-methyl-tetrahydro-2-furanone by reacting genuine 3-methyl-2-furanone or 4-methyl-2-furanone with sulfate radical anions. The latter were generated through S(IV)-autoxidation chain reactions (described in details in chapter 5.1.5). The experiments for both furanone precursors were carried out separately, which greatly simplified the chromatographic analysis of the reaction products and allowed for the distinction of six different isomers of the MW 212 OSs.

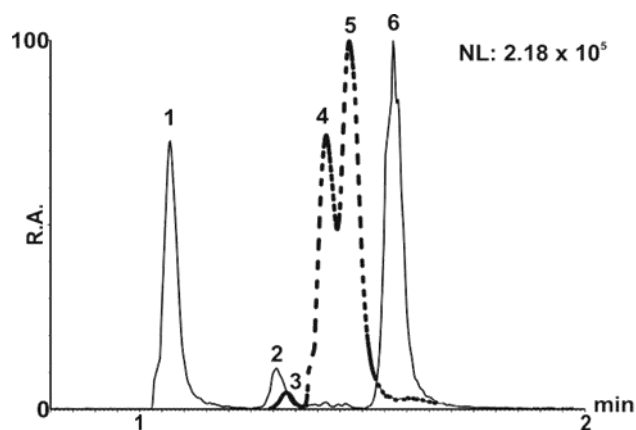


Figure 5.5 Overlapped LC/ESI-HRMS extracted ion chromatograms at the m/z 211 channel for the synthesized sulfate esters of 3,4-dihydroxy-3-methyl-tetrahydro-2-furanone (dashed line, peaks 3, 4, 5) and 3,4-dihydroxy-4-methyl-tetrahydro-2-furanone (solid line, peaks 1, 2, 6). Retention times for subsequent peaks (1-6): 1.07, 1.31, 1.33, 1.42, 1.48 and 1.57 min.

The performed synthesis of standards in solution resulted in a mixture of six m/z 211 compounds (Fig. 5.5) with the same or similar RTs as those observed in the ambient fine $PM_{2.5}$ SOA samples (Fig. 5.1 A-C).

The most informative data was collected for the 3,4-dihydroxy-4-methyl-tetrahydro-2-furanone sulfate ester. Three isomers of the MW 212 OSs were produced (Fig. 5.5, peaks 1, 2, and 6), of which peaks 1 and 6 showed rich fragmentation patterns (MS^2 spectra of m/z 211 are given in Figure 5.6 A,C).

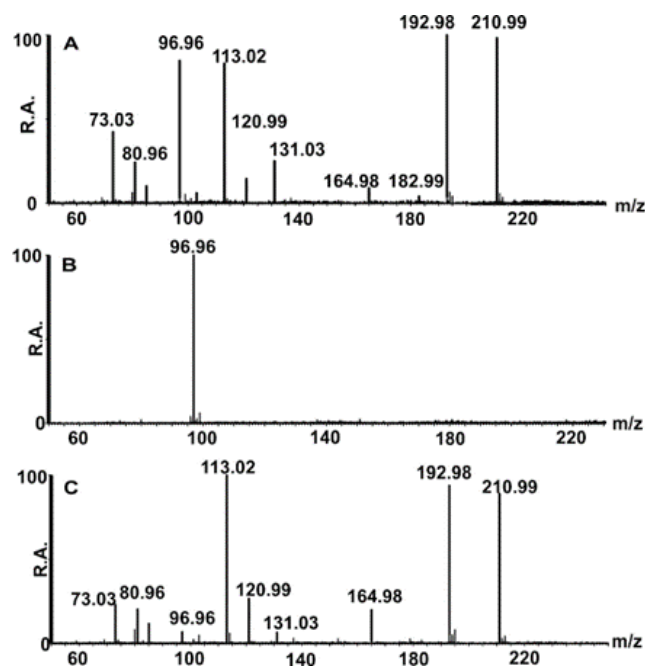


Figure 5.6 The MS² data acquired for 4-methyl-2(5H)-furanone SOA for peaks with retention times at (A) 1.07 min. (B) 1.31 min. and (C) 1.57 min, respectively. CID were collected at the collision energy (CE) of 25 eV.

These results correspond well with the MS² data collected for the PM_{2.5} K-pusztá sample (Figure 5.3 A, D), although the MS² data acquired for peak 1 at the RT 1.05 min. showed weaker fragmentation than the synthesized sulfate esters 3,4-dihydroxy-3-methyl-tetrahydro-2-furanone (Figure 5.6 A, RT 1.07 min).

The additional observations were made for the peak 2 in ambient samples (Fig. 5.1 A: RT 1.29 min.; Fig. 1B: RT 1.31 min.; Fig. 1C: RT 1.27 min.). In samples of the fine ambient PM_{2.5} SOA this peak was observed as a single, slightly broadened peak. However, *m/z* 211 EIC of 3,4-dihydroxy-3-methyl-tetrahydro-2-furanone and 3,4-dihydroxy-4-methyl-tetrahydro-2-furanone revealed two different peaks for each compound (Fig. 5.5, peaks 2 and 3). The first peak at the RT of 1.31 min. corresponds to the positional isomer of the sulfate ester with a methyl substituent at C-4, while the second peak at the RT of 1.33 min. is the isomer of the sulfate ester with a methyl substituent at C-3. The MS² data (Figures 23 B and Figure 5.7 C, consecutively) confirmed the presence of two different isomers, however, revealed limited structural information (*m/z* 97).

The sufficient separation was achieved for 4-dihydroxy-3-methyl-tetrahydro-2-furanone to record product ion spectra (Figure 5.7 B, C) close to the eluting isomers.

These results confirm the presence of two different isomers with a slightly different fragmentation pattern. The relative intensities are similar for either isomer.

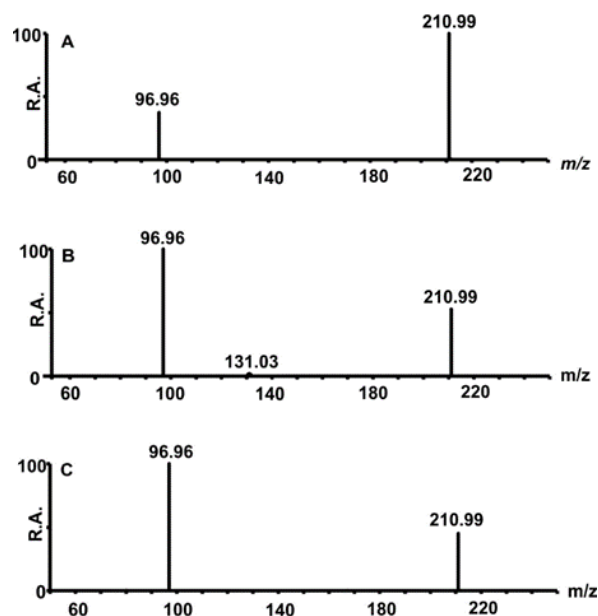
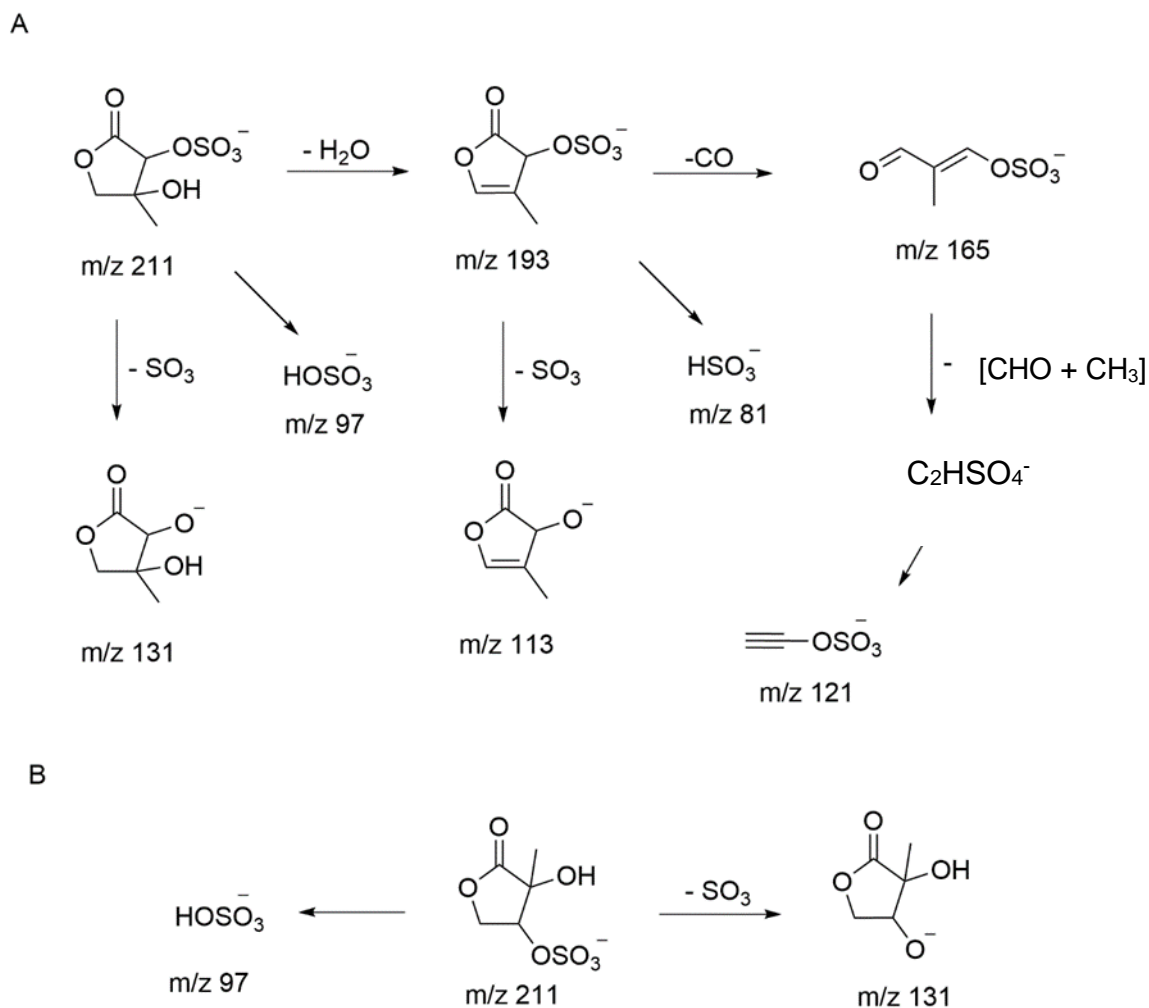


Figure 5.7 The MS² data recorded for 3-methyl-2(5H)-furanone SOA for peaks with retention times at (A) 1.33 min., (B) 1.42 min. and (C) 1.44 min. CID were collected at the collision energy of 15 eV.

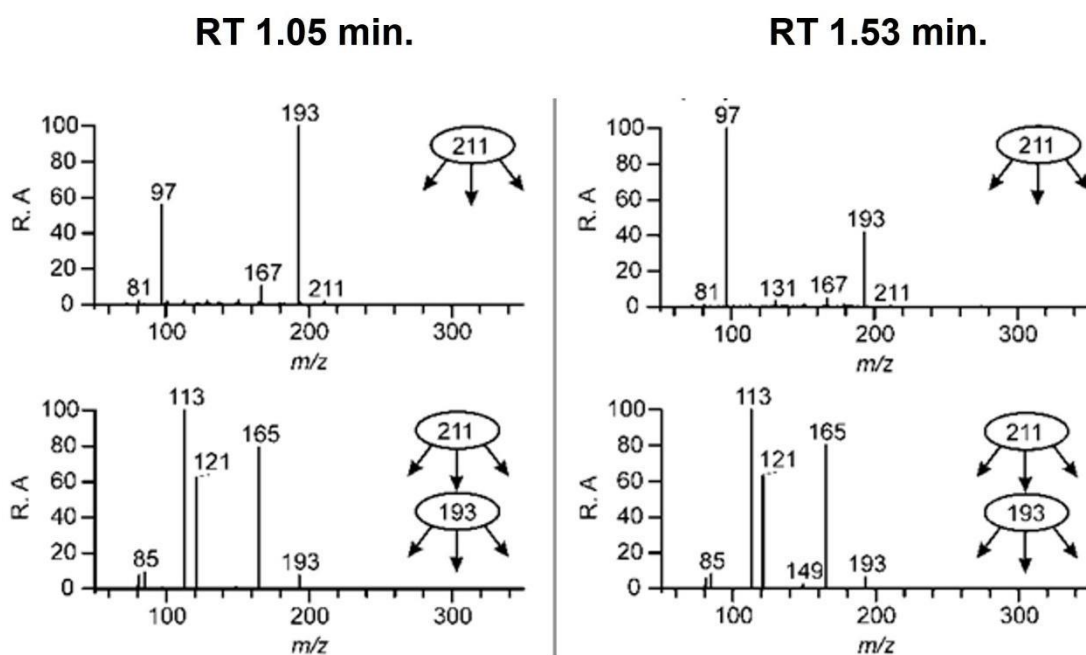
In case of the peak 4, the ion at m/z 131 is observed (Fig. 5.7 B). However, for other samples (i.e., fine ambient PM_{2.5} SOA, isoprene smog chamber-generated SOA, and SOA mimicking the aqueous phase of isoprene), separation of closely eluting peaks was not achieved at that stage of my research.

Based on a detailed analysis of the MS data for both fine ambient PM_{2.5} aerosol samples and synthesized sulfate esters of 3,4-dihydroxy-3-methyltetrahydro-2-furanone and 3,4-dihydroxy-4-methyl-tetrahydro-2-furanone, I proposed possible fragmentation pathways for the observed m/z 211 OS isomers with a methyl substituent at C-4 (Scheme 5.1 A) and C-3 (Scheme 5.1 B).



Scheme 5.1 Plausible fragmentation pathways for the m/z 211 ionic products, assigned to positional isomeric sulfate esters of A) 3,4-dihydroxy-4-methyl-tetrahydro-2-furanone, and B) 3,4-dihydroxy-3-methyl-tetrahydro-2-furanone, based on the combined LC/MS/MS, MS³ and accurate mass MS² data.

The data confirmed that fragmentation of m/z 211 mainly results in the loss of water (m/z 193) and bisulfate ion (m/z 97). Further fragmentation of m/z 193 results in the loss of CO (m/z 165), and ions at m/z 121 and 113 and are in line with previously reported ion trap mass spectrometric data⁹⁵(Scheme 5.1)¹¹¹. It is proposed that the loss of water leading to the m/z 193 ion preferentially involves a hydrogen atom adjacent to the lactone oxygen atom at the 5-position hydrogen. However, elimination involving the hydrogen from the methyl substituent should also be considered, as indicated by quantum chemical calculation performed in collaboration with the Warsaw University (dr Kacper Błaziak; Scheme 5.3 in chapter 5.1.2).³⁶



Scheme 5.2 Ion trap LC/MS² and MS³ product ion spectra of *m/z* 211 and *m/z* 193 obtained for the peak eluting with the RT 1.05 min. (left panels) and RT 1.53 min. (right panels) from *K*-puszta fine ambient PM_{2.5} aerosol sample (Fig. 5.1 A). Details of the experiment were described elsewhere.¹⁸⁹

5.1.2 Quantum-chemical calculations

In order to get more insights into fragmentation patterns of sulfate esters of 3,4-dihydroxy-3-methyl-tetrahydro-2-furanone and 3,4-dihydroxy-4-methyl-tetrahydro-2-furanone stereoisomers, which would aid for better interpretation of their MS² spectra and the spectra of the MW 212 OS isomers, I deployed theoretical calculation suit.³⁶ More specifically, the aim of this part of study was to investigate dissociation channels of target molecules and identify the appropriate activation energy barriers for each stereoisomer. These calculations were performed in collaboration with dr Kacper Błaziak from the Warsaw University. Below, I am providing the most relevant outputs of conducted calculations; their detailed description is given elsewhere.³⁶

Density Functional Theory (DFT)-based calculations were utilized to examine the two principal fragmentation pathways observed in the *m/z* 211 MS² spectra. These pathways were identified as a water loss leading to *m/z* 193 ion and the formation of bisulfate ion (*m/z* 97) through collision induced dissociation (CID) experiments using the

Synapt G2-S HDMS instrument, with ion collision energies ranging from 2.3 to 3.2 eV (230 to 307 kJ/mol) at the center of mass frame (CM). Although multiple ion-to-gas collisions are possible under experimental conditions, the spectra should still be dominated by the processes with the lowest activation energy.

To explain the observed differences in fragmentation patterns, a semi-qualitative structural analyses based on the results of quantum chemistry calculations were performed. A density functional theory (DFT) was used to calculate the relative dissociation energies of the two competing reaction channels: water loss and HSO_4^- ion formation. All likely fragmentation mechanisms were evaluated through calculations, with the calculated reaction activation barriers, corresponding to the transition state electron energies, as shown in Scheme 5.3.

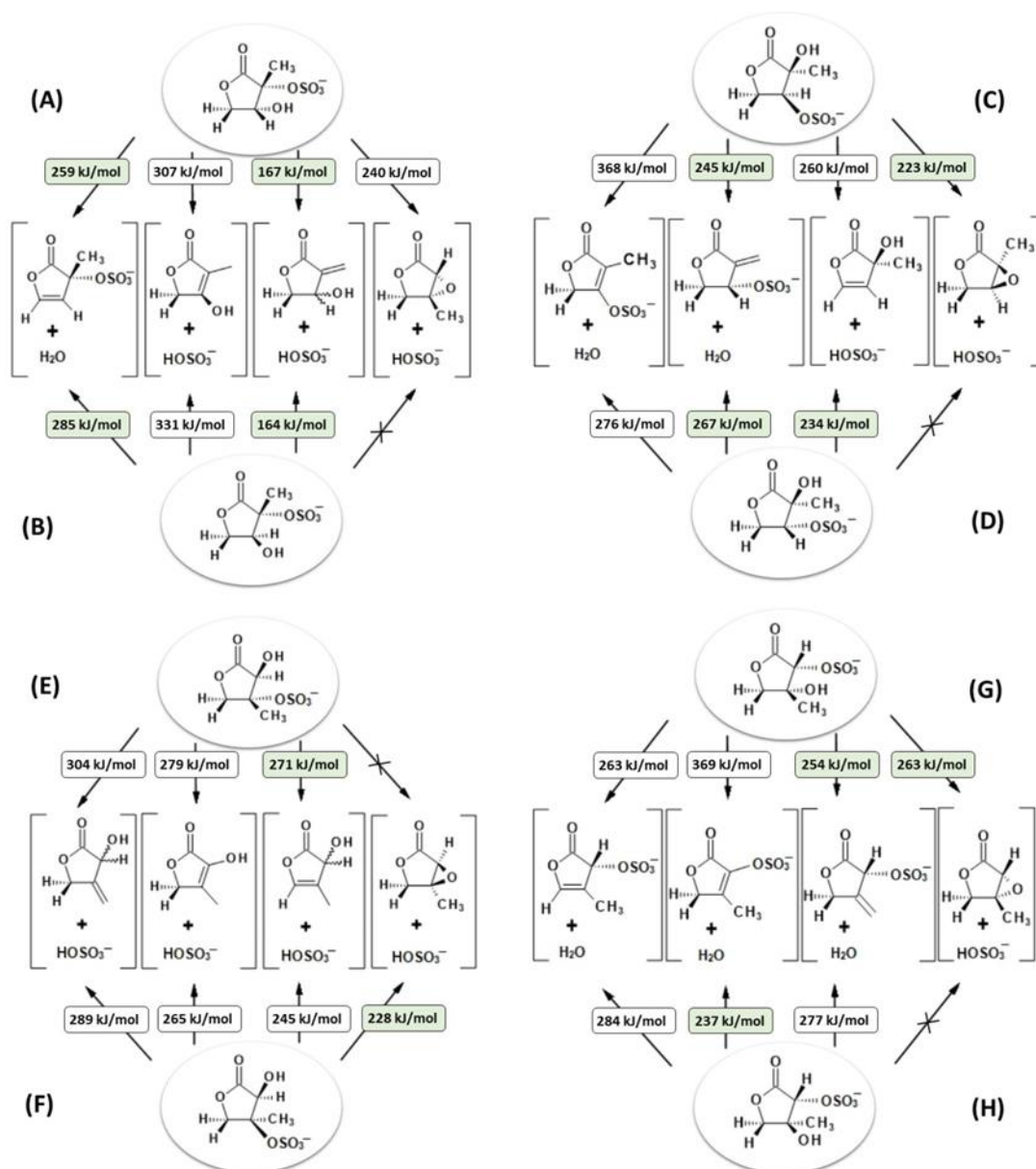
The study of stereoisomers assigned to structure (A) revealed one pathway for water loss and three pathways for HSO_4^- ion formation. Kinetically, the most preferred reaction is the neutral loss of 114 Da, forming the bisulfate ion (m/z 97). A water loss is less favorable, due to a higher activation energy (259 kJ/mol). Bisulfate ion formation should be the dominant or only observed fragmentation process.

The conclusions for the diastereoisomer (B) are similar, where the hydroxyl and sulfate groups are in a *trans* configuration. However, only three fragmentation channels were observed: one for a water loss and two for bisulfate ion formation. The *trans* orientation of the key functional groups (-OH and $-\text{OSO}_3^-$) causes significant steric hindrance, making the appropriate epoxide formation impossible.

For structure (C) shown in Scheme 5.3 (hydroxyl group located at C-3, the sulfate ligand at C-4), four transformation pathways were found, among which the formation of the HSO_4^- ion and a neutral epoxide species with an activation energy barrier of 228 kJ/mol is the most preferable reaction channel. For diastereoisomer (D), due to the *trans*-steric effects, bisulfate ion formation leads to a different neutral lactone-containing product.

Theoretical investigations of the reaction kinetic properties of sulfate esters of 3,4-dihydroxy-3-methyl-tetrahydro-2-furanone stereoisomers (A) – (D) show that in all cases,

the m/z 211 precursor ions undergo most likely the fragmentation to the bisulfate ion (m/z 97) upon CID runs.



Scheme 5.3 Calculated activation energy barriers for eight MW 212 OS diastereoisomers for the water elimination reaction and bisulfate ion formation. The transition state electron energies and the ZPE correction were calculated at a B3LYP/6-311+g(2d,p) level of theory. The lowest energy values are highlighted in green color.³⁶

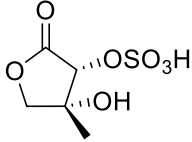
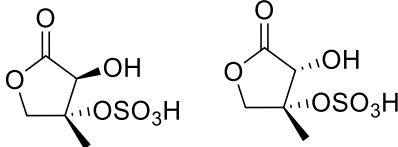
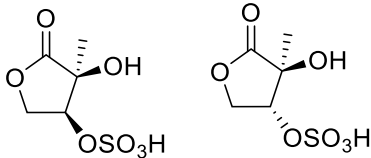
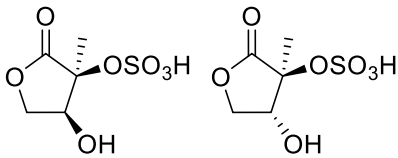
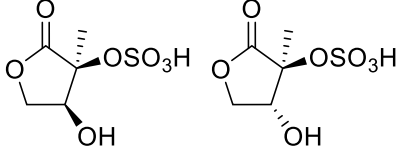
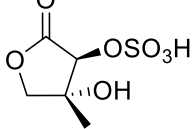
This observation is in good agreement with the experimental fragmentation patterns recorded for chromatographic peaks shown in Figure 4, where the HSO_4^- ion is the only product.

In the next step, activation energy barriers were calculated for a set of stereoisomers of sulfate esters of 3,4-dihydroxy-4-methyl-tetrahydro-2-furanone. For the first two stereoisomers, the reaction pathway leading to the loss of water was not found. In this respect, the only fragmentation pathway found for (E-F) ions is a neutral loss of 114 Da. Additionally, during the bisulfate ion formation process, different neutral lactone-containing molecules are formed from each stereoisomer.

Finally, in the last stereoisomer case (H), the sulfate and the hydroxyl groups are in a *trans* configuration thus, the only identified dissociation channel for these molecules leads to water elimination *via* the lowest energy barrier.

The research on the fragmentation patterns of sulfate esters of 3,4-dihydroxy-3-methyl-tetrahydro-2-furanone and 3,4-dihydroxy-4-methyl-tetrahydro-2-furanone stereoisomers provides a better understanding of the chemical properties of these molecules. By utilizing quantum-chemical calculations to examine the fragmentation pathways of target molecules and identify the appropriate activation energy barriers for each stereoisomer, I could propose a preliminary structural assignment of sulfated lactones A-H to the peaks present in the chromatogram. This thorough analysis of scheme and fragmentation spectra allows for a more detailed understanding of the chemical properties of discussed organosulfur SOA components and allows a preliminary assignment of sulfated lactones A-H to the peaks present in LC/ESI-HRMS chromatograms. The assignments are summarized in Table 5-III.

Table 5-III Tentative structural assignments of the compounds A – H shown in Scheme 5.3 for peaks appearing on real LC/ESI-HRMS chromatograms shown in Fig. 5.5.

Peak No.	RT (min)	Compound(s) caption	Proposed structure
1	1.07	H	
2	1.31	E or F	
3	1.33	C or D	
4	1.42	A or B	
5	1.48	A or B	
6	1.57	G	

5.1.3 Improved and complementary chromatographic analysis for the MW 212 OS with use of RP-C18 and HILIC methods

Among a broad scope of the research, I have explored the capacity of two different methods for the analysis of aerosol polar fraction with a target put to organosulfates: HILIC chromatography separation with a BEH Amide column and RP-C18 mode. The results obtained with use of the latter method, I discussed in the above sections.

Both methods have their advantages and disadvantages.^{5,117} The HILIC method was found to be less dependent on sample solvent, making it a suitable method for the analysis of polar SOA-bound compounds. However, it has lower versatility, when it comes to targets with different polarity. On the other hand, the RP-C18 mode was more versatile, but it was more dependent on sample solvent (Figure 5.8). The optimization conducted for the sample preparation before LC/MS organosulfate analysis showed that the best solvent for the sample reconstitution is pure aqueous ammonium buffer used as a mobile phase A (Figure 5.8).

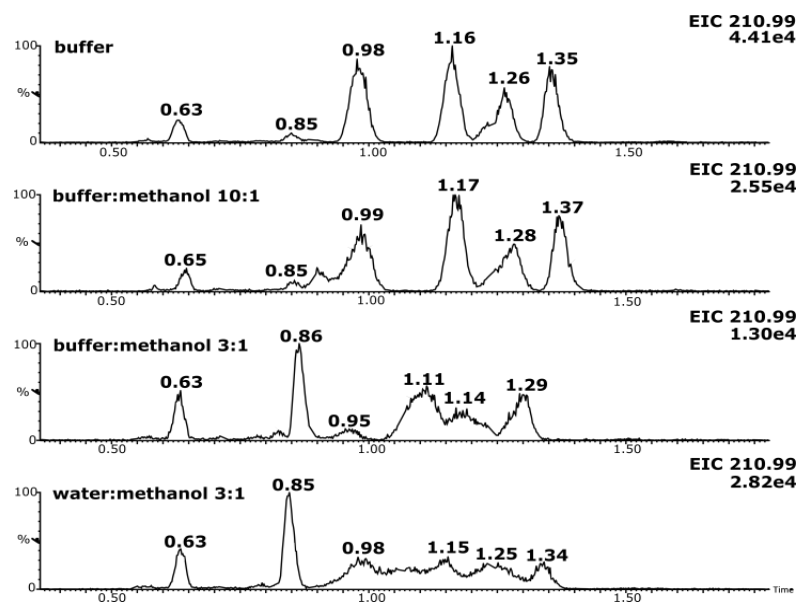


Figure 5.8 The RP-C18 separation power of organosulfate isomers with the MW 212 depending on the sample solvent deployed (chromatography (Acquity HSS T3 1.8 μm column; 2.1 x 100 mm; Waters).¹¹⁶

In the analysis of such chemically complex matrices as fine ambient SOA extracts, it should be minded that it is extremely important to interfere with the sample as little as

possible so as not to affect its chemical composition or possible physicochemical processes. The addition of the buffer, despite a very good effect on the chromatography, could have been too far-reaching interference in the chemical composition of the samples. For this reason, we verified the hypothesis whether the separation of the target analytes would get significantly worse when using ultrapure water in the reconstitution process. It turned out that the use of ultrapure water gave rise to the comparably good results with the use of a buffer (Figure 5.9). In addition to a better retention on the LC column with the use of water alone as the sample solvent, the quality of the chromatographic separation did not deteriorate depending on the injection volume.

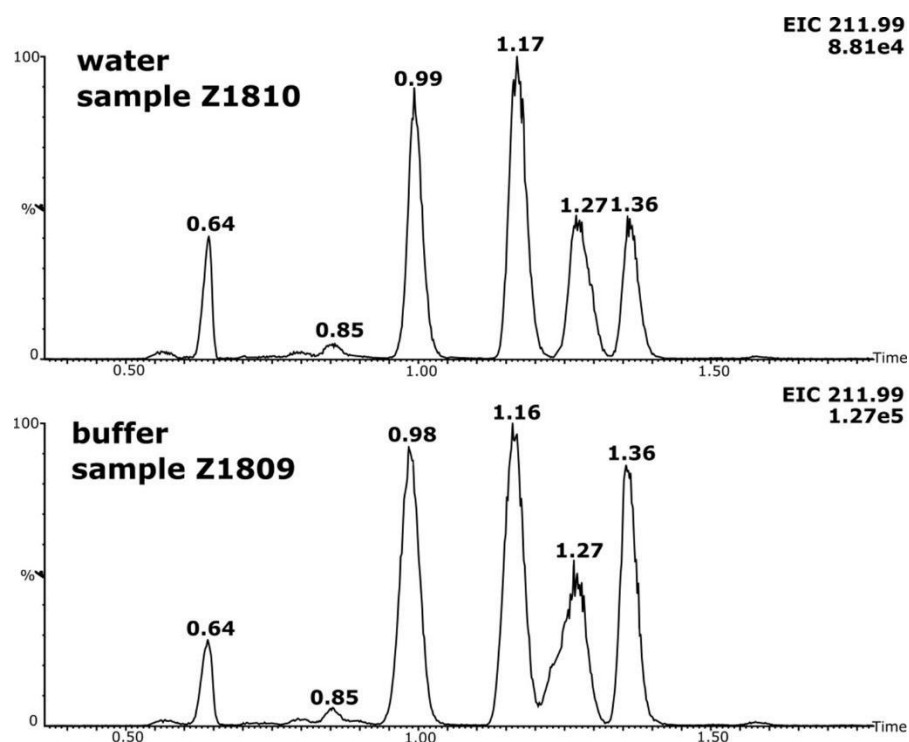


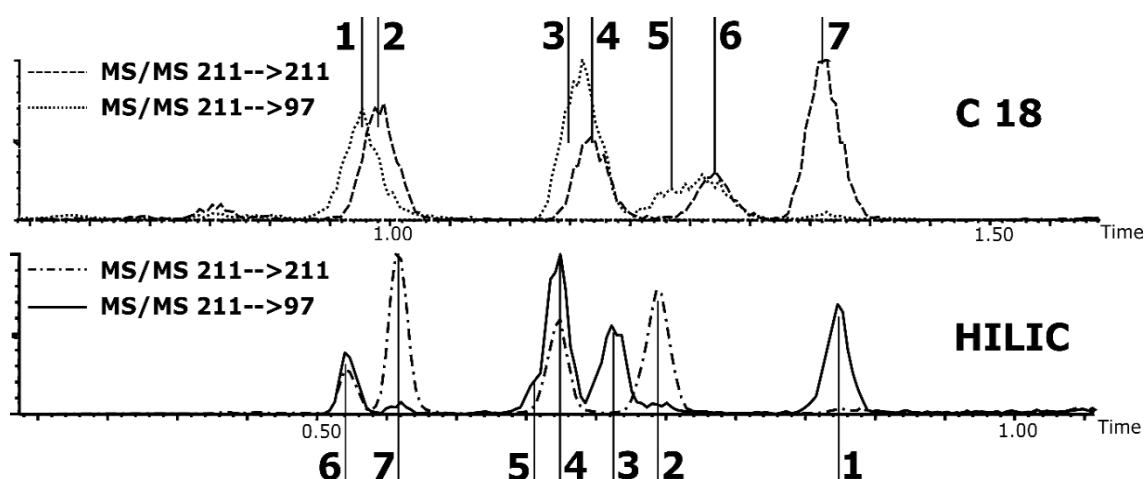
Figure 5.9 Comparison of differences in the RP-C-18 chromatographic separation of the MW 212 organosulfate isomers in fine ambient PM_{2.5} aerosol samples (sampling location: Diabla Góra; sampling time: 12h; sampling regime: day-time sampling during sunny summer time) depending on the sample solvent used. Column used: Acquity HSS T3 1.8 μm column; 2.1 x 100 mm; Waters.¹¹⁶

Another factor affecting the quality of the chromatographic separation was the use of the appropriate column temperature and the pH of mobile phase A. The latter showed not much influence on the chromatographic quality. The optimal temperature in the separation of the polar SOA fraction in the case of RP-C18 chromatography was 40 °C, while in the case of HILIC chromatography the best results were achieved with 45 °C. As

the results on method optimization described in details elsewhere showed,¹¹⁶ selecting the appropriate methodology according to the purpose of analysis, taking into account its advantages and disadvantages, is essential.

In the analysis of the MS/MS experimental data for the m/z 211 ion recorded in a RP-C-18 mode and a HILIC method, it was discovered that there were seven structurally similar isomers present, which significantly expanded the existing knowledge based on my previous studies of natural aerosol samples, as well as the results of mimic experiments.

First of all, the use of two fragmentation channels (m/z 211/211 and m/z 211/97) allowed not only to confirm the presence of seven the MW 212 organosulfate isomers but also to obtain the far more accurate data from fragmentation experiments (Scheme 5.4).



Scheme 5.4 Chromatographic separation of the MW 212 organosulfate isomers using an RP-C-18 chromatography (upper trace) and the HILIC method (bottom trace). The scheme overlaps two fragmentation reaction channels at m/z 211/211 and m/z 211/97, respectively for each method.

The identification and assignment of structures to the MW 212 OS single isomers (Figure 5.10) were based on their distinct fragmentation behaviors.

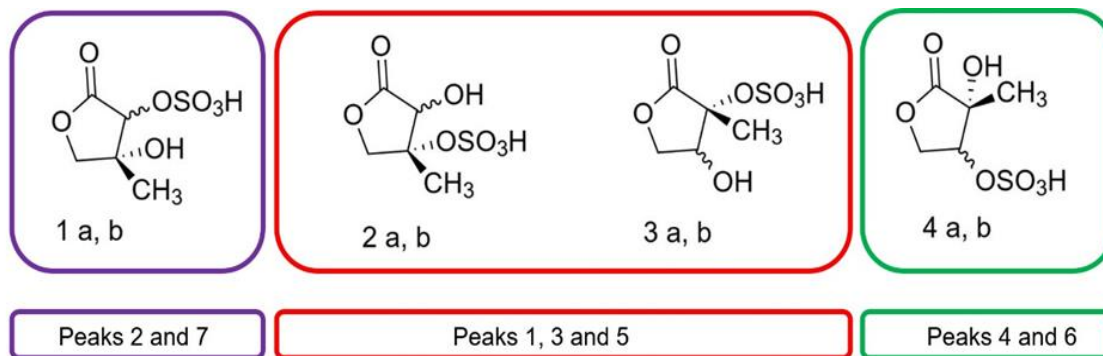


Figure 5.10 Proposed structures of organosulfate isomers with the MW 212 and corresponding chromatographic peaks.

In the case of the peak eluting at the RT 1.05 min. in ambient aerosol samples, I noticed that we are dealing with two coeluting isomers. In the earlier m/z 211 ion fragmentation spectra for this peak, two fragmentation paths were superimposed (Fig. 5.3, RT 1.05).

Among the seven isomers, two of them were identified as lactone diastereoisomers, where the abundance of the m/z 97 ion was close to zero, and the m/z 193 peaks were observed (Figure 5.11). These two lactone isomers, compounds 1a and 1b, corresponding to peak 2 and 7 (Scheme 5.4, RP-C18 column), bear both methyl and free hydroxyl groups in position 4.

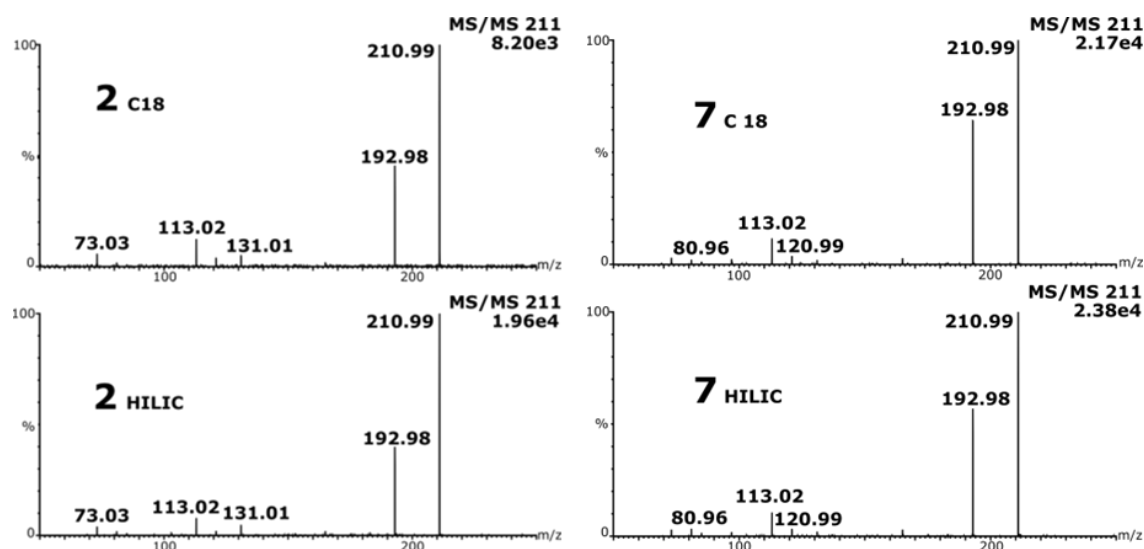


Figure 5.11 Negative ion electrospray product ion mass spectra recorded for the m/z 211 isomers collected for peaks 2 and 7 (Scheme 5.4). CID collected with CE energy of 20 eV.

However, the structures of the other five hydrogen sulfates cannot be established unequivocally. Still, reasonable proposals can be formulated based on the MS/MS spectra of the m/z 211 ions that correspond to chromatographic peaks 1, 3, and 5 in Figure 5.13. In these cases, the m/z 97 fragment ion is the only one or at least the most abundant.

In contrast, in the case of chromatographic peaks 4 and 6, the relative intensities of the parent ion (m/z 211) and the fragment ion peak (m/z 97) are comparable, thus indicating that elimination of the HSO_4^- ion is still possible, but the fragmentation reaction is hampered (Figure 5.13).

Comparing the structures of likely isomers, it is apparent that in the case of organosulfates 4a and 4b, there is only one vicinal hydrogen atom *cis* to the $-\text{OSO}_3^-$ residue, so there is only one fragmentation channel leading to the elimination of the HSO_4^- ion. In the case of compounds 2 and 3, there are at least three hydrogen atoms in positions that enable the *cis*-elimination reaction, so the m/z 97 ion should be more abundant. Consequently, it is very likely that chromatographic peaks 1, 3, and 5 correspond to three to four possible structures: 2a, b and 3a, b.

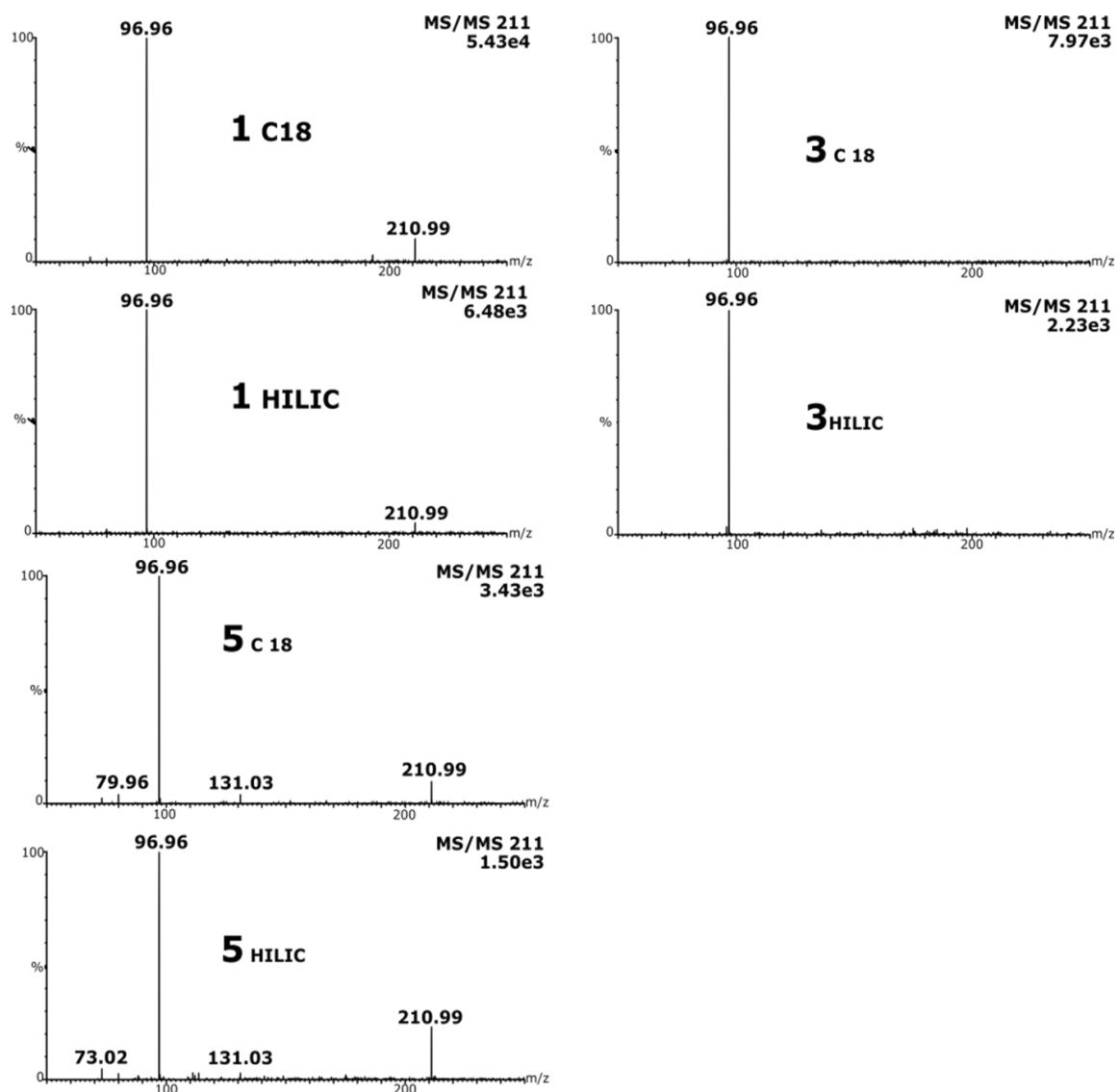


Figure 5.12 Negative ion electrospray product ion mass spectra recorded for the m/z 211 isomers collected for peaks 1,3 and 5 (Scheme 5.4). CID collected with CE energy of 15 eV.

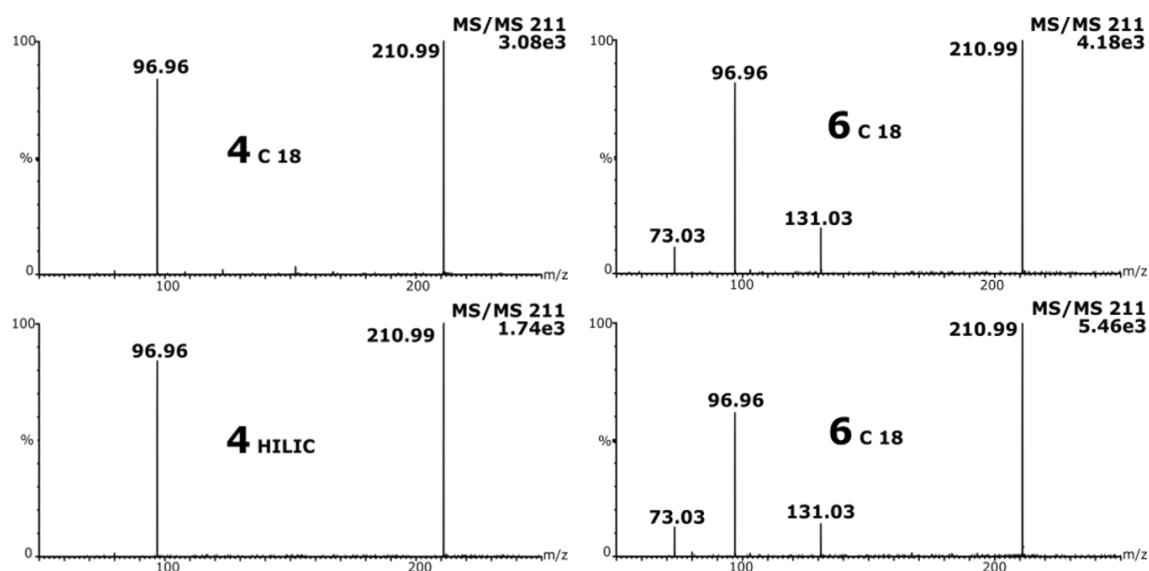


Figure 5.13 Negative ion electrospray product ion mass recorded for the m/z 211 isomers collected for peaks 2 and 7 (Scheme 5.4). CID collected with CE energy of 15 eV.

The fragmentation studies carried out for individual isomers of organosulfate with the MW 212, regardless of the method, show a large convergence in the results obtained. The differences that can be observed in the fragmentation spectra for the non-optimized and optimized methods result firstly from insufficient separation in the case of the first method, and secondly from the differences that may occur during the collection of spectra for a given isomer. In the case of samples with such a rich matrix, this is not an easy task. Surely, the unambiguous determination of likely structures for the group of discussed organosulfates with MW 212 and assigning them to the appropriate chromatographic peaks in natural aerosol samples would be fully possible with the successful synthesis of the analytical standards. Attempts to synthesize the standard were undertaken in several trials, including epoxidation of 3- and 4-methylfuranones and subsequent opening of the epoxide ring in an acidic environment in the presence of sulfuric acid. *Anti*-hydroxylation using a peroxyacid, in this case *m*-perchlorobenzoic acid,^{190,191} or another oxidizing agent, such as potassium permanganate, is a fairly well-documented synthesis procedure, unfortunately the yields of the epoxide product obtained were unsatisfactory. Considering the probable reasons of the problem of performing this procedure on a furanone backbone with methyl substituent, the only explanation that seems plausible is that the structure of the furanone ring with a methyl substituent could form a sterically or stereo selectively inconvenient structure for the epoxidation mechanism to occur.

5.1.4 Heterogeneous formation of the 212 organosulfate via aqueous-phase oxidative degradation of isoprene – mechanism investigation

The experiments described in this subchapter were a part of Patrycja Grzesiak's master thesis¹⁹² I was a scientific advisor of.

The study on the formation mechanism of organosulfate with the MW 212 Da, I started from conducting experiments, which would verify the hypothesis that the formation of this specific and abundant organosulfates can be explain through the oxidative degradation of isoprene in aqueous droplets during the atmospheric S(IV) autoxidation process. For this purpose, I planned and co-conducted a series of comparative experiments, in which in the first step the molecular oxygen $^{16}\text{O}_2$ was used, and in the second one, ultrapure water was first deoxygenated and then saturated with an isotopically labeled oxygen $^{18}\text{O}_2$. The degradation of isoprene in the experiments was continuously monitored – UV spectra were recorded for pure water, after the addition of the MnSO_4 salt solution, and after the addition of isoprene solution. From the moment of initiating the S(IV) autoxidation reaction, UV spectra were recorded every 2 minutes (Chart 5-1).

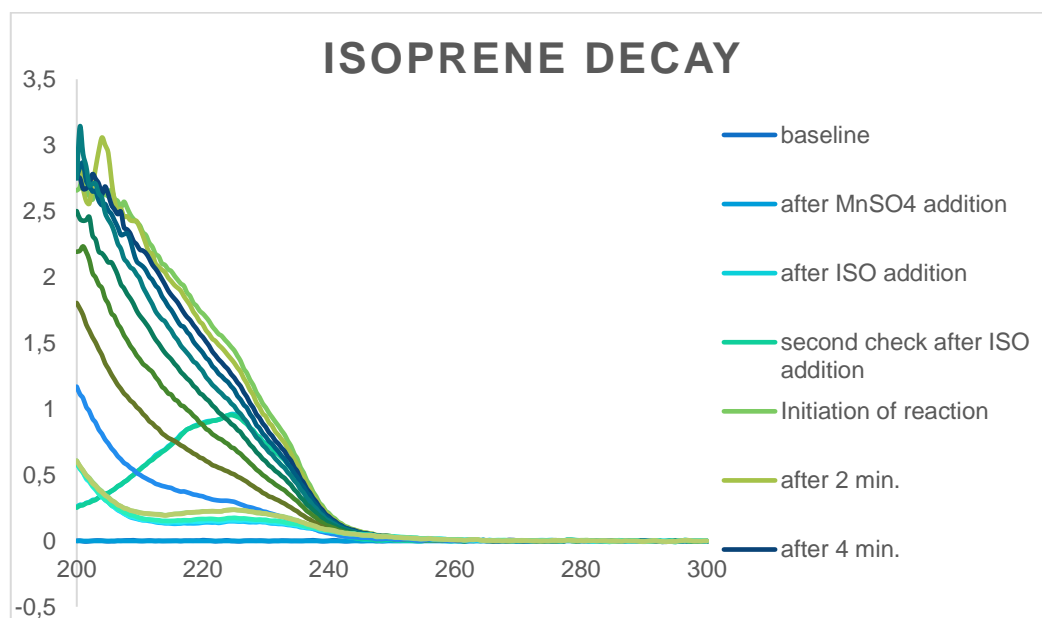


Chart 5-1 The isoprene decay profiles during its aqueous-phase degradation in the presence of *in situ*-generated sulfate radicals recorded with the UV-Vis spectroscopy (x-axis shows the wavelength units of the light in nanometers).

The results of the conducted experiments confirmed the formation of the MW 212 OS structures in the case of the aqueous-phase reaction performed under $^{16}\text{O}_2$ conditions, and the MW 222 structures in the case of the aqueous-phase reaction carried out under $^{18}\text{O}_2$ conditions (Figure 5.14).

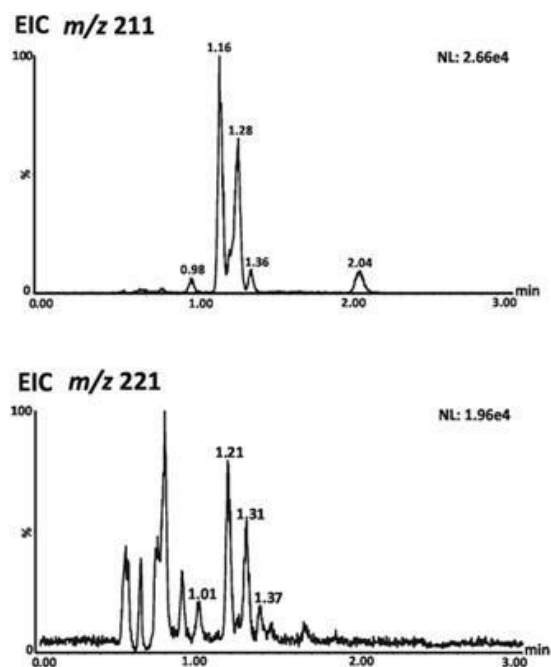


Figure 5.14 Representative LC/MS extracted ion chromatograms for organosulfates produced *via* the aqueous-phase SO_4 radicals-driven reactions of isoprene in the presence of: A) $^{16}\text{O}_2$ (m/z 211 channel; upper chromatogram) and B) $^{18}\text{O}_2$ (m/z 221 channel; bottom chromatogram). The data obtained using non-optimized RP-C18 chromatography.

The comparison of these results unequivocally implies a key role of the molecular oxygen in the reaction mechanism. The observed mass shifts from m/z 212 to m/z 222 for the most prominent peaks, i.e., 1.16 min and 1.28 min (Figure 5.14, panel A) and 1.21 min and 1.31 min. (Figure 5.14, panel B), reveals that five 16-oxygen atoms were replaced by five 18-oxygen atoms. As shown in the Figure 5.14 (panel B), in the labeling experiment, not only was the formation of organosulfate with the MW 222 observed, but also a number of other isotopologs of organosulfates, in which less than five 16-oxygen atoms were replaced by the 18-oxygen isotopes. The highest intensity of chromatographic peaks was observed for ions in the structure of which there were five atoms of the ^{18}O oxygen isotope, i.e., the m/z 221 ion. A detailed analysis of the fragmentation spectra (Figure 5.15) was carried out for this ion in order to confirm the identity of the structures of compounds differing only in the presence of ^{18}O oxygen atoms. Peak distribution in

the range of 1.00 – 1.50 min. in the chromatogram for the ion m/z 211 ($^{16}\text{O}_2$) and m/z 221 ($^{18}\text{O}_2$) and the retention times are similar. Slight shifts in the retention times are the most likely due to differences in injection volumes. The peaks present in the chromatogram of the labeled sample range from 0.00-1.00 min. come from compounds the structures of other compounds formed as a result of the conducted reaction and are not taken into account.

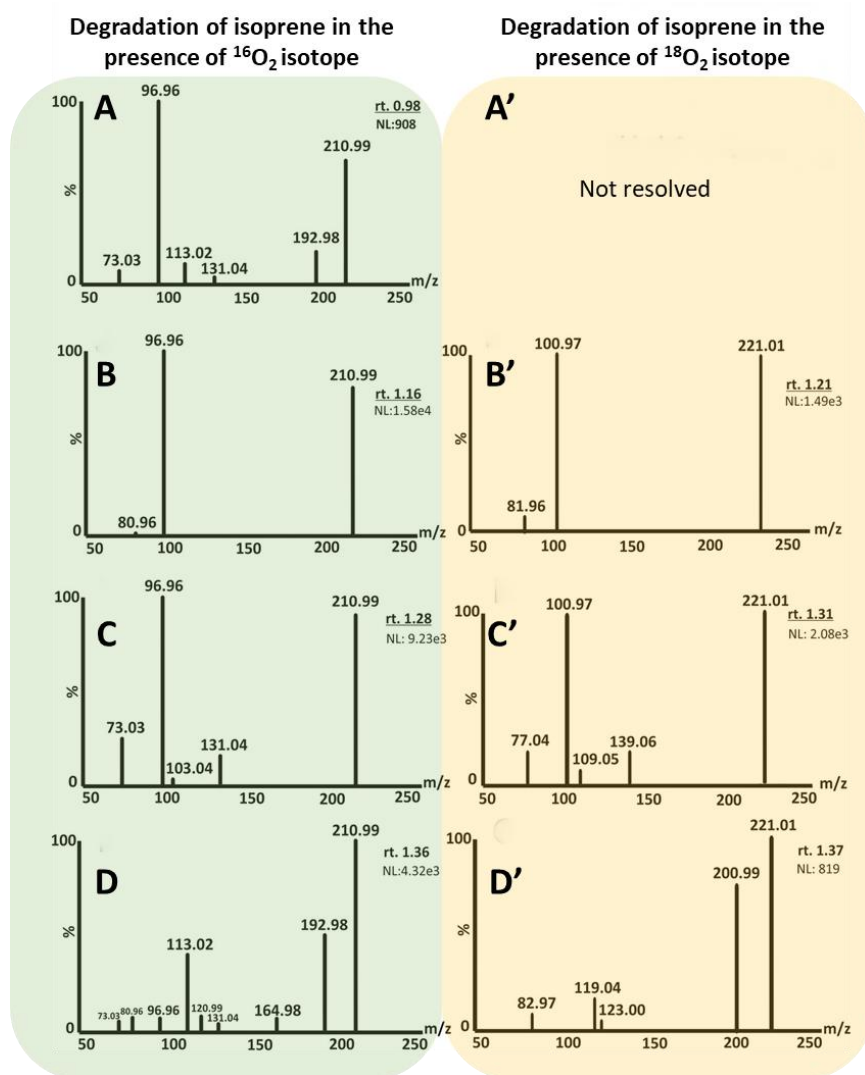
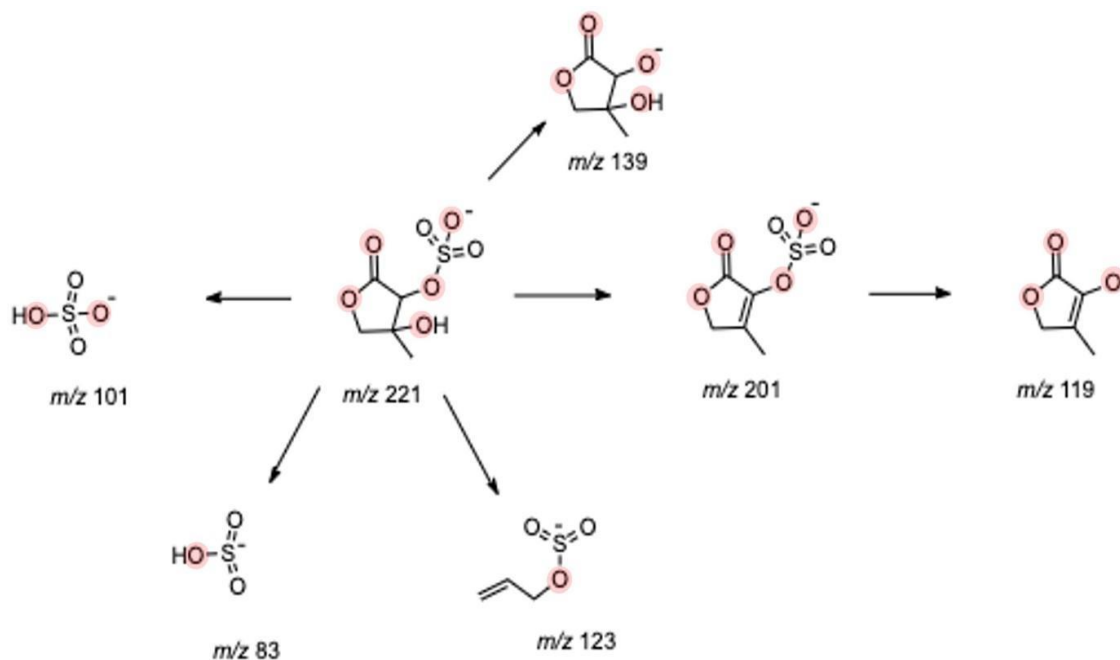


Figure 5.15 Product ion mass spectra acquired for m/z 211 (left panel) and 221(right panel) resulted from the aqueous-phase SO_4 radicals-induced reactions of isoprene in the presence of oxygen-16 (left panel) and oxygen-18 isotope (right panel), respectively: peaks at the RT 0.98 min. (A) and 1.01 (A'); 1.16 (B) and 1.21 (B'); 1.28 (C) and 1.31 (C'); 1.36 (D) and 1.37 (D'). In the case of the first eluting peak at the RT 1.01 min. overlapping of two structures occurred and sufficient separation of the spectra was not obtained.

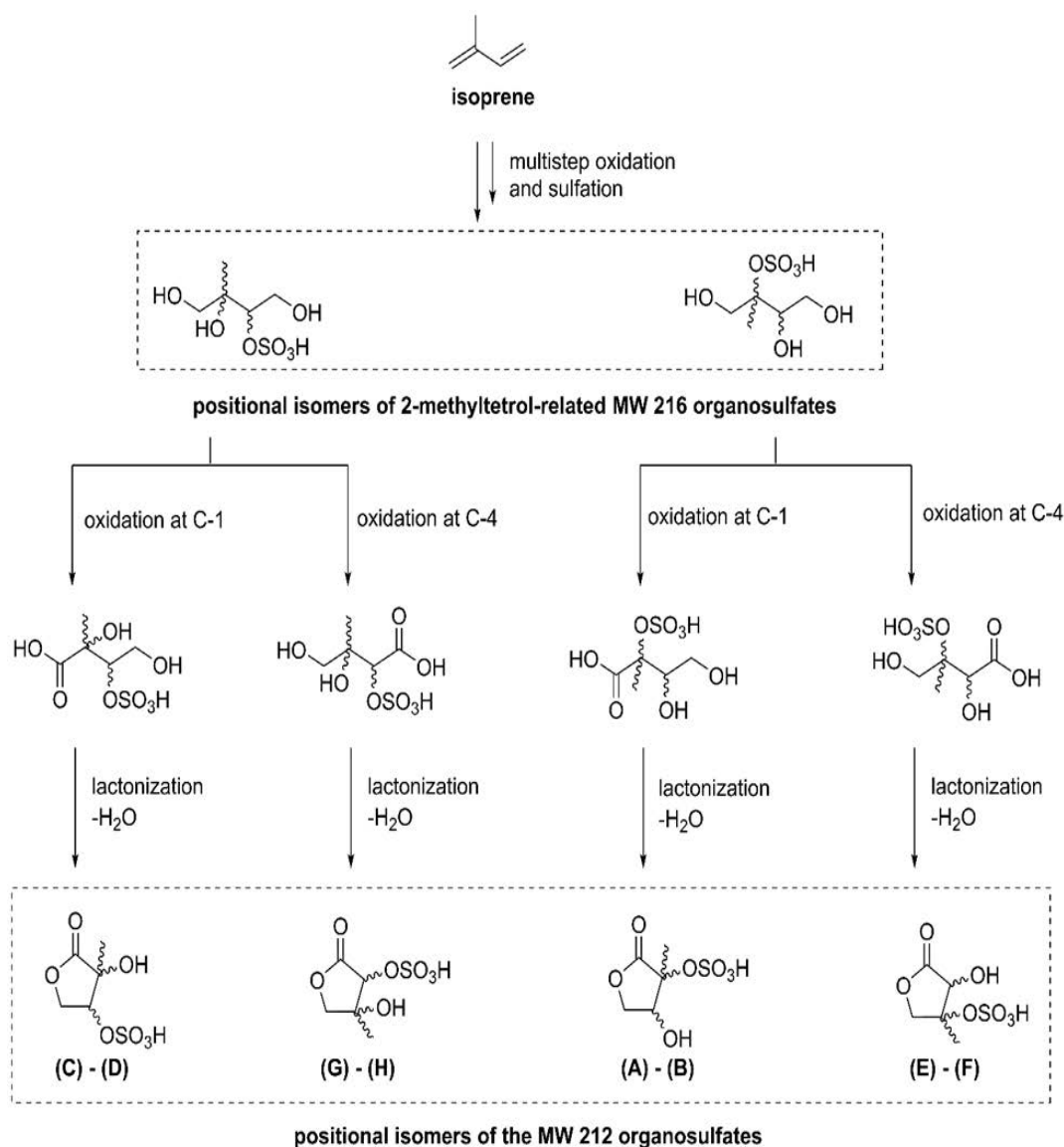
At the retention time of 1.01 min. for a sample from the reaction carried out in the presence of the oxygen-18-isotope, two products overlap, which cannot be baseline-separated, so it was not possible to extract the pure product ion mass spectrum for the ion at m/z 221. Similarly, the spectrum obtained for the peak with retention time of 1.36 min. due to the low signal intensity, it is of poor quality, and thus a reliable comparison is fairly impossible. The analysis of the remaining two spectra shows that they are qualitatively identical to each other, and the noticeable differences result only from the isotope shift of the masses. The spectra of the sample from the isoprene reaction in the presence of the 16-oxygen isotope (A, B, C, D in Figure 5.15) showed a signal coming from the ion at m/z 211 with the elemental formula $C_5H_7O_7S$. On the other hand, in the spectra of the sample from the isoprene reaction in the presence of the 18-oxygen isotope (B', C', D' in Figure 5.15) there is a signal from the m/z 221 ion, which originates from the organosulfate with the formula $C_5H_7^{16}O_2^{18}O_5S$, in which five 16-oxygen atoms are replaced by 18-oxygen isotopes. The signal at m/z 97 comes from the sulfate group HSO_4^- and is also observed in the MS/MS spectra recorded for the sample from the reaction with $^{18}O_2$ at m/z 101, where two 16-oxygen atoms are substituted with the isotope of 18-oxygen. In the C spectrum (Figure 5.15) for the reaction with $^{16}O_2$, the m/z 103 signal corresponds to an ion with the molecular formula $C_4H_7O_3$, which is also visible in the C' (Figure 5.15) spectrum at m/z 109, but its structure contains three 16-oxygen atoms replaced by 18-oxygen isotopes ($C_4H_7^{18}O_3$), hence the difference in the mass ratio to the charge of the observed ions. Similarly, an ion at m/z 131 observed in the reaction with 16-oxygen ($C_5H_7O_4$) is visible in the fragment spectrum of the sample from the reaction with ^{18}O isotope at m/z 139 ($C_5H_7^{18}O_4$). This ion was formed as a result of the detachment of the $S^{16}O_2^{18}O$ group. In the D' spectrum (Figure 5.15) with a retention time of 1.37 min. a signal of m/z 201 appears, which corresponds to an ion with the formula $C_5H_5^{16}O_2^{18}O_4S$, formed as a result of the elimination of a H_2O molecule containing the oxygen isotope ($H_2^{18}O$). The proposed fragmentation channels for the m/z 221 ion are shown in Scheme 5.5.



Scheme 5.5 Proposed fragmentation pathways for the oxygen-18-labeled organosulfates (the MW 222 Da) bearing five incorporated oxygen-18 isotopes (marked with red color).

5.1.5 Tentative Proposal for the Formation Mechanism for the MW 212 OSs under atmospheric conditions

Considering that the MW 216 methyltetrol-related organic sulfates (OSs) are abundantly present in ambient $PM_{2.5}$ (particulate matter with diameter less than $2.5 \mu m$), it was reasonable to propose that they act as precursors for the MW 212 OSs. These can be formed by the oxidation of a hydroxyl group to a carboxylic acid group, followed by lactonization (Scheme 6.6). This suggests that the MW 212 OSs are further oxidation or aged forms of the MW 216 methyltetrol-related OSs. It's worth noting that in a study by Lam et al., 3-methyltetrol OS, a minor isomer of the abundant MW 216 MTs-related OSs, underwent heterogeneous OH oxidation.¹⁹³ However, the study did not identify molecular-level organic products, and further investigation is needed, especially by examining the major isomer of the MW 216 MTs-related OSs.

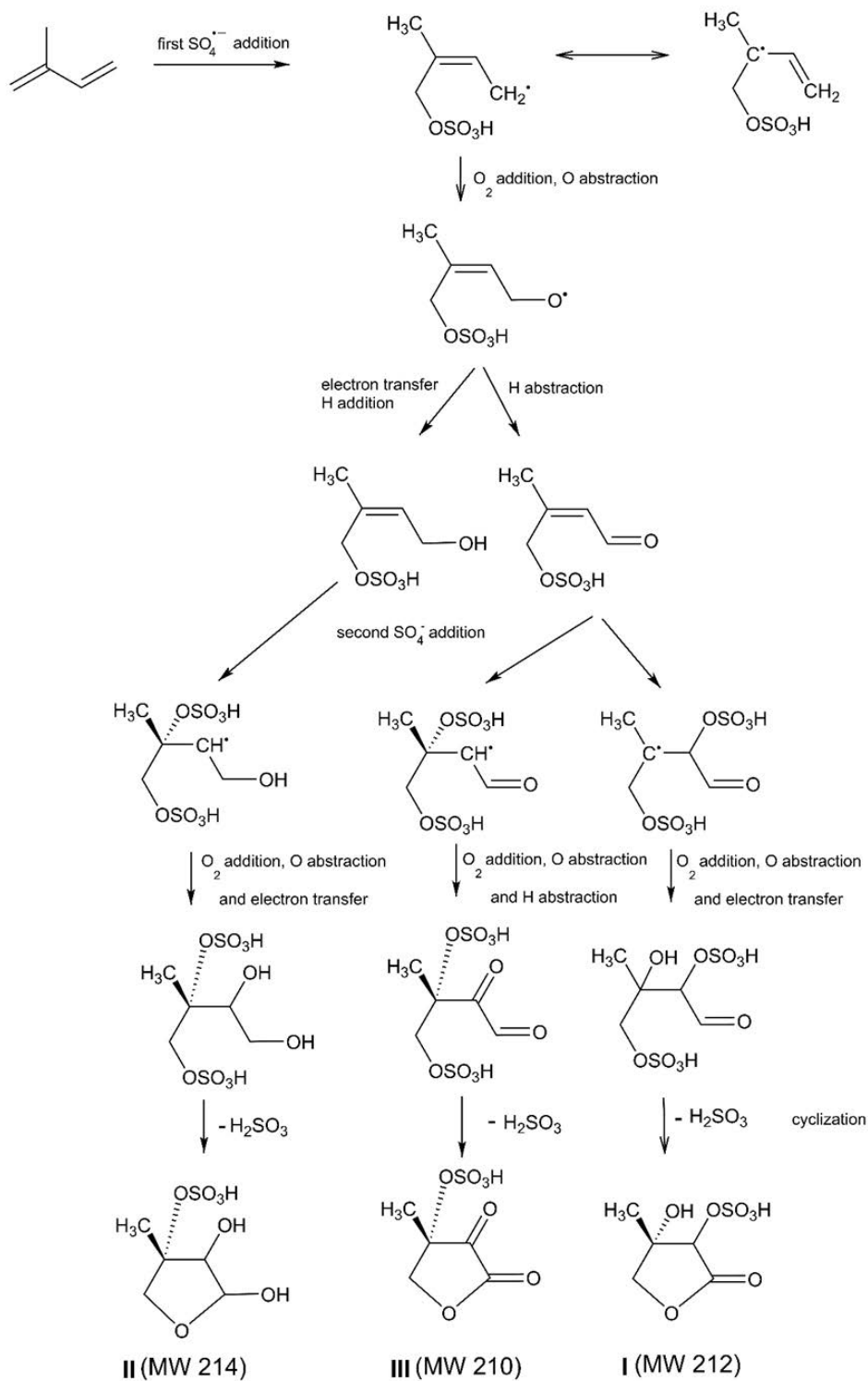


Scheme 5.6 Tentative mechanism of the MW 212 OSs formation from the heterogeneous oxidation 2-methyltetrol-related OSs, involving heterogeneous oxidation of a terminal hydroxyl group to a carboxylic acid group, followed by lactonization.³⁶

However, my laboratory endeavors revealed that an alternative mechanism (Scheme 5.7) is to be considered to explain the abundant presence of the particle-bound MW 212 organosulfate. According to my data, the target MW 212 organosulfate can originate from the isoprene oxidation with sulfate radicals in the aqueous phase. Such a reaction can preferentially occur onto the surface of aqueous droplets, where the contact between volatile species, i.e., isoprene and molecular oxygen and droplet active bulk containing S(IV) species, e.g., $\text{SO}_3^{2-}/\text{HSO}_3^-$ ions, achieves a maximum stage. The atmospheric hydrometeors are rich in transition ion metals, e.g., Fe(II) and Mn(II), which enhances

the proceed of the atmospheric S(IV) \rightarrow S(VI) oxidation and consequently serves as a powerful source of tropospheric sulfur radicals.^{184,194} Bulk aqueous reactions between isoprene (and other VOCs), molecular oxygen and sulfur radicals are also feasible, however are markedly constrained in the atmospheric framework by the limited solubility of volatiles reagents in the aqueous phase at a given ambient temperature and pressure.

According to the proposed mechanism, the possible formation of the MW 212 organosulfate starts from the reactive capture of sulfate radical-anions by the isoprene unsaturated bond systems in an aqueous environment. The process begins by adding sulfate radicals, which are continuously produced through S(IV)-autoxidation mechanism, to one of the double bonds of the isoprene molecule, which leads to alkene radicals (Scheme 5.7). The latter is quenched by the molecular oxygen to afford peroxy radicals. In the next step, peroxy radicals can undergo the cross-reduction with available S(IV) species, such as HSO_3^- ions, to form alkoxy radicals. The newly form alkoxy radical can then follow two reaction pathways: (i) electron transfer to another reactant, such as SO_3^{2-} species and final protonation; or (ii) hydrogen abstraction, if available at the radical C atom, by another reactant, such as molecular oxygen O_2 . In the first scenario, hydroxyl alkene sulfates are formed, while in the second one, carbonyl alkene sulfates are produced. In both cases, reactive unsaturated polar intermediates are formed that open up further chain reactions: SO_3^- and HO_2 , respectively. Each alkene sulfate formed has a double C=C bond to which available sulfate radicals can add (second addition). Then, all the reactions that followed the first addition of the sulfate radical can take place. In each case, the reaction sequence concludes with the formation of methyl alkane disulfates that can undergo spontaneous cyclization to a lactone sulfate, with H_2SO_3 (H_2O and SO_2) as a leaving group. If the first and second series of the reactions include one electron transfer step and one hydrogen abstraction step, a methyl lactone sulfate (I) containing one hydroxyl and one carbonyl group (MW 212) is formed (Scheme 5.7). If the two series include two electron transfer steps, the product (II) contains two hydroxyl groups (MW 214 Da). If the series includes two hydrogen abstractions, the product (III) contains two carbonyl groups (MW 210 Da). The hydroxyl alkene sulfates and carbonyl alkene sulfates, which were identified as intermediates, were discussed in earlier experiments on the isoprene transformation coupled to S(IV)-autoxidation¹⁸³.



Scheme 5.7 The plausible formation mechanism of the MW 212 OS from isoprene in the aqueous solution is indispensably combined with the S(IV)-autooxidation process. A key step in this approach is an addition of the sulfate radical-anions onto the C=C bond.³⁶

5.1.6 Conclusions

In the research on the novel marker compound for isoprene aging processes in the atmosphere, the organosulfate with the MW 212 Da, a number of experiments were carried out to determine the probable structure of this compound, as well as to determine the enantiomers present in samples of natural atmospheric aerosol. Based on LC-MS analysis and fragmentation spectra performed with fine ambient PM_{2.5} aerosol samples and the results of semi-synthetic reactions in the aqueous phase, it was possible to identify seven peaks corresponding to the MW 212 OSs and assign their structures as 3-hydroxy-4-methyl-4-sulf-oxy-2(3H)-dihydrofuranones and 2,3-dihydroxy-4-methyl-4-sulfoxytetrahydrofuranes. The mechanisms that could lead to the formation of this important marker under atmospheric conditions have also been proposed. The work also showed the importance of optimizing analytical methods for the tested environmental samples and the importance of using complementary methods, as in the case of the use of reverse phase chromatography RP-C18 and the HILIC method, especially for the separation of polar compounds present in different positional isomeric and diastereomeric forms. According to my knowledge, the studies that make up the subsection described are the most comprehensive approach to research on the structure of organosulfates with MW 212 in the literature.¹⁹⁵

5.2 Radical oxidation of methyl vinyl ketone and methacrolein in aqueous droplets: characterization of organosulfates and atmospheric implications

The sulfate radical-anions are a strong driving factor in the aqueous droplets processing of isoprene and C4-C5 carbonyls, which leads to a series of organosulfates that are suitable markers of the polar fraction of SOA. The scope of the presented research was to study the molecular composition of aqueous SOA (aqSOA) generated by sunlight-induced aqueous photochemistry. This process is one of the potentially important routes in atmospheric SOA organosulfates formation. To verify this hypothesis, I used two main atmospherically-relevant products of isoprene oxidation, which are soluble in water – methacrolein (MACR) and methyl vinyl ketone (MVK). These model compounds were exposed to sulfate radicals. Potassium persulfate was used as a radical precursor under solar conditions. When looking for appropriate reaction products, literature reports presenting various methods of generating sulfate anion radicals in reactions with MVK were considered,^{196,197} according to the state of my current knowledge, no one used natural solar irradiation as a source of the UV light. The assumption of the research was to deploy reaction conditions, which are closest to natural ones, i.e., high dilutions of reaction solutions were used, and the source of UV radiation was only natural sunlight.

Parallely to the reactions carried out under exposure to radiation, a series of *dark tests* were carried out, which were identical in composition to the irradiated samples, except that reactions were carried out without access to light.

The decomposition of organic compounds (MVK, MACR) and the course of the reaction during each experiment was monitored by UV-Vis spectroscopy. The irradiation results were compared with those recorded under dark conditions to rule out chemical artifacts. For methyl vinyl ketone and methacrolein, the absorption maxima were measured in a short-wave UV range - an intense absorption bands are at the wavelengths of approx. 210 nm (MVK) and approx. 220 nm (MACR), corresponding to the $\pi \rightarrow \pi^*$ transition, respectively.

The products obtained during the reactions were characterized by ultra-high-performance liquid chromatography coupled with mass spectrometry. The data obtained from the experiments were compared with ambient PM_{2.5} samples collected during the

2014 summer campaign in northeastern rural areas of Poland (Masurian Voivodeship). The region is dominated by deciduous forests, a local source of isoprene and isoprene-oxidized volatile organic compounds, including MACR and MVK.

5.2.1 Reaction progress monitoring using UV-Vis

The study of the progress of the reaction over time using UV-Vis spectrophotometry (Fig. 5.16) clearly showed the disappearance of the characteristic absorption bands inherent in MACR and MVK, which could be expected that new products are formed during the ongoing process.

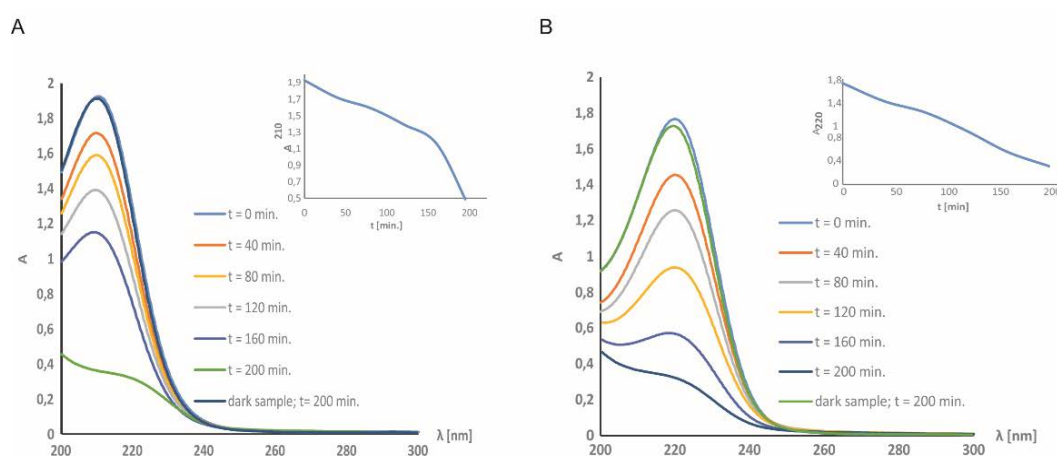


Figure 5.16 Decay of UV absorption bands recorded for A) methyl vinyl ketone (λ_{\max} 210 nm) and B) methacrolein (λ_{\max} 220 nm) during the reaction in the aqueous phase with sulfate radicals. The insets show the maxima of the absorption bands as a function of time.

The acquired UV spectra for reaction mixtures containing MVK and potassium persulfate before sun exposure and the dark sample (t = 200 min.) without sun exposure are comparable. The experiment was carried out for ca. 200 min. During this time, under the influence of solar radiation, the absorption loss is visible up to 160 min. of the experiment, in which there is a rapid decrease in absorption until its complete disappearance is about 200 min. The difference between a sample irradiated with the sun and a sample stored in a dark environment is clear (Fig. 5.16 A), indicating that naturally occurring UV light significantly accelerates the formation of secondary products due to the effective formation of radicals through photolysis.

Similar results were obtained in case of the experiment conducted with MACR. Although its decay proceeds far milder than in case of MVK, after 200 min. of the reaction, the absorption band for methacrolein indicates the consumption of a significant amount of the precursor. In the case of a dark sample, the absorption band does not markedly alter (Fig. 5.16 B).

5.2.2 Characteristics of MVK photooxidation reaction products in the aqueous phase

During the analysis of the reaction products, the focus was put on characterization of low-molecular weight organosulfates, containing from 3 to 4 carbon atoms in the structure, which are ubiquitous in ambient SOA masses.^{126,198} The results of MS analyzes are summarized in Table 5-IV. Their presence in ambient PM_{2.5} samples and aqueous-phase mimicking reactions is also compared, together with suggested structures.

Table 5-IV Organosulfates identified as reaction products in aqueous MVK processing in the presence of sulfate radicals.³⁸

Organic precursor	[M – H] ⁻	Error [mDa]	Formula	No. of isomers	Aqueous-phase reaction	Ambient sample	Suggested structure
MVK	152.9859	+ 0.1	C ₃ H ₅ O ₅ S	1	present	present	
MVK	154.9652	+ 0.2	C ₂ H ₃ O ₆ S	1	present	present	
MVK	167.0018	+ 0.4	C ₄ H ₇ O ₅ S	1	present	not	
MVK	182.9958	- 0.5	C ₄ H ₇ O ₆ S	2	present	one isomer is present (on the upper side)	
MVK	198.9911	- 0.1	C ₄ H ₇ O ₇ S	1	present	not	

5.2.2.1 SOA-derived organosulfate with the MW 154

The MW 154 organosulfate (formula $C_3H_5O_5S$) was determined as a single peak in the LC/MS analysis, both as one of aqueous-phase reaction products from MVK and as a component of the ambient $PM_{2.5}$ sample. The result of the experiment I conducted is consistent with previous literature reports.^{170,196} The plausible formation pathways for this organosulfate is the addition of SO_4 radicals to the unsaturated MVK bond system, which results in hydroxy acetone sulfate.^{170,196}

5.2.2.2 SOA- derived organosulfate with the MW 156

The MW 156 organosulfate (formula $C_2H_3O_6S$) is also present as a reaction product of MVK photo-oxidation in the aqueous phase and in ambient $PM_{2.5}$ samples. Like OS 154, it appears as a single chromatographic peak. It is a downstream oxidation product compared to the MW 154 OS. The mechanism by which the organosulfate is formed remains unknown. The available data suggest the formation of sulfated glycolic acid (Table 1) as a result of the reactive uptake of glyoxal by aerosol of ammonium sulfate seeds under the influence of irradiation.¹⁷⁰ The mechanism I propose differs from the one suggested so far; namely, under reaction conditions in the aqueous phase, the MW 156 OS may be formed as a result of adding a hydroxyl radical to hydroxy acetone sulfate.

5.2.2.3 SOA- derived organosulfate with the MW 168

The MW 168 organosulfate (formula $C_4H_7O_5S$) also appears as a reaction product in the aqueous phase, and as a component of secondary atmospheric load in ambient $PM_{2.5}$ samples; however, a detailed chromatographic analysis revealed that the MW 168 organosulfate may exist as two isobaric species, which emerge at different retention times. On this basis, it should be assumed that the oxidation of MVK in the aqueous phase is not a key process leading to the formation of the organosulfate in the atmospheric PM matter.

5.2.2.4 SOA- derived organosulfate with the MW 184

As a result of MVK photo-oxidation experiments in the presence of sulfate radical-anions, I also observed the presence of the MW 184 organosulfate in a form of two chromatographically-resolved peaks. This indicated the presence of two positional

isomers eluting sequentially at rt. 0.92 and 0.96 minutes, respectively (Fig 5.17 B, C₄H₇O₆S; HRMS: 182.9965; error: 0.2 mDa).

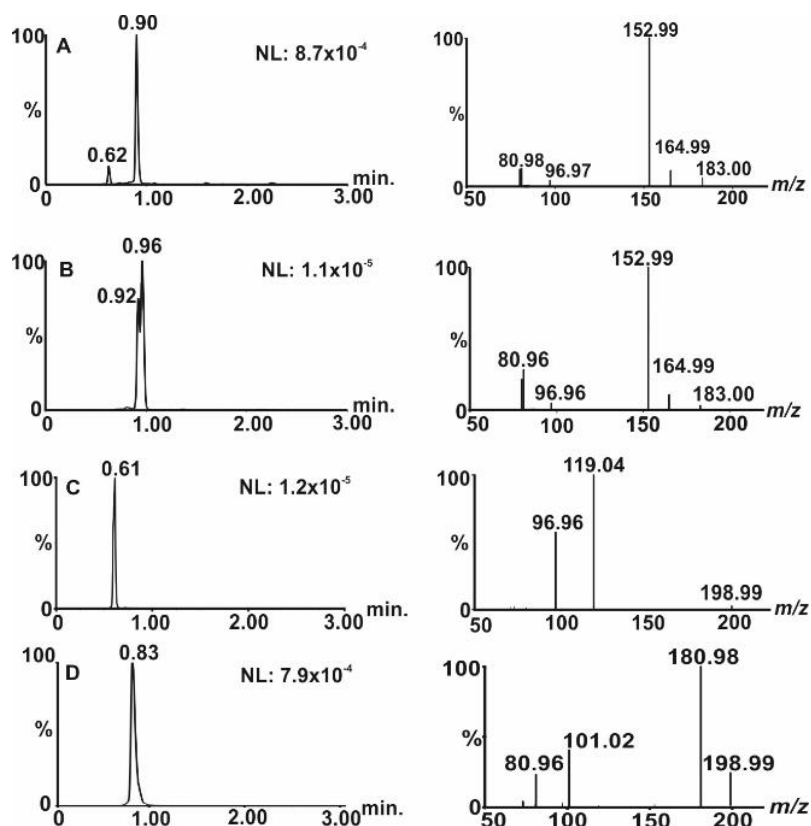


Figure 5.17 Extracted ion chromatograms along with negative ion electrospray product ion spectra recorded for A) m/z 183 ion in the fine ambient PM_{2.5} aerosol sample; B) m/z 183 ion in the MVK aqueous photo-oxidation sample (the product ion spectrum for the RT 0.92 min isomer shown in Fig 3); C) m/z 199 ion in the ambient PM_{2.5} aerosol sample; D) m/z 199 ion in the MVK aqueous photo-oxidation sample.³⁸

The fragmentation spectra recorded for both isomers showed some structural differences. The product ion mass spectrum m/z 183 recorded for the isomer at RT 0.96 min. shows the loss of a neutral formaldehyde molecule (m/z 183 \rightarrow m/z 153) as the major fragmentation pathway (Fig. 5.17 B), indicating the presence of a terminal primary OH group (Scheme 5.8 B2). In contrast, the second isomer with the RT 0.92 min. is dominated by the loss of HSO₄⁻ ion (m/z 97) (Fig. 5.18), suggesting the presence of a sulfated primary OH group and a secondary OH group in the backbone retained by MVK (Scheme 5.8 B1).

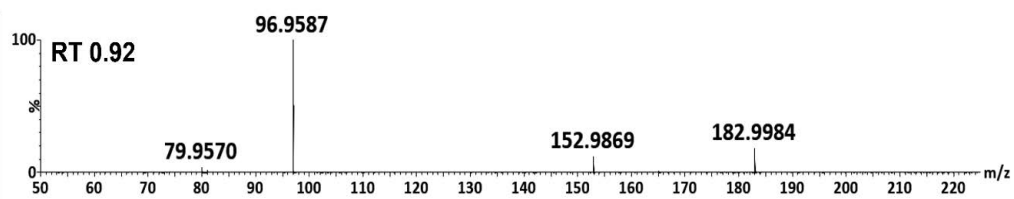
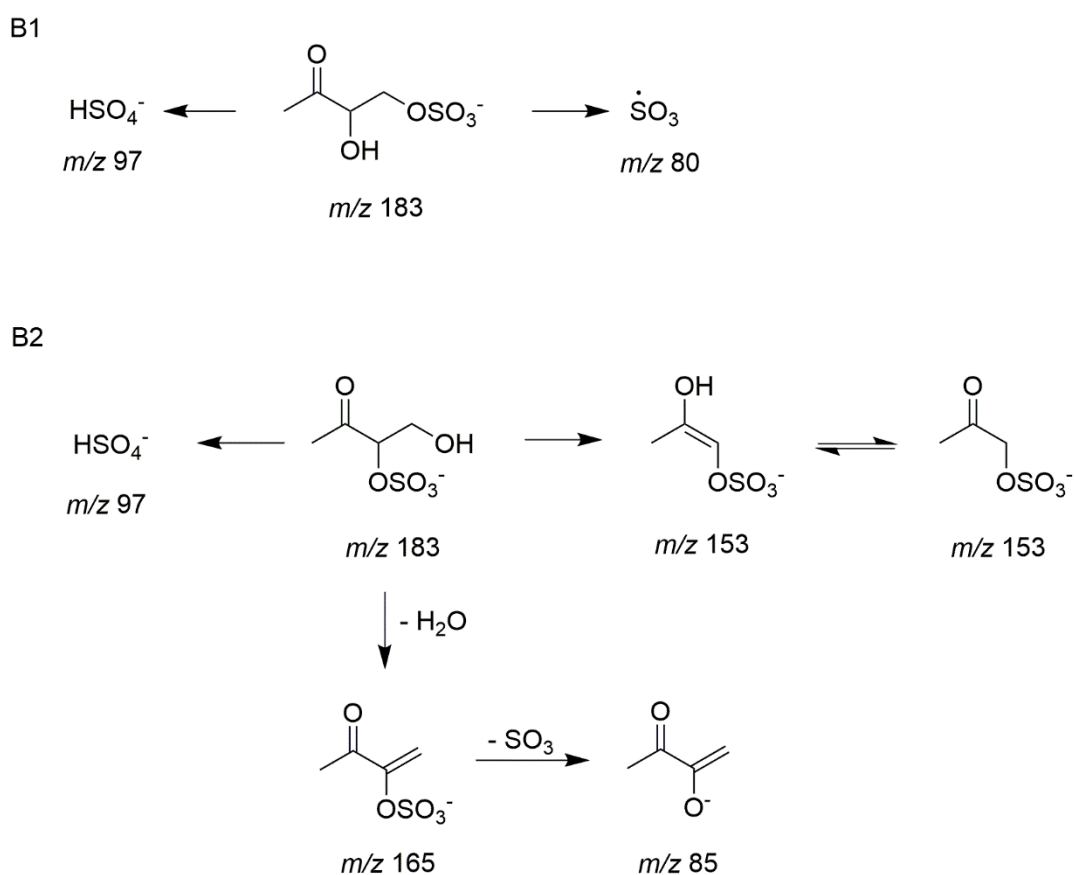


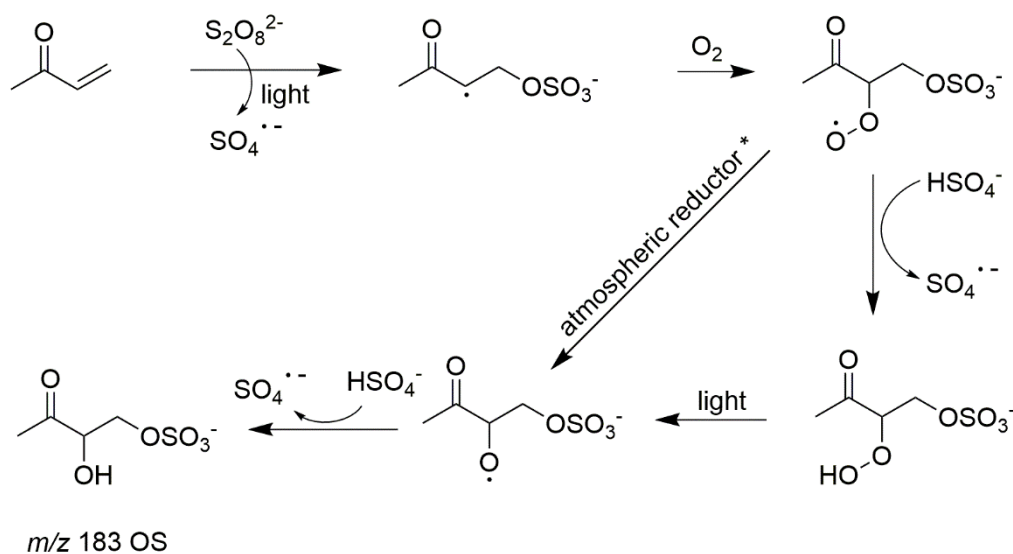
Figure 5.18 The negative ion electrospray product ion mass spectrum recorded for the m/z 183 diagnostic ion from the MVK aqueous photo-oxidation experiment reveals a characteristic m/z 183 \rightarrow m/z 97 transition.

Figure 5.18



Scheme 5.8 Proposed fragmentation pathways of the MW 184 organosulfate originating from MVK aqueous photo-oxidation mimicking experiments: B1) early-eluting isomer with retention time 0.92 min. and B2) late-eluting isomer with a retention time of 0.96 min.³⁸

A possible reaction path for the formation of the MW184 organosulfate with MVK is shown in Scheme 5.9. Sulfate radicals formed as a result of homolytic dissociation of peroxydisulfate initiate the reaction by addition to the C=C double bond of methyl vinyl ketone, giving rise to a dystonic radical with a negative charge located on the sulfate group and a radical on the carbon atom. This step is followed by adding a molecular oxygen to a radical center, which leads to a corresponding peroxy radical. In the further reaction, the latter detaches the hydrogen atom from the bisulfate ion, which is ubiquitous in experimental solutions, and turns into hydroperoxide. Under the influence of solar radiation, hydroperoxide can dissociate into OH and alkoxy radicals, which can then uptake a hydrogen atom and transform into an organosulfur product with the MW of 184 Da. There is also possibility of the peroxy radical \rightarrow alkoxy transition in atmospheric aqueous environment by other dissolved compounds, such as the ubiquitous S(IV) compounds.¹⁹⁹



Scheme 5.9 A tentative reaction mechanism explaining the formation of the MW 184 organosulfate from aqueous photo-oxidation of MVK. (with * was noted atmospherically- available red-ox systems, e.g., $\text{HSO}_3^-/\text{SO}_3^{2-} \rightarrow \text{HSO}_4^-/\text{SO}_4^{2-}$ ³⁸)

5.2.2.5 Organosulfate with the MW 200

The MW 200 organosulfate formed as a result of MVK transformations in the atmosphere was previously noted in the literature as a component of secondary

atmospheric aerosol.¹⁹⁶ In conducted experiments, I could determine the presence of this organosulfate in the post-reaction samples (RT 0.83 min; C₄H₇O₇S; measured mass: 198.9901; error: -1.1 mDa). However, I failed to confirm their presence in ambient aerosol samples using tandem mass spectrometric analysis. (Fig. 5.17 C,D).

5.2.3 Chemical signatures of MACR photooxidation reaction products in the aqueous-phase mimicking experiments

Similarly to the previous part of the experiment, the focus during the analysis of methacrolein photooxidation reaction products (Table 5-V) was on low-molecular organosulfates containing 3 to 4 carbon atoms. The extracted ion chromatograms for the discussed further methacrolein oxidation derived products are shown in Figure 5.19.

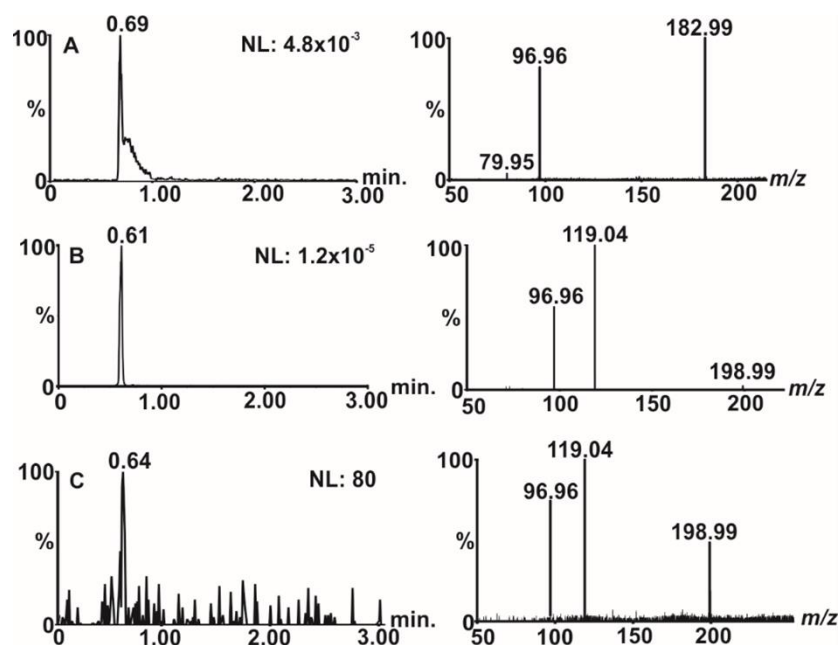


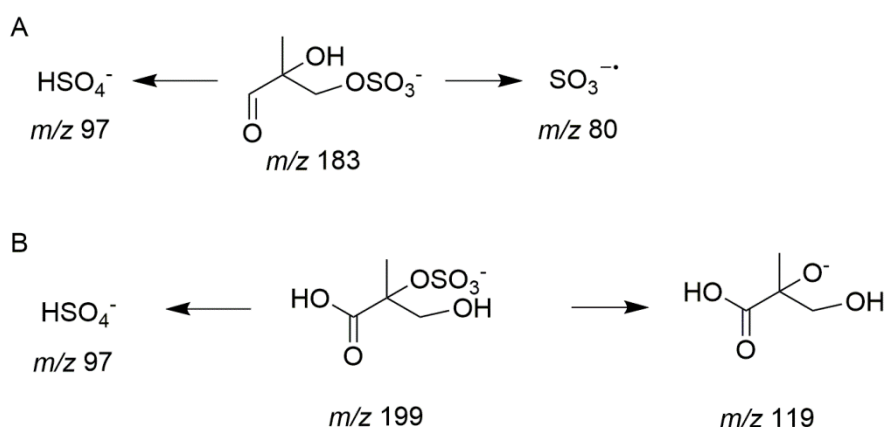
Figure 5.19 Extracted ion current chromatograms acquired for: A) m/z 183 from aqueous-photo oxidation of MACR 2) m/z 199 present in PM_{2.5} aerosol and C) m/z 199 resulting as a product of MACR photo-oxidation, along with product ion spectra for the mentioned ions.³⁸

5.2.3.1 Organosulfate with the MW 154

The organosulfate with the MW of 154 (RT 0.99 min; measured mass 152.9857; error 0.1 mDa; formula C₃H₅O₅S) is also formed as a result of MACR photo-oxidation in the presence of oxygenated sulfur radicals, as in the case of MVK (subs. 5.2.2.1).

5.2.3.2 Organosulfate with the MW 184

The organosulfate with the MW 184 (formula $C_4H_7O_6S$) formed in the reaction with MACR in the aqueous phase using a sulfate radical anion system, in contrast to the previously described product of the same mass in section 5.2.2.4, was observed in a fine ambient $PM_{2.5}$ aerosol sample (Fig. 5.19 A). Analyzing the fragmentation spectra for an ion with m/z 183 and taking into account that there is no loss of a neutral formaldehyde molecule observed, the probable position of the sulfate group is terminal. Scheme 5.10 A shows the proposed fragmentation pathways for the polar SOA component.



Scheme 5.10 Proposed fragmentation channels for forming MACR-derived organosulfates A) the MW 184 and B) the MW 200 formed *via* aqueous photo-oxidation reactions.³⁸

5.2.3.3 Organosulfate with MW 200

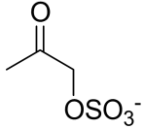
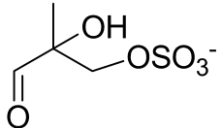
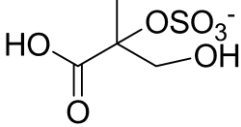
The MW 200 organosulfate was determined both as a product of the MACR photo-oxidation reaction in the presence of trace concentrations of sulfate radicals (RT 0.64; $C_4H_7O_7S$; measured mass 198.9927; error: 1.5 mDa) and in the ambient fine aerosol $PM_{2.5}$ sample (RT 0.61 min; $C_4H_7O_7S$; measured mass 198.9915, error: 0.3 mDa). Both compounds reveal similar elution times and show the identical fragmentation profiles (Fig. 5.19 B, C). A detailed interpretation of the product ion mass spectra along with the HRMS measurements indicate a structure containing a carboxyl group, a hydroxymethyl group, and a sulfate group located at the tertiary hydroxyl position. The formation of the bisulfate ion at m/z 97 (HSO_4^-) requires access to the proton on the adjacent carbon atom

(Scheme 5.10 B). The sulfate group located on the terminal carbon would make this fragmentation route the least likely.¹⁸⁸ Differences in retention times are observed between the ambient PM_{2.5} sample and the aqSOA sample. They are similar to those observed in the MW 184 MVK-derived organosulfates. In the ambient PM_{2.5} sample, the peak elutes slightly earlier, indicating a similar matrix effect.

5.2.4 Summary

In the course of the conducted project, I was able to demonstrate that SOA-bound low-molecular weight organosulfates present in ambient aerosol masses could form as a result of aqueous photo-oxidation reactions of α,β -unsaturated carbonyl compounds in the presence of sulfate radicals. Such processes may proceed in the water bulk, however for less soluble carbonyl precursors, e.g. MVK, multiphase chemical processes may play a dominant role in the atmosphere. Regardless of the process, through the laboratory efforts, I was able to characterize a number of organosulfur SOA components and confirm their presence in ambient aerosol samples. This also proved that laboratory mimicking experiments have a great potential in understanding the chemical composition of ambient aerosol loads. For instance, a thorough analysis of the LC/MS/MS data allowed to verify the structure of MVK-derived organosulfate with the MW 184 Da and to determine that it has a terminal sulfate group.

Table 5-V Organosulfates identified as reaction products in aqueous MACR processing in the presence of sulfate radicals.³⁸

Organic precursor	[M – H] ⁻	Error [mDa]	Formula	No. of isomers	Aqueous-phase reaction	Ambient sample	Suggested structure
MACR	152.9857	-0.1	C ₃ H ₅ O ₅ S	1	present	present	
MACR	182.9962	-0.1	C ₄ H ₇ O ₆ S	1	present	not	
MACR	198.9939	+1.5	C ₄ H ₇ O ₇ S	1	present	present	

5.3 Secondary Organic Aerosol markers in atmospheric waters

The identification of key SOA-bound components through the aqueous-phase processing of MVK and MAC prompted me to consider the presence of important components of secondary atmospheric aerosol in precipitation samples, such as rain, snow, and hail. Although cloud processes have been recognized as the relevant source of atmospheric SOA,^{200,201} precipitation analyses are rare, possibly due to the low sensitivity of the methods used to identify SOA markers at the molecular level. Having considered strong links between atmospheric chemistry and the importance of interfacial processes in the formation of secondary atmospheric aerosol components,^{136,202} and the fact that molecules with a high oxygen content in their structure significantly contribute to cloud condensation processes,²⁰³ this is certainly an area of atmospheric chemistry to be developed. It seems logical to launch a systematic study of the chemical composition of precipitation in order to extend the knowledge on the mechanisms of formation of secondary aerosol particles in the atmosphere. Until our research, there were not many literature reports on the chemical profile of atmospheric precipitation linked to secondary organic aerosol.²⁰⁴⁻²⁰⁷ None of them have performed the chromatography separation with identification of the species on a molecular level. Additionally, I found SOA organosulfates components, which contrast with the lately reported results by Bianco et al.²⁰⁸ Differences in results of measurements may result from different spectrometric techniques used in the studies.

Hydrometeors are able to transport particles of organic matter as well as solid particles on their surface or inside the droplet.²⁰⁹ During the research, we assumed that due to the dynamic nature of hail formation, it should not contain pollutants from the air, the core of the hail can be a representative sample of the chemical composition of water from the clouds. Similar assumptions were made in the case of snow and rain, but only for the purpose of conducting research.

The improved analytical methodology definitely facilitated the research process, because the sensitivity of the method allowed for direct testing of samples only after their prior concentration. Due to the fact that water was the best chromatographic solvent for the UHPLC-MS runs for organosulfates-targeted analyses, the snow and rain samples were only concentrated up to 100 μ L, as well as the hail samples after washing the outer

layer with ultrapure water. This concentration level was sufficient for the analysis. For abundant analytes, 1 μl injection volume was enough for satisfactory results, in other cases the injection volume was increased to 10 μl .

Organosulfates were the first individuals whose presence we decided to check, mainly due to the fact that we already had an experience with analyzing this particular group of compounds, as well as we had a library of filters and a database to which we could relate the new results. In the following paragraph, I will describe the results of the analyzes focusing on these particular SOA species.

5.3.1 Organosulfates MW 184, MW 212, MW 214 and MW 216 in atmospheric precipitates

Organosulfates with the MW 184 have been observed in both rain and hail samples. The extracted ion currents for the m/z 183 ion showed a major peak at RT 0.90 min.(Figure 5.19), with a high intensity similar to the ones observed in samples of hail and the PM_{2.5} fine ambient aerosol samples. The intensity for this organosulfate in the rain was significantly lower than for the other two samples, despite the increase in sample injection up to 10 μL .

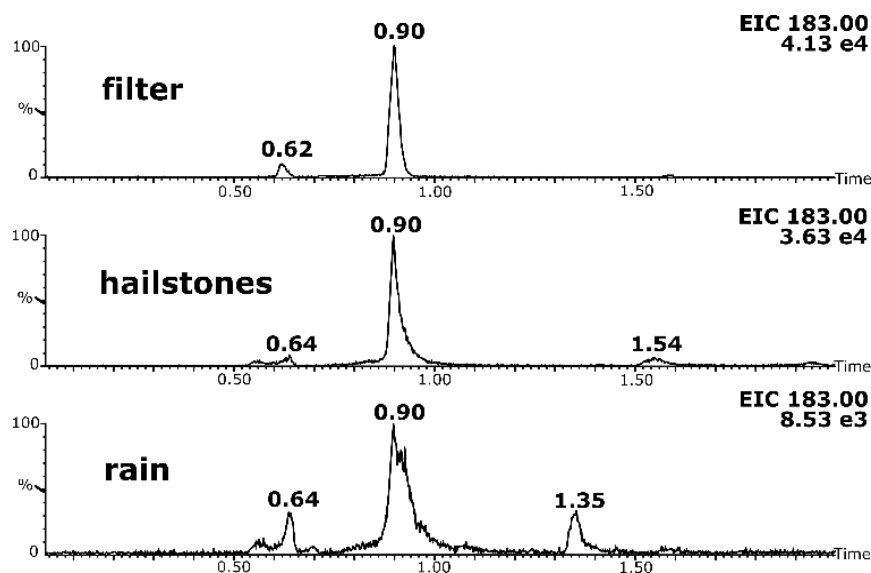


Figure 5.20 LC/MS extracted ion chromatograms for a target m/z 183 ion in PM_{2.5} fine ambient aerosol, hailstone and rain sample.

Due to the low intensity of the parent ion in the rain samples, the fragmentation spectra were not considered conclusive (Fig. 5.17 A), however, characteristic fragmentation ions for this compound are visible, the same as in the case of MW 184 OS present in PM_{2.5} samples (Fig. 5.21 B) or in the reactions of methyl vinyl ketone photooxidation (Fig. 5.17 B).

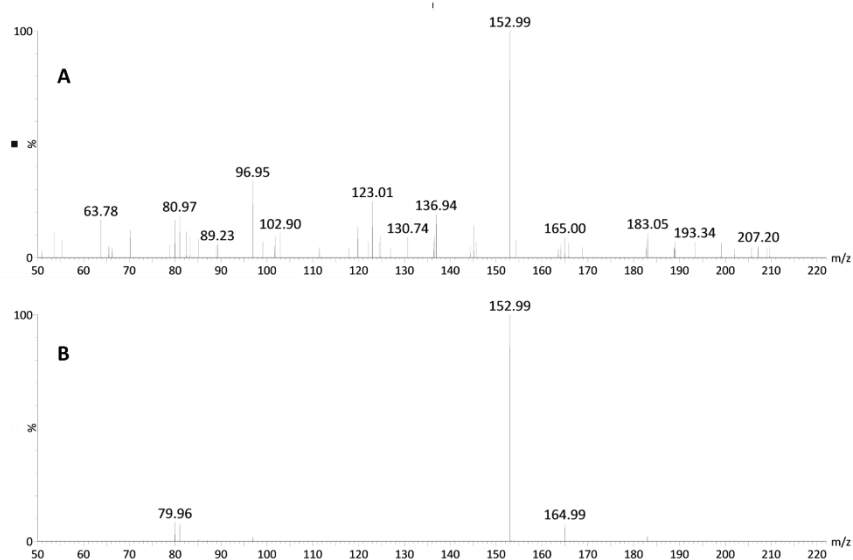


Figure 5.21 Negative electrospray product ion mass spectra for the m/z 183 ion present in a rain sample (A) and PM_{2.5} fine ambient aerosol (B).

In the case of methyl-dihydroxy- γ -lactones sulfate esters (organosulfates with the MW 212 Da) and methyl-trihydroxyaldehydes cyclic hemiacetals sulfate esters (organosulfates with the MW 214 Da), well-known isoprene-derived organosulfates,^{5,186} the intensities in hailstone and rain samples are lower than in PM_{2.5} fine ambient aerosol samples (Fig. 5.22). The chromatographic profile of the peaks is the same in all three compared samples. Due to the same chromatographic profile, it can be assumed that these components correspond to the same positional isomers and moreover, that they are formed by the same chemical processes.

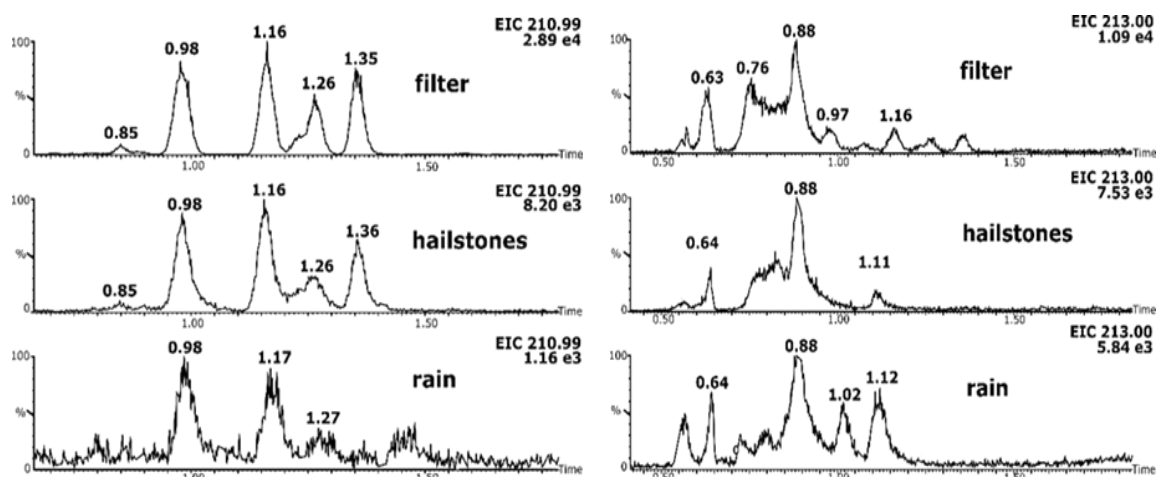


Figure 5.22 Extracted ion chromatograms for ions m/z 211 (left side) and m/z 214 (right side) in $PM_{2.5}$ fine ambient aerosol, hailstone and rain samples.

Other organosulfates, which were determined in atmospheric water precipitates, were one of the most abundant SOA markers with the MW 216 OS (i.e., 2-methyltetrols sulfate esters)^{30,57}. The presence of these compounds was recorded in both hail and rain samples with very good intensities, comparable in each of the tested samples to the content of this marker in samples of $PM_{2.5}$ fine ambient aerosol (Fig. 5.23).

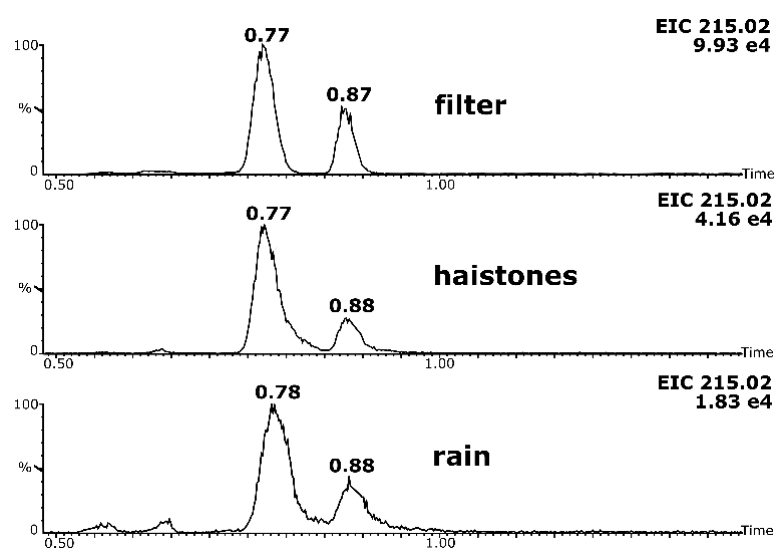


Figure 5.23 LC/MS extracted ion chromatograms for the m/z 215 ion in $PM_{2.5}$ ambient fine aerosol, hailstone and rain samples.

Due to the high content of organosulfates in the samples, it was possible to acquire the fragmentation spectra, which allowed to confirm the identity of the observed m/z 215 ions eluting with RT 0.77 min. and RT 0.88 min. (Figure 5.24).

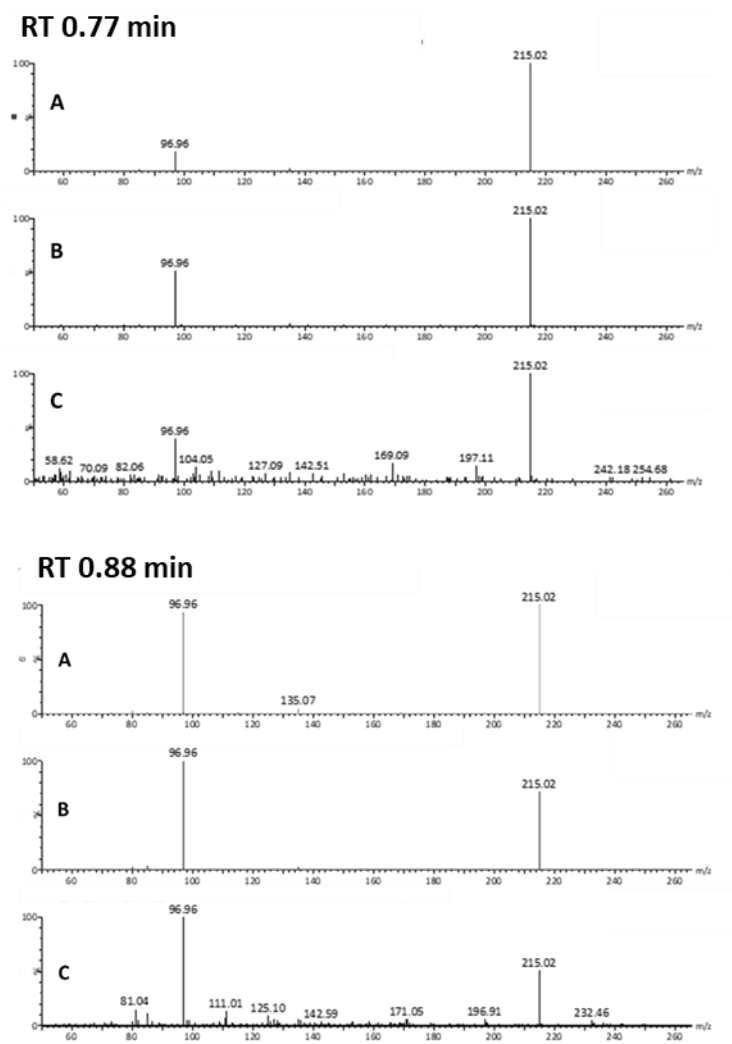


Figure 5.24 Negative electrospray product ion mass spectra of the m/z 215 ions sequentially eluting at RT 0.77 min. (upper) and 0.88 min. (bottom), respectively in A: PM_{2.5} ambient fine aerosol (injection volume 2 μ l), B: hailstone (injection volume 5 μ l), C: rain (injection volume 10 μ l). Spectra were recorded with CE 20 eV.

The differences in the relative intensity of the MW 212 OS and the MW 214 OS compared to the MW 216 OS were observed in a great number of samples analyzed. Due to the structural similarities of these organosulfates, I put forward the hypothesis that their formation could be linked to further oxidation (aging) processes of SOA-bound 2-methyltetrol. At least it would explain the presence in their structures of either hemiacetal or 5-membered lactone residues.

Another important observation was the differences noted between the samples collected in the summer and winter (Chart 5-2). It was noted that samples taken during the winter had significantly higher responses for hydroxy acetone sulfate (the MW 154

OS). Due to the limited number of samples and the lack of analytical standards, these observations were made only on the basis of relative peak intensities, however, taking into account the structural and chemical similarity of the tested compounds, some trends noticeable in the tested samples can be estimated on this basis.

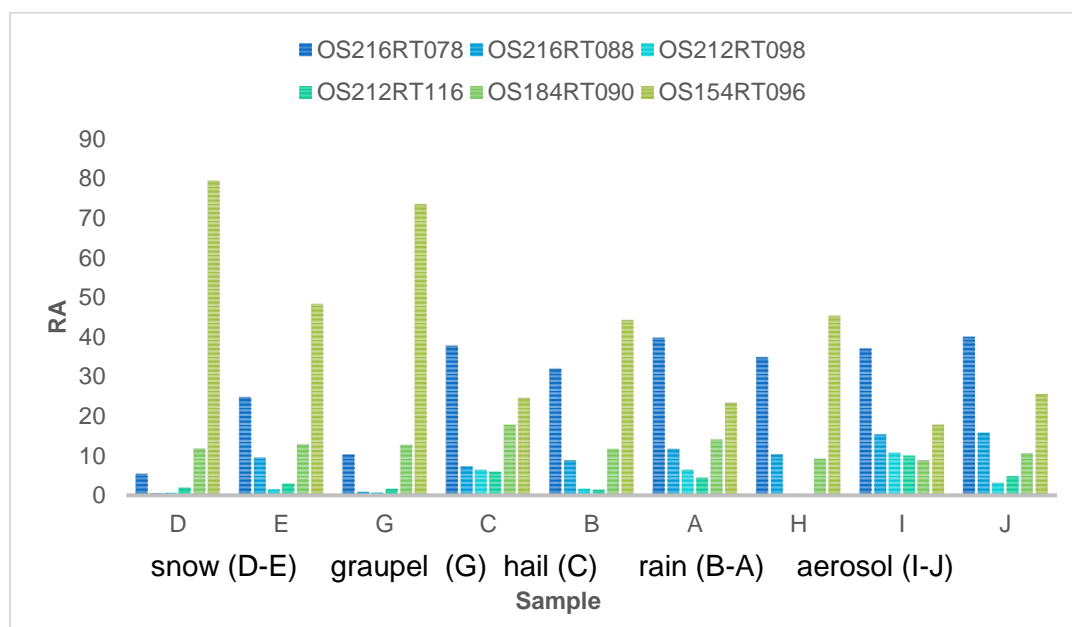


Chart 5-2 The relative abundance for selected organosulfates detected in the atmospheric waters samples collected in Poland during different seasons and locations: (A) summer rural rain sample collected in Woziwoda; B) autumn urban rain sample collected in Warsaw; C) late summer hailstone sample collected in Warsaw; D) and E) urban snow samples collected in Warsaw; F) winter rural snow sample collected in Puszcza Borecka; G) urban graupel sample collected in Skawina during late winter; H-J) PM_{2.5} fine ambient aerosol samples collected in Puszcza Borecka. The legend: OS nominal mass followed by retention time of structural isomer×100.

5.3.2 Conclusions

In the course of a project devoted to determination of secondary atmospheric aerosol components in precipitation, I identified the presence of important markers of isoprene transformations in the atmosphere, i.e., 2-MT and the MW 212 organosulfate, either confirmed in ambient aerosol samples. While the abundance of these individuals in precipitates samples is lower than in the case of fine ambient PM_{2.5} aerosol, it is sufficient to perform full LC-MS analysis on only concentrated samples and sufficient to perform fragmentation spectra to confirm the identity of the observed organosulfate isomers. In the course of research on contribution of secondary atmospheric aerosol in

precipitates, apart from organosulfates, other organic compounds and nitroxyorganosulfates were firmly identified.¹⁹

6 Summary

During my doctoral studies at the Institute of Physical Chemistry of the Polish Academy of Sciences, I planned and executed a number of experiments covering the chemical analysis of selected abundant polar fraction-residing components of secondary atmospheric aerosol. The most extensive part of the research was concerned with the elucidation of the isoprene aerosol aging marker, namely the abundant MW 212 organosulfate, noted in numerous field, smog chamber and laboratory studies, however without a firm structural signature. As a part of the qualitative research, I performed LC/MS and LC/MS/MS analyses for fine ambient PM_{2.5} aerosol samples collected from various continental rural sites and conducted a series of aqueous-phase oxidation mimicking reactions with sulfate radicals in order to authenticate the proposed chemical structure(s) for the target MW 212 OS compound. The optimization of the LC/MS experimental conditions at the initial phase resulted in the satisfactory findings, allowing the firm identification of four main chromatographic peaks for the [M-H]⁻ ion (*m/z* 211) in the laboratory-generated SOA samples and ambient aerosol. The further efforts on improving the analytical LC/MS method for the target MW 212 OS, combined with a thorough interpretation of product ion mass spectra for their individual stereoisomers, allowed for the first time for the identification of its seven isomeric structures, namely, of 3-hydroxy-4-methyl-4-sulf-oxy-2(3H)-dihydrofuranones and 2,3-dihydroxy-4-methyl-4-sulfoxytetrahydrofuranes, respectively. The high resolution mass data for diagnostic ions in their MS/MS spectra made it possible to propose rational structures for their four isomers (in the remaining three cases the fragmentation was too poor for unambiguous structural determination). During my study, I also proposed the tentative mechanism for the formation of organosulfates with the MW 212 Da in the atmosphere. The process assumes a chain of chemical aging reactions, i.e., the oxidation of SOA-bound 2-MT with the formation of a carboxyl group with a subsequent lactonization of the terminal hydroxyl group with the carboxyl group. The current state of knowledge allows me to conclude that there are at least several possible ways of the formation of the MW 212 organosulfates, this is only one of the possible ways. Due to the fact that I was

able to obtain the same products as a result of the degradation of isoprene in the aqueous phase in the presence of sulfate anion radicals and transition metal cations, I proposed another likely mechanism, starting with the addition of sulfate radical-anions to the isoprene double bond, followed by a series of reactions as a result of which one of the final products may arise as the structure of hydroxymethyl-sulfoxytetrahydrofuranone.

The second area of my research was the verification of the hypothesis that through aqueous-phase oxidative degradation of α , β -unsaturated carbonyls under close-to-natural conditions, I was able to mimic the formation of numerous components of secondary organic aerosol in the atmosphere. For this purpose, I carried out a series of experiments, in which the source of radiation was sunlight radiation, while the source of radical oxidants were sulfate radicals formed as a result of photolytic decomposition. In the reactions with unsaturated carbonyls, such as methyl vinyl ketone and methacrolein, I succeeded in the firm identification of three MVK-derived organosulfates and two MACR-derived organosulfates that I contribute to ambient aerosol masses. These findings shed light for alternative organosulfate formation mechanisms in the tropospheric aerosol through the multiphase sulfoxy radicals uptake by the double bonds of unsaturated precursors in atmospheric water droplets. The access for these radicals is allowed *via* a transition metal ion-catalyzed oxidation chain of S(IV)-species, that is a process, which underlines the acid rain formation in the atmosphere.

Undoubtedly, an important part of the research results was the verification of the structure of the MVK-derived MW 184 organosulfate observed in SOA - after a thorough analysis of the fragmentation spectra, I assigned the correct structure of the isomer found in the natural environment.

In the last part of my research, I examined samples of atmospheric precipitation (i.e., rain, snow, hail) for the presence of organic SOA compounds that are observed in atmospheric aerosol samples. In particular, I was interested in organosulfates, which I had previously observed in fine ambient PM_{2.5} samples, that is MW 154 OS, MW 184 OS MW 212 OS and MW 216 OS. The conducted LC/MS and LC/MS/MS analyses proved that the chemical screening of aqueous SOA samples from laboratory experiments can provide valuable information about the role of cloud droplets in the atmospheric formation of aerosol particles through multiphase chemistry.

Understanding the complex interactions between aerosols, clouds, and precipitation is crucial to reduce the uncertainty of climate change prediction. Recent satellite observations²¹⁰ have found a positive correlation between aerosols and precipitation, suggesting that the impact of aerosols on precipitation is more complex than previously thought. Additionally, the study of secondary organic aerosol markers in atmospheric waters has the potential to provide valuable insights into the transport and transformation of pollutants in the atmosphere, and to improve our understanding of the Earth's climate system. Although the study of organosulfates in atmospheric precipitation is still in its early stages, further research is warranted to fully comprehend the behavior of SOA in aqueous environments and to develop more accurate methods for their analysis.

Until research described within this thesis, the chemical characterization of SOA components at the molecular level was carried out mainly on ambient aerosol samples. Studies have shown that the components identified in fine ambient aerosol are also present in precipitation samples, with varying abundance, with respect to relative intensities. These studies may lead to the conclusion that chemistry at the interface or in-cloud water droplets may play an important role in determining the transformations of the main components of secondary atmospheric aerosols. Moreover, the information gathered from these studies can be used to develop more accurate models of atmospheric chemistry and improve our understanding of the Earth's climate system.

The data reported here advances the chemical research on secondary organic aerosol composition with an emphasis on the organosulfate formation through multiphase processing. At this stage, however, it should be noted that further efforts are still required to better understand the chemical processes occurring in the atmosphere¹⁹⁵. A particular attention is paid for further development of robust LC/MS methods to explain the organosulfates' origin in environmental samples.¹³⁹ It is also a challenge to design the synthetic protocols for analytical standards for unquestionable confirmation of the structures of the identified SOA-derived components, as well as the possibility of performing a full quantitative analysis. Advances in these areas will help deepen our understanding of the transformations of volatile organic compounds in the atmosphere, which in turn may contribute to a full understanding of their role in the atmospheric system.

7 References

- (1) Kroll, J. H.; Seinfeld, J. H. Chemistry of secondary organic aerosol: Formation and evolution of low-volatility organics in the atmosphere. *Atmospheric Environment* **2008**, *42*, 3593-3624.
- (2) Kroll, J. H.; Smith, J. D.; Che, D. L.; Kessler, S. H.; Worsnop, D. R.; Wilson, K. R. Measurement of fragmentation and functionalization pathways in the heterogeneous oxidation of oxidized organic aerosol. *Physical Chemistry Chemical Physics* **2009**, *11*, 8005-8014.
- (3) Yu, L.; Smith, J.; Laskin, A.; George, K. M.; Anastasio, C.; Laskin, J.; Dillner, A. M.; Zhang, Q. Molecular transformations of phenolic SOA during photochemical aging in the aqueous phase: competition among oligomerization, functionalization, and fragmentation. *Atmospheric Chemistry and Physics* **2016**, *16*, 4511-4527.
- (4) Hallquist, M.; Wenger, J. C.; Baltensperger, U.; Rudich, Y.; Simpson, D.; Claeys, M.; Dommen, J.; Donahue, N. M.; George, C.; Goldstein, A. H.; Hamilton, J. F.; Herrmann, H.; Hoffmann, T.; Iinuma, Y.; Jang, M.; Jenkin, M. E.; Jimenez, J. L.; Kiendler-Scharr, A.; Maenhaut, W.; McFiggans, G.; Mentel, T. F.; Monod, A.; Prévôt, A. S. H.; Seinfeld, J. H.; Surratt, J. D.; Szmigielski, R.; Wildt, J. The formation, properties and impact of secondary organic aerosol: current and emerging issues. *Atmos. Chem. Phys.* **2009**, *9*, 5155.
- (5) Noziere, B.; Kalberer, M.; Claeys, M.; Allan, J.; D'Anna, B.; Decesari, S.; Finessi, E.; Glasius, M.; Grgic, I.; Hamilton, J. F.; Hoffmann, T.; Iinuma, Y.; Jaoui, M.; Kahnt, A.; Kampf, C. J.; Kourttchev, I.; Maenhaut, W.; Marsden, N.; Saarikoski, S.; Schnelle-Kreis, J.; Surratt, J. D.; Szidat, S.; Szmigielski, R.; Wisthaler, A. The molecular identification of organic compounds in the atmosphere: state of the art and challenges. *Chem. Rev.* **2015**, *115*, 3919-3983.
- (6) Turner, J. a. C., I.: Physical and Chemical Properties of Atmospheric Aerosols. In *Environmental Chemistry of Aerosols*; Colbeck, I., Ed., 2009; pp 1-29.
- (7) Aaltonen, V.; Lihavainen, H.; Kerminen, V.-M.; Komppula, M.; Hatakka, J.; Eneroth, K.; Kulmala, M.; Viisanen, Y. Measurements of optical properties of atmospheric aerosols in Northern Finland. *Atmospheric Chemistry and Physics* **2006**, *6*, 1155-1164.
- (8) Jacobson, M. C.; Hansson, H.-C.; Noone, K. J.; Charlson, R. J. Organic atmospheric aerosols: Review and state of the science. *Reviews of Geophysics* **2000**, *38*, 267-294.
- (9) Shiraiwa, M.; Selzle, K.; Pöschl, U. Hazardous components and health effects of atmospheric aerosol particles: reactive oxygen species, soot, polycyclic aromatic compounds and allergenic proteins. *Free Radical Research* **2012**, *46*, 927-939.
- (10) WHO. *Health risks of air pollution in Europe - HRAPIE project: New emerging risks to health from air pollution - Results from the survey of experts.*: Copenhagen2013.
- (11) Whitby, K. T.; Sverdrup, G. M. California aerosols - their physical and chemical characteristics. *Adv. Environ. Sci. Technol.* **1980**, *9*.
- (12) Gordon, G. E. *Chemistry of the Natural Atmosphere*. Peter Warneck. Academic Press, San Diego, CA, 1988. xiv, 757 pp., illus. \$85. International Geophysics Series, vol. 41. *Science* **1988**, *242*, 121-122.
- (13) Andreae, M. O.; Elbert, W.; de Mora, S. J. Biogenic sulfur emissions and aerosols over the tropical South Atlantic: 3. Atmospheric dimethylsulfide, aerosols and cloud condensation nuclei. *Journal of Geophysical Research: Atmospheres* **1995**, *100*, 11335-11356.

- (14) Pacyna, J. M.: Sources, Particle Size Distribution and Transport of Aerosols. In *Airborne Particulate Matter. The Handbook of Environmental Chemistry*; T., K., C., S., Eds.; Springer: Berlin, 1995; Vol. 4/4D.
- (15) Spijksma, F. T. M. *Bioaerosols Handbook*. Edited by C. S. Cox and C. M. Wathes. Boca Raton & London: CRC/Lewis (1995), pp.623, £58.00. ISBN 1-87371-615-9. *Experimental Agriculture* **1997**, *33*, 113-119.
- (16) Hinds, W. C.: *Aerosol Technology: Properties, Behavior, and Measurement of Airborne Particles*; Wiley, 1999.
- (17) Pöschl, U. Atmospheric Aerosols: Composition, Transformation, Climate and Health Effects. *Angewandte Chemie International Edition* **2005**, *44*, 7520-7540.
- (18) Winiwarter, W.; Bauer, H.; Caseiro, A.; Puxbaum, H. Quantifying emissions of primary biological aerosol particle mass in Europe. *Atmospheric Environment* **2009**, *43*, 1403-1409.
- (19) Spolnik, G.; Wach, P.; Rudziński, K. J.; Szmigielski, R.; Danikiewicz, W. Tracing the biogenic secondary organic aerosol markers in rain, snow and hail. *Chemosphere* **2020**, *251*, 126439.
- (20) Rodigast, M.; Mutzel, A.; Schindelka, J.; Herrmann, H. A new source of methylglyoxal in the aqueous phase. *Atmospheric Chemistry and Physics* **2016**, *16*, 2689-2702.
- (21) Nozière, B. Don't forget the surface. *Science* **2016**, *351*.
- (22) Sareen, N.; Carlton, A. G.; Surratt, J. D.; Gold, A.; Lee, B.; Lopez-Hilfiker, F. D.; Mohr, C.; Thornton, J. A.; Zhang, Z.; Lim, Y. B.; Turpin, B. J. Identifying precursors and aqueous organic aerosol formation pathways during the SOAS campaign. *Atmos. Chem. Phys.* **2016**, *16*, 14409-14420.
- (23) Lighty, J. S.; Veranth, J. M.; Sarofim, A. F. Combustion Aerosols: Factors Governing Their Size and Composition and Implications to Human Health. *Journal of the Air & Waste Management Association* **2000**, *50*, 1565-1618.
- (24) Okazaki, K. Submicron particle formation in pulverized coal combustion. *J. Aerosols. Res. Jpn.* **1993**, *7*, 289-291.
- (25) Guenther, A. B.; Jiang, X.; Heald, C. L.; Sakulyanontvittaya, T.; Duhl, T.; Emmons, L. K.; Wang, X. The Model of Emissions of Gases and Aerosols from Nature version 2.1 (MEGAN2.1): an extended and updated framework for modeling biogenic emissions. *Geosci. Model Dev.* **2012**, *5*, 1471-1492.
- (26) Sharkey, T. D.; Wiberley, A. E.; Donohue, A. R. Isoprene Emission from Plants: Why and How. *Annals of Botany* **2007**, *101*, 5-18.
- (27) Sharkey, T. D.; Singsaas, E. L. Why plants emit isoprene. *Nature* **1995**, *374*, 769-769.
- (28) Benjamin, M. T.; Sudol, M.; Bloch, L.; Winer, A. M. Low-emitting urban forests: A taxonomic methodology for assigning isoprene and monoterpene emission rates. *Atmospheric Environment* **1996**, *30*, 1437-1452.
- (29) Loreto, F.; Velikova, V. Isoprene Produced by Leaves Protects the Photosynthetic Apparatus against Ozone Damage, Quenches Ozone Products, and Reduces Lipid Peroxidation of Cellular Membranes. *Plant Physiology* **2001**, *127*, 1781-1787.
- (30) Claeys, M.; Graham, B.; Vas, G.; Wang, W.; Vermeylen, R.; Pashynska, V.; Cafmeyer, J.; Guyon, P.; Andreae, M. O.; Artaxo, P.; Maenhaut, W. Formation of secondary organic aerosols through photooxidation of isoprene. *Science* **2004**, *303*, 1173-1176.
- (31) Chan, M. N.; Surratt, J. D.; Claeys, M.; Edgerton, E. S.; Tanner, R. L.; Shaw, S. L.; Zheng, M.; Knipping, E. M.; Eddingsaas, N. C.; Wennberg, P. O.; Seinfeld, J. H. Characterization and quantification of isoprene-derived epoxydiols in ambient aerosol in the southeastern United States. *Environ. Sci. Technol.* **2010**, *44*, 4590-4596.

- (32) Cheung, K.; Guo, H.; Ou, J. M.; Simpson, I. J.; Barletta, B.; Meinardi, S.; Blake, D. R. Diurnal profiles of isoprene, methacrolein and methyl vinyl ketone at an urban site in Hong Kong. *Atmospheric Environment* **2014**, *48*, 323-331.
- (33) Darer, A. I.; Cole-Filipiak, N. C.; O'Connor, A. E.; Elrod, M. J. Formation and stability of atmospherically relevant isoprene-derived organosulfates and organonitrates. *Environ Sci Technol* **2011**, *45*, 1895-1902.
- (34) Surratt, J. D.; Murphy, S. M.; Kroll, J. H.; Ng, N. L.; Hildebrandt, L.; Sorooshian, A.; Szmigielski, R.; Vermeylen, R.; Maenhaut, W.; Claeys, M.; Flagan, R. C.; Seinfeld, J. H. Chemical Composition of Secondary Organic Aerosol Formed from the Photooxidation of Isoprene. *J. Phys. Chem. A* **2006**, *110*, 9665-9690.
- (35) Riva, M.; Budisulistiorini, S. H.; Chen, Y.; Zhang, Z.; D'Ambro, E. L.; Zhang, X.; Gold, A.; Turpin, B. J.; Thornton, J. A.; Canagaratna, M. R.; Surratt, J. D. Chemical Characterization of Secondary Organic Aerosol from Oxidation of Isoprene Hydroxyhydroperoxides. *Environ. Sci. Technol.* **2016**, *50*, 9889-9899.
- (36) Wach, P.; Spólnik, G.; Surratt, J. D.; Blaziak, K.; Rudziński, K. J.; Lin, Y.-H.; Maenhaut, W.; Danikiewicz, W.; Claeys, M.; Szmigielski, R. Structural Characterization of Lactone-Containing MW 212 Organosulfates Originating from Isoprene Oxidation in Ambient Fine Aerosol. *Environmental Science & Technology* **2020**, *54*, 1415-1424.
- (37) Szmigielski, R. Evidence for C5 organosulfur secondary organic aerosol components from in-cloud processing of isoprene: Role of reactive SO₄ and SO₃ radicals. *Atmos. Environ.* **2016**, *130*, 14-22.
- (38) Wach, P.; Spólnik, G.; Rudziński, K. J.; Skotak, K.; Claeys, M.; Danikiewicz, W.; Szmigielski, R. Radical oxidation of methyl vinyl ketone and methacrolein in aqueous droplets: characterization of organosulfates and atmospheric implications. *Chemosphere* **2019**, *214*, 1.
- (39) Guenther, A.; Hewitt, C. N.; Erickson, D.; Fall, R.; Geron, C.; Graedel, T.; Harley, P.; Klinger, L.; Lerdau, M.; McKay, W. A.; Pierce, T.; Scholes, B.; Steinbrecher, R.; Tallamraju, R.; Taylor, J.; Zimmerman, P. A global model of natural volatile organic compound emissions. *Journal of Geophysical Research: Atmospheres* **1995**, *100*, 8873-8892.
- (40) Tomasi, C. a. L., A.: Coagulation, Condensation, Dry and Wet Deposition, and Cloud Droplet Formation in the Atmospheric Aerosol Life Cycle. In *Atmospheric Aerosols*; Tomasi, C., Fuzzi, S., Kokhanovsky, A., Eds., 2016; pp 115-182.
- (41) Ervens, B.; Turpin, B. J.; Weber, R. J. Secondary organic aerosol formation in cloud droplets and aqueous particles (aqSOA): a review of laboratory, field and model studies. *Atmospheric Chemistry and Physics* **2011**, *11*, 11069-11102.
- (42) Bianco, A.; Deguillaume, L.; Vařtilingom, M.; Nicol, E.; Baray, J.-L.; Chaumerliac, N.; Bridoux, M. Molecular Characterization of Cloud Water Samples Collected at the Puy de Dôme (France) by Fourier Transform Ion Cyclotron Resonance Mass Spectrometry. *Environmental Science & Technology* **2018**, *52*, 10275-10285.
- (43) EEA. *Air quality in Europe — 2019 report* for Publications Office of the European Union: Luxembourg 2019.
- (44) Atkinson, S. M. A. a. R. Formation Yields of Methyl Vinyl Ketone and Methacrolein from the Gas-Phase Reaction of O₃ with Isoprene. *Environ. Sci. Technol.* **1994**, *28*, 1539-1542.
- (45) Barrie, L.; Platt, U. Arctic tropospheric chemistry: an overview. *Tellus B* **1997**, *49*, 450-454.
- (46) Oum, K. W.; Lakin, M. J.; Finlayson-Pitts, B. J. Bromine activation in the troposphere by the dark reaction of O₃ with seawater ice. *Geophysical Research Letters* **1998**, *25*, 3923-3926.
- (47) Seinfeld, J. H.; Pankow, J. F. Organic Atmospheric Particulate Material. *Annual Review of Physical Chemistry* **2003**, *54*, 121-140.

- (48) Pandis, S. N.; Harley, R. A.; Cass, G. R.; Seinfeld, J. H. Secondary organic aerosol formation and transport. *Atmospheric Environment. Part A. General Topics* **1992**, *26*, 2269-2282.
- (49) Shrivastava, M.; Cappa, C. D.; Fan, J.; Goldstein, A. H.; Guenther, A. B.; Jimenez, J. L.; Kuang, C.; Laskin, A.; Martin, S. T.; Ng, N. L.; Petaja, T.; Pierce, J. R.; Rasch, P. J.; Roldin, P.; Seinfeld, J. H.; Shilling, J.; Smith, J. N.; Thornton, J. A.; Volkamer, R.; Wang, J.; Worsnop, D. R.; Zaveri, R. A.; Zelenyuk, A.; Zhang, Q. Recent advances in understanding secondary organic aerosol: Implications for global climate forcing. *Reviews of Geophysics* **2017**, *55*, 509-559.
- (50) Went, F. W. Blue Hazes in the Atmosphere. *Nature* **1960**, *187*, 641-643.
- (51) Rasmussen, R. A.; Went, F. W. VOLATILE ORGANIC MATERIAL OF PLANT ORIGIN IN THE ATMOSPHERE. *Proceedings of the National Academy of Sciences of the United States of America* **1965**, *53*, 215-220.
- (52) Ziemann, P. J.; Atkinson, R. Kinetics, products, and mechanisms of secondary organic aerosol formation. *Chemical Society Reviews* **2012**, *41*, 6582-6605.
- (53) Seinfeld, J. H.; Pandis, S. N.: *Atmospheric Chemistry and Physics: From Air Pollution to Climate Change*, 2012.
- (54) Keywood, M. D.; Varutbangkul, V.; Bahreini, R.; Flagan, R. C.; Seinfeld, J. H. Secondary Organic Aerosol Formation from the Ozonolysis of Cycloalkenes and Related Compounds. *Environmental Science & Technology* **2004**, *38*, 4157-4164.
- (55) Pierotti, D.; Wofsy, S. C.; Jacob, D.; Rasmussen, R. A. Isoprene and its oxidation products: Methacrolein and methyl vinyl ketone. *J. Geophys. Res. Atmos.* **1990**, *95*, 1871-1881.
- (56) Kroll, J. H.; Ng, N. L.; Murphy, S. M.; Flagan, R. C.; Seinfeld, J. H. Secondary Organic Aerosol Formation from Isoprene Photooxidation. *Environ. Sci. Technol.* **2006**, *40*, 1869-1877.
- (57) Edney, E. O.; Kleindienst, T. E.; Jaoui, M.; Lewandowski, M.; Offenberg, J. H.; Wang, W.; Claeys, M. Formation of 2-methyl tetrols and 2-methylglyceric acid in secondary organic aerosol from laboratory irradiated isoprene/NO_x/SO₂/air mixtures and their detection in ambient PM_{2.5} samples collected in the eastern United States. *Atmos. Environ.* **2005**, *39*, 5281-5289.
- (58) Pankow, J. F.; Asher, W. E. SIMPOL.1: a simple group contribution method for predicting vapor pressures and enthalpies of vaporization of multifunctional organic compounds. *Atmos. Chem. Phys.* **2008**, *8*, 2773-2796.
- (59) Ng, N. L.; Chhabra, P. S.; Chan, A. W. H.; Surratt, J. D.; Kroll, J. H.; Kwan, A. J.; McCabe, D. C.; Wennberg, P. O.; Sorooshian, A.; Murphy, S. M.; Dalleska, N. F.; Flagan, R. C.; Seinfeld, J. H. Effect of NO_x level on secondary organic aerosol (SOA) formation from the photooxidation of terpenes. *Atmospheric Chemistry and Physics Discussions* **2007**, *7*, 10131-10177.
- (60) Szmigielski, R.; Surratt, J. D.; Vermeylen, R.; Szmigielska, K.; Kroll, J. H.; Ng, N. L.; Murphy, S. M.; Sorooshian, A.; Seinfeld, J. H.; Claeys, M. Characterization of 2-methylglyceric acid oligomers in secondary organic aerosol formed from the photooxidation of isoprene using trimethylsilylation and gas chromatography/ion trap mass spectrometry. *Journal of Mass Spectrometry* **2007**, *42*, 101-116.
- (61) Nestorowicz, K.; Jaoui, M.; Rudzinski, K. J.; Lewandowski, M.; Kleindienst, T. E.; Spólnik, G.; Danikiewicz, W.; Szmigielski, R. Chemical composition of isoprene SOA under acidic and non-acidic conditions: effect of relative humidity. *Atmos. Chem. Phys.* **2018**, *18*, 18101-18121.
- (62) Atkinson, R. Atmospheric chemistry of VOCs and NO_x. *Atmospheric Environment* **2000**, *34*, 2063-2101.
- (63) Cai, X.; Griffin, R. J. Secondary aerosol formation from the oxidation of biogenic hydrocarbons by chlorine atoms. *Journal of Geophysical Research: Atmospheres* **2006**, *111*.

- (64) Paulson, S. E.; Orlando, J. J. The reactions of ozone with alkenes: An important source of HOx in the boundary layer. *Geophysical Research Letters* **1996**, *23*, 3727-3730.
- (65) Zhang, S.-H.; Shaw, M.; Seinfeld, J. H.; Flagan, R. C. Photochemical aerosol formation from α -pinene- and β -pinene. *Journal of Geophysical Research: Atmospheres* **1992**, *97*, 20717-20729.
- (66) Atkinson, R.; Arey, J. Gas-phase tropospheric chemistry of biogenic volatile organic compounds: a review. *Atmos. Environ.* **2003**, *37*, 197-219.
- (67) Calvert, J. G.; Atkinson, R. W.; Becker, K. H.; Kamens, R. M.; Seinfeld, J. H.; Wallington, T. J.; Yarwood, G.: *The mechanisms of atmospheric oxidation of aromatic hydrocarbons*; Oxford University Press: New York, 2002.
- (68) Calvert, J. G.; Mellouki, A.; Orlando, J. J.; Pilling, M. J.; Wallington, T. J.: *The Mechanisms of Atmospheric Oxidation of the Oxygenates*; Oxford University Press: New York, 2011.
- (69) Calogirou, A.; Larsen, B. R.; Kotzias, D. Gas-phase terpene oxidation products: a review. *Atmospheric Environment* **1999**, *33*, 1423-1439.
- (70) Bianchi, F.; Kurtén, T.; Riva, M.; Mohr, C.; Rissanen, M. P.; Roldin, P.; Berndt, T.; Crouse, J. D.; Wennberg, P. O.; Mentel, T. F.; Wildt, J.; Junninen, H.; Jokinen, T.; Kulmala, M.; Worsnop, D. R.; Thornton, J. A.; Donahue, N.; Kjaergaard, H. G.; Ehn, M. Highly Oxygenated Organic Molecules (HOM) from Gas-Phase Autoxidation Involving Peroxy Radicals: A Key Contributor to Atmospheric Aerosol. *Chemical Reviews* **2019**, *119*, 3472-3509.
- (71) Blanco, M. B.; Barnes, I.; Wiesen, P. Kinetic investigation of the OH radical and Cl atom initiated degradation of unsaturated ketones at atmospheric pressure and 298 K. *J Phys Chem A* **2012**, *116*, 6033-6040.
- (72) Barnes, I.; Bastian, V.; Becker, K. H.; Tong, Z. Kinetics and products of the reactions of nitrate radical with monoalkenes, dialkenes, and monoterpenes. *The Journal of Physical Chemistry* **1990**, *94*, 2413-2419.
- (73) Faxon, C. B.; Allen, D. T. Chlorine chemistry in urban atmospheres: a review. *Environmental Chemistry* **2013**, *10*, 221-233.
- (74) Canosa-Mas, C. E.; Hutton-Squire, H. R.; King, M. D.; Stewart, D. J.; Thompson, K. C.; Wayne, R. P. Laboratory Kinetic Studies of the Reactions of Cl Atoms with Species of Biogenic Origin: δ 3-Carene, Isoprene, Methacrolein and Methyl Vinyl Ketone. *Journal of Atmospheric Chemistry* **1999**, *34*, 163-170.
- (75) Riedel, T. P.; Lin, Y. H.; Zhang, Z.; Chu, K.; Thornton, J. A.; Vizuete, W.; Gold, A.; Surratt, J. D. Constraining condensed-phase formation kinetics of secondary organic aerosol components from isoprene epoxydiols. *Atmospheric Chemistry and Physics* **2016**, *16*, 1245-1254.
- (76) Riva, M.; Tomaz, S.; Cui, T.; Lin, Y. H.; Perraudin, E.; Gold, A.; Stone, E. A.; Villenave, E.; Surratt, J. D. Evidence for an unrecognized secondary anthropogenic source of organosulfates and sulfonates: gas-phase oxidation of polycyclic aromatic hydrocarbons in the presence of sulfate aerosol. *Environ. Sci. Technol.* **2015**, *49*, 6654.
- (77) Criegee, R. Mechanism of Ozonolysis. *Angewandte Chemie International Edition in English* **1975**, *14*, 745-752.
- (78) Donahue, N. M.; Drozd, G. T.; Epstein, S. A.; Presto, A. A.; Kroll, J. H. Adventures in ozoneland: down the rabbit-hole. *Physical Chemistry Chemical Physics* **2011**, *13*, 10848-10857.
- (79) Paulson, S. E.; Chung, M.; Sen, A. D.; Orzechowska, G. Measurement of OH radical formation from the reaction of ozone with several biogenic alkenes. *Journal of Geophysical Research: Atmospheres* **1998**, *103*, 25533-25539.
- (80) Yamasaki, H.; Kuwata, K.; Miyamoto, H. Effects of ambient temperature on aspects of airborne polycyclic aromatic hydrocarbons. *Environmental Science & Technology* **1982**, *16*, 189-194.

- (81) Pankow, J. F. An absorption model of gas/particle partitioning of organic compounds in the atmosphere. *Atmospheric Environment* **1994**, *28*, 185-188.
- (82) Gray, H. A.; Cass, G. R.; Huntzicker, J. J.; Heyerdahl, E. K.; Rau, J. A. Characteristics of atmospheric organic and elemental carbon particle concentrations in Los Angeles. *Environmental Science & Technology* **1986**, *20*, 580-589.
- (83) Mazurek, M. A. Molecular Identification of Organic Compounds in Atmospheric Complex Mixtures and Relationship to Atmospheric Chemistry and Sources. *Environmental Health Perspectives* **2002**, *110*, 995-1003.
- (84) Grosjean, D.; Seinfeld, J. H. Parameterization of the formation potential of secondary organic aerosols. *Atmospheric Environment (1967)* **1989**, *23*, 1733-1747.
- (85) Odum, J. R.; Hoffmann, T.; Bowman, F.; Collins, D.; Flagan, R. C.; Seinfeld, J. H. Gas/Particle Partitioning and Secondary Organic Aerosol Yields. *Environmental Science & Technology* **1996**, *30*, 2580-2585.
- (86) Szmigielski, R.; Surratt, J. D.; Gómez-González, Y.; Van der Veken, P.; Kourtchev, I.; Vermeylen, R.; Blockhuys, F.; Jaoui, M.; Kleindienst, T. E.; Lewandowski, M.; Offenberg, J. H.; Edney, E. O.; Seinfeld, J. H.; Maenhaut, W.; Claeys, M. 3-methyl-1,2,3-butanetricarboxylic acid: An atmospheric tracer for terpene secondary organic aerosol. *Geophysical Research Letters* **2007**, *34*.
- (87) Tolocka, M. P.; Jang, M.; Ginter, J. M.; Cox, F. J.; Kamens, R. M.; Johnston, M. V. Formation of Oligomers in Secondary Organic Aerosol. *Environmental Science & Technology* **2004**, *38*, 1428-1434.
- (88) Gao, S.; Ng, N. L.; Keywood, M.; Varutbangkul, V.; Bahreini, R.; Nenes, A.; He, J.; Yoo, K. Y.; Beauchamp, J. L.; Hodyss, R. P.; Flagan, R. C.; Seinfeld, J. H. Particle Phase Acidity and Oligomer Formation in Secondary Organic Aerosol. *Environmental Science & Technology* **2004**, *38*, 6582-6589.
- (89) De Haan, D. O.; Tolbert, M. A.; Jimenez, J. L. Atmospheric condensed-phase reactions of glyoxal with methylamine. *Geophysical Research Letters* **2009**, *36*.
- (90) Hoffmann, T.; Bandur, R.; Marggraf, U.; Linscheid, M. Molecular composition of organic aerosols formed in the α -pinene/O₃ reaction: Implications for new particle formation processes. *Journal of Geophysical Research: Atmospheres* **1998**, *103*, 25569-25578.
- (91) Yasmeen, F.; Vermeylen, R.; Maurin, N.; Perraudin, E.; Doussin, J.-F.; Claeys, M. Characterisation of tracers for aging of α -pinene secondary organic aerosol using liquid chromatography/negative ion electrospray ionisation mass spectrometry. *Environmental Chemistry* **2012**, *9*, 236-246.
- (92) Surratt, J. D.; Lewandowski, M.; Offenberg, J. H.; Jaoui, M.; Kleindienst, T. E.; Edney, E. O.; Seinfeld, J. H. Effect of Acidity on Secondary Organic Aerosol Formation from Isoprene. *Environ. Sci. Technol.* **2007**, *41*, 5363-5369.
- (93) Donahue, N. M.; Henry, K. M.; Mentel, T. F.; Kiendler-Scharr, A.; Spindler, C.; Bohn, B.; Brauers, T.; Dorn, H. P.; Fuchs, H.; Tillmann, R.; Wahner, A.; Saathoff, H.; Naumann, K.-H.; Möhler, O.; Leisner, T.; Müller, L.; Reinnig, M.-C.; Hoffmann, T.; Salo, K.; Hallquist, M.; Frosch, M.; Bilde, M.; Tritscher, T.; Barmet, P.; Praplan, A. P.; DeCarlo, P. F.; Dommen, J.; Prévôt, A. S. H.; Baltensperger, U. Aging of biogenic secondary organic aerosol via gas-phase OH radical reactions. *Proceedings of the National Academy of Sciences* **2012**, *109*, 13503-13508.
- (94) Rudich, Y.; Donahue, N. M.; Mentel, T. F. Aging of organic aerosol: bridging the gap between laboratory and field studies. *Annu Rev Phys Chem* **2007**, *58*, 321-352.
- (95) Kroll, J. H.; Smith, J. D.; Che, D. L.; Kessler, S. H.; Worsnop, D. R.; Wilson, K. R. Measurement of fragmentation and functionalization pathways in the heterogeneous oxidation of oxidized organic aerosol. *Phys Chem Chem Phys* **2009**, *11*, 8005-8014.

- (96) Kołodziejczyk, A. Badania fizykochemiczne produktów utleniania alfa-pinenu w aspekcie powstawania wtórnego aerozolu atmosferycznego. Doctoral Dissertation, Institute of Physical Chemistry, Polish Academy of Sciences 2020.
- (97) Tritscher, T.; Dommen, J.; DeCarlo, P. F.; Gysel, M.; Barmet, P. B.; Praplan, A. P.; Weingartner, E.; Prévôt, A. S. H.; Riipinen, I.; Donahue, N. M.; Baltensperger, U. Volatility and hygroscopicity of aging secondary organic aerosol in a smog chamber. *Atmos. Chem. Phys.* **2011**, *11*, 11477-11496.
- (98) Wagstrom, K. M.; Pandis, S. N. Determination of the age distribution of primary and secondary aerosol species using a chemical transport model. *Journal of Geophysical Research: Atmospheres* **2009**, *114*.
- (99) Chen, Z. M.; Wang, H. L.; Zhu, L. H.; Wang, C. X.; Jie, C. Y.; Hua, W. Aqueous-phase ozonolysis of methacrolein and methyl vinyl ketone: a potentially important source of atmospheric aqueous oxidants. *Atmos. Chem. Phys.* **2008**, *8*, 2255-2265.
- (100) Lim, Y. B.; Turpin, B. J. Laboratory evidence of organic peroxide and peroxyhemiacetal formation in the aqueous phase and implications for aqueous OH. *Atmos. Chem. Phys.* **2015**, *15*, 12867.
- (101) Couvidat, F.; Sartelet, K.; Seigneur, C. Investigating the impact of aqueous-phase chemistry and wet deposition on organic aerosol formation using a molecular surrogate modeling approach. *Environ Sci Technol* **2013**, *47*, 914-922.
- (102) Giorio, C.; Monod, A.; Bregonzio-Rozier, L.; DeWitt, H. L.; Cazaunau, M.; Temime-Roussel, B.; Gratien, A.; Michoud, V.; Pangui, E.; Ravier, S.; Zielinski, A. T.; Tapparo, A.; Vermeylen, R.; Claeys, M.; Voisin, D.; Kalberer, M.; Doussin, J. F. Cloud Processing of Secondary Organic Aerosol from Isoprene and Methacrolein Photooxidation. *J Phys Chem A* **2017**, *121*, 7641-7654.
- (103) Srivastava, D.; Favez, O.; Perraudin, E.; Villenave, E.; Albinet, A. Comparison of Measurement-Based Methodologies to Apportion Secondary Organic Carbon (SOC) in PM_{2.5}: A Review of Recent Studies. *Atmosphere* **2018**, *9*, 452.
- (104) Sheppard, P. A. Atmospheric tracers and the study of the general circulation of the atmosphere. *Reports on Progress in Physics* **1963**, *26*, 213-267.
- (105) Claeys, M.; Wang, W.; Ion, A. C.; Kourtchev, I.; Gelencsér, A.; Maenhaut, W. Formation of secondary organic aerosols from isoprene and its gas-phase oxidation products through reaction with hydrogen peroxide. *Atmospheric Environment* **2004**, *38*, 4093-4098.
- (106) González, N. J.; Borg-Karlson, A. K.; Redeby, J. P.; Nozière, B.; Krejci, R.; Pei, Y.; Dommen, J.; Prévôt, A. S. New method for resolving the enantiomeric composition of 2-methyltetrols in atmospheric organic aerosols. *Journal of chromatography. A* **2011**, *1218*, 9288-9294.
- (107) Nozière, B.; González, N. J. D.; Borg-Karlson, A.-K.; Pei, Y.; Redeby, J. P.; Krejci, R.; Dommen, J.; Prevot, A. S. H.; Anthonsen, T. Atmospheric chemistry in stereo: A new look at secondary organic aerosols from isoprene. *Geophysical Research Letters* **2011**, *38*.
- (108) Surratt, J. D.; Kroll, J. H.; Kleindienst, T. E.; Edney, E. O.; Claeys, M.; Sorooshian, A.; Ng, N. L.; Offenberg, J. H.; Lewandowski, M.; Jaoui, M.; Flagan, R. C.; Seinfeld, J. H. Evidence for Organosulfates in Secondary Organic Aerosol. *Environ. Sci. Technol.* **2007**, *41*, 517-527.
- (109) Birdsall, A. W.; Zentner, C. A.; Elrod, M. J. Study of the kinetics and equilibria of the oligomerization reactions of 2-methylglyceric acid. *Atmospheric Chemistry & Physics Discussions* **2012**, *12*, 30039.
- (110) Claeys, M.; Szmigielski, R.; Kourtchev, I.; Van der Veken, P.; Vermeylen, R.; Maenhaut, W.; Jaoui, M.; Kleindienst, T. E.; Lewandowski, M.; Offenberg, J. H.; Edney, E. O. Hydroxycarboxylic Acids: Markers for Secondary Organic Aerosol from the Photooxidation of α -Pinene. *Environmental Science & Technology* **2007**, *41*, 1628-1634.

- (111) Gomez-Gonzalez, Y.; Surratt, J. D.; Cuyckens, F.; Szmigielski, R.; Vermeylen, R.; Jaoui, M.; Lewandowski, M.; Offenberg, J. H.; Kleindienst, T. E.; Edney, E. O.; Blockhuys, F.; Van Alsenoy, C.; Maenhaut, W.; Claeys, M. Characterization of organosulfates from the photooxidation of isoprene and unsaturated fatty acids in ambient aerosol using liquid chromatography/(-) electrospray ionization mass spectrometry. *J Mass Spectrom* **2008**, *43*, 371-382.
- (112) Lin, Y. H.; Zhang, Z.; Docherty, K. S.; Zhang, H.; Budisulistiorini, S. H.; Rubitschun, C. L.; Shaw, S. L.; Knipping, E. M.; Edgerton, E. S.; Kleindienst, T. E.; Gold, A.; Surratt, J. D. Isoprene epoxydiols as precursors to secondary organic aerosol formation: acid-catalyzed reactive uptake studies with authentic compounds. *Environ. Sci. Technol.* **2012**, *46*, 250-258.
- (113) Zhang, H.; Lin, Y.-H.; Zhang, Z.; Zhang, X.; Shaw, S. L.; Knipping, E. M.; Weber, R. J.; Gold, A.; Kamens, R. M.; Surratt, J. D. Secondary organic aerosol formation from methacrolein photooxidation: roles of NO_x level, relative humidity and aerosol acidity. *Environmental Chemistry* **2012**, *9*, 247-262.
- (114) Zhang, Z.; Lin, Y. H.; Zhang, H.; Surratt, J. D.; Ball, L. M.; Gold, A. Technical Note: Synthesis of isoprene atmospheric oxidation products: isomeric epoxydiols and the rearrangement products cis- and trans-3-methyl-3,4-dihydroxytetrahydrofuran. *Atmospheric Chemistry and Physics* **2012**, *12*, 8529.
- (115) Lin, Y. H.; Zhang, H.; Pye, H. O.; Zhang, Z.; Marth, W. J.; Park, S.; Arashiro, M.; Cui, T.; Budisulistiorini, S. H.; Sexton, K. G.; Vizuete, W.; Xie, Y.; Luecken, D. J.; Piletic, I. R.; Edney, E. O.; Bartolotti, L. J.; Gold, A.; Surratt, J. D. Epoxide as a precursor to secondary organic aerosol formation from isoprene photooxidation in the presence of nitrogen oxides. *Proc Natl Acad Sci U S A* **2013**, *110*, 6718-6723.
- (116) Spolnik, G.; Wach, P.; Rudzinski, K. J.; Skotak, K.; Danikiewicz, W.; Szmigielski, R. Improved UHPLC-MS/MS Methods for Analysis of Isoprene-Derived Organosulfates. *Anal. Chem.* **2018**, *90*, 3416-3423.
- (117) Hettiyadura, A. P. S.; Stone, E. A.; Kundu, S.; Baker, Z.; Geddes, E.; Richards, K.; Humphry, T. Determination of atmospheric organosulfates using HILIC chromatography with MS detection. *Atmos. Meas. Tech.* **2015**, *8*, 2347-2358.
- (118) Jacobs, M. I.; Burke, W. J.; Elrod, M. J. Kinetics of the reactions of isoprene-derived hydroxynitrates: gas phase epoxide formation and solution phase hydrolysis. *Atmos. Chem. Phys.* **2014**, *14*, 8933-8946.
- (119) Moglioni, A. G.; García-Expósito, E.; Aguado, G. P.; Parella, T.; Branchadell, V.; Moltrasio, G. Y.; Ortuño, R. M. Divergent Routes to Chiral Cyclobutane Synthons from (-)- α -Pinene and Their Use in the Stereoselective Synthesis of Dehydro Amino Acids. *The Journal of Organic Chemistry* **2000**, *65*, 3934-3940.
- (120) Fache, F.; Piva, O.; Mirabel, P. First synthesis of hydroxy-pinonaldehyde and hydroxy-pinonic acid, monoterpene degradation products present in atmosphere. *Tetrahedron Letters* **2002**, *43*, 2511-2513.
- (121) Claeys, M.; Iinuma, Y.; Szmigielski, R.; Surratt, J. D.; Blockhuys, F.; Van Alsenoy, C.; Böge, O.; Sierau, B.; Gómez-González, Y.; Vermeylen, R.; Van der Veken, P.; Shahgholi, M.; Chan, A. W. H.; Herrmann, H.; Seinfeld, J. H.; Maenhaut, W. Terpenylic Acid and Related Compounds from the Oxidation of α -Pinene: Implications for New Particle Formation and Growth above Forests. *Environmental Science & Technology* **2009**, *43*, 6976-6982.
- (122) Yasmeen, F.; Vermeylen, R.; Szmigielski, R.; Iinuma, Y.; Böge, O.; Herrmann, H.; Maenhaut, W.; Claeys, M. Terpenylic acid and related compounds: precursors for dimers in secondary organic aerosol from the ozonolysis of α - and β -pinene. *Atmospheric Chemistry and Physics* **2010**, *10*, 9383-9392.

- (123) Iinuma, Y.; Böge, O.; Keywood, M.; Gnauk, T.; Herrmann, H. Diaterebic Acid Acetate and Diaterpenylic Acid Acetate: Atmospheric Tracers for Secondary Organic Aerosol Formation from 1,8-Cineole Oxidation. *Environmental Science & Technology* **2009**, *43*, 280-285.
- (124) Parshintsev, J.; Nurmi, J.; Kilpeläinen, I.; Hartonen, K.; Kulmala, M.; Riekkola, M.-L. Preparation of β -caryophyllene oxidation products and their determination in ambient aerosol samples. *Analytical and Bioanalytical Chemistry* **2008**, *390*, 913-919.
- (125) van Eijck, A.; Opatz, T.; Taraborrelli, D.; Sander, R.; Hoffmann, T. New tracer compounds for secondary organic aerosol formation from β -caryophyllene oxidation. *Atmospheric Environment* **2013**, *80*, 122-130.
- (126) Carlton, A. G.; Wiedinmyer, C.; Kroll, J. H. A review of Secondary Organic Aerosol (SOA) formation from isoprene. *Atmos. Chem. Phys.* **2009**, *9*, 4987-5005.
- (127) Surratt, J. D.; Chan, A. W.; Eddingsaas, N. C.; Chan, M.; Loza, C. L.; Kwan, A. J.; Hersey, S. P.; Flagan, R. C.; Wennberg, P. O.; Seinfeld, J. H. Reactive intermediates revealed in secondary organic aerosol formation from isoprene. *Proc. Natl. Acad. Sci. U S A* **2010**, *107*, 6640-6645.
- (128) Paulot, F.; Crouse, J. D.; Kjaergaard, H. G.; Kürten, A.; St. Clair, J. M.; Seinfeld, J. H.; Wennberg, P. O. Unexpected Epoxide Formation in the Gas-Phase Photooxidation of Isoprene. *Science* **2009**, *325*, 730-733.
- (129) Nguyen, T. B.; Coggon, M. M.; Bates, K. H.; Zhang, X.; Schwantes, R. H.; Schilling, K. A.; Loza, C. L.; Flagan, R. C.; Wennberg, P. O.; Seinfeld, J. H. Organic aerosol formation from the reactive uptake of isoprene epoxydiols (IEPOX) onto non-acidified inorganic seeds. *Atmospheric Chemistry and Physics* **2014**, *14*, 3497-3510.
- (130) Nguyen, T. B.; Bates, K. H.; Crouse, J. D.; Schwantes, R. H.; Zhang, X.; Kjaergaard, H. G.; Surratt, J. D.; Lin, P.; Laskin, A.; Seinfeld, J. H.; Wennberg, P. O. Mechanism of the hydroxyl radical oxidation of methacryloyl peroxyxynitrate (MPAN) and its pathway toward secondary organic aerosol formation in the atmosphere. *Physical Chemistry Chemical Physics* **2015**, *17*, 17914-17926.
- (131) Glasius, M.; Bering, M. S.; Yee, L. D.; de Sá, S. S.; Isaacman-VanWertz, G.; Wernis, R. A.; Barbosa, H. M. J.; Alexander, M. L.; Palm, B. B.; Hu, W.; Campuzano-Jost, P.; Day, D. A.; Jimenez, J. L.; Shrivastava, M.; Martin, S. T.; Goldstein, A. H. Organosulfates in aerosols downwind of an urban region in central Amazon. *Environ. Sci.: Processes & Impacts* **2018**, *20*, 1546-1558.
- (132) Ye, J.; Abbatt, J. P. D.; Chan, A. W. H. Novel pathway of SO₂ oxidation in the atmosphere: reactions with monoterpene ozonolysis intermediates and secondary organic aerosol. *Atmos. Chem. Phys.* **2018**, *18*, 5549.
- (133) Passananti, M.; Kong, L.; Shang, J.; Dupart, Y.; Perrier, S.; Chen, J.; Donaldson, D. J.; George, C. Organosulfate formation through the heterogeneous reaction of sulfur dioxide with unsaturated fatty acids and long-chain alkenes. *Angew. Chem., Int. Ed.* **2016**, *55*, 10336.
- (134) Wang, S.; Zhou, S.; Tao, Y.; Tsui, W. G.; Ye, J.; Yu, J. Z.; Murphy, J. G.; McNeill, V. F.; Abbatt, J. P. D.; Chan, A. W. H. Organic Peroxides and Sulfur Dioxide in Aerosol: Source of Particulate Sulfate. *Environmental Science & Technology* **2019**, *53*, 10695-10704.
- (135) Zheng, B.; Zhang, Q.; Zhang, Y.; He, K. B.; Wang, K.; Zheng, G. J.; Duan, F. K.; Ma, Y. L.; Kimoto, T. Heterogeneous chemistry: a mechanism missing in current models to explain secondary inorganic aerosol formation during the January 2013 haze episode in North China. *Atmos. Chem. Phys.* **2015**, *15*, 2031.
- (136) McNeill, V. F.; Woo, J. L.; Kim, D. D.; Schwier, A. N.; Wannell, N. J.; Sumner, A. J.; Barakat, J. M. Aqueous-phase secondary organic aerosol and organosulfate formation in atmospheric aerosols: a modeling study. *Environ Sci Technol* **2012**, *46*, 8075-8081.
- (137) Schone, L.; Schindelka, J.; Szeremeta, E.; Schaefer, T.; Hoffmann, D.; Rudzinski, K. J.; Szmigielski, R.; Herrmann, H. Atmospheric aqueous phase radical chemistry of the isoprene

oxidation products methacrolein, methyl vinyl ketone, methacrylic acid and acrylic acid--kinetics and product studies. *Phys. Chem. Chem. Phys.* **2014**, *16*, 6257-6272.

(138) Riva, M.; Chen, Y.; Zhang, Y.; Lei, Z.; Olson, N. E.; Boyer, H. C.; Narayan, S.; Yee, L. D.; Green, H. S.; Cui, T.; Zhang, Z.; Baumann, K.; Fort, M.; Edgerton, E.; Budisulistiorini, S. H.; Rose, C. A.; Ribeiro, I. O.; e Oliveira, R. L.; dos Santos, E. O.; Machado, C. M. D.; Szopa, S.; Zhao, Y.; Alves, E. G.; de Sá, S. S.; Hu, W.; Knipping, E. M.; Shaw, S. L.; Duvoisin Junior, S.; de Souza, R. A. F.; Palm, B. B.; Jimenez, J.-L.; Glasius, M.; Goldstein, A. H.; Pye, H. O. T.; Gold, A.; Turpin, B. J.; Vizuete, W.; Martin, S. T.; Thornton, J. A.; Dutcher, C. S.; Ault, A. P.; Surratt, J. D. Increasing Isoprene Epoxydiol-to-Inorganic Sulfate Aerosol Ratio Results in Extensive Conversion of Inorganic Sulfate to Organosulfur Forms: Implications for Aerosol Physicochemical Properties. *Environ. Sci. & Technol.* **2019**, *53*, 8682-8694.

(139) Brüggemann, M.; Xu, R.; Tilgner, A.; Kwong, K. C.; Mutzel, A.; Poon, H. Y.; Otto, T.; Schaefer, T.; Poulain, L.; Chan, M. N.; Herrmann, H. Organosulfates in Ambient Aerosol: State of Knowledge and Future Research Directions on Formation, Abundance, Fate, and Importance. *Environmental Science & Technology* **2020**, *54*, 3767-3782.

(140) Hatch, L. E.; Creamean, J. M.; Ault, A. P.; Surratt, J. D.; Chan, M. N.; Seinfeld, J. H.; Edgerton, E. S.; Su, Y.; Prather, K. A. Measurements of isoprene-derived organosulfates in ambient aerosols by aerosol time-of-flight mass spectrometry - part 1: single particle atmospheric observations in Atlanta. *Environ. Sci. Technol.* **2011**, *45*, 5105-5111.

(141) Laskin, J.; Laskin, A.; Nizkorodov, S. A. Mass Spectrometry Analysis in Atmospheric Chemistry. *Analytical Chemistry* **2018**, *90*, 166-189.

(142) Pratt, K. A.; Prather, K. A. Mass spectrometry of atmospheric aerosols--recent developments and applications. Part I: Off-line mass spectrometry techniques. *Mass spectrometry reviews* **2012**, *31*, 1-16.

(143) Pratt, K. A.; Prather, K. A. Mass spectrometry of atmospheric aerosols—Recent developments and applications. Part II: On-line mass spectrometry techniques. *Mass spectrometry reviews* **2012**, *31*, 17-48.

(144) McMurry, P. H. A review of atmospheric aerosol measurements. *Atmospheric Environment* **2000**, *34*, 1959-1999.

(145) Danikiewicz, W.: *Spektrometria Mas*; Wydawnictwo Naukowe PWN SA: Warszawa, 2020.

(146) Jaoui, M.; Szmigielski, R.; Nestorowicz, K.; Kolodziejczyk, A.; Sarang, K.; Rudzinski, K. J.; Konopka, A.; Bulska, E.; Lewandowski, M.; Kleindienst, T. E. Organic Hydroxy Acids as Highly Oxygenated Molecular (HOM) Tracers for Aged Isoprene Aerosol. *Environmental Science & Technology* **2019**, *53*, 14516-14527.

(147) Jaoui, M.; Lewandowski, M.; Kleindienst, T. E.; Offenberg, J. H.; Edney, E. O. β -caryophyllinic acid: An atmospheric tracer for β -caryophyllene secondary organic aerosol. *Geophysical Research Letters* **2007**, *34*.

(148) El Haddad, I.; Marchand, N.; Termine-Roussel, B.; Wortham, H.; Piot, C.; Besombes, J.-L.; Baduel, C.; Voisin, D.; Armengaud, A.; Jaffrezo, J.-L. Insights into the secondary fraction of the organic aerosol in a Mediterranean urban area: Marseille. *Atmospheric Chemistry and Physics* **2011**, *11*, 2059-2079.

(149) Niederer, M. Determination of polycyclic aromatic hydrocarbons and substitutes (Nitro-, Oxy-PAHs) in urban soil and airborne particulate by GC-MS and NCI-MS/MS. *Environmental Science and Pollution Research* **1998**, *5*, 209-216.

(150) Hearn, J. D.; Smith, G. D. A Chemical Ionization Mass Spectrometry Method for the Online Analysis of Organic Aerosols. *Analytical Chemistry* **2004**, *76*, 2820-2826.

(151) Zhao, R.; Lee, A. K. Y.; Abbatt, J. P. D. Investigation of Aqueous-Phase Photooxidation of Glyoxal and Methylglyoxal by Aerosol Chemical Ionization Mass

Spectrometry: Observation of Hydroxyhydroperoxide Formation. *The Journal of Physical Chemistry A* **2012**, *116*, 6253-6263.

(152) Kubátová, A.; Vermeylen, R.; Claeys, M.; Cafmeyer, J.; Maenhaut, W.; Roberts, G.; Artaxo, P. Carbonaceous aerosol characterization in the Amazon basin, Brazil: novel dicarboxylic acids and related compounds. *Atmospheric Environment* **2000**, *34*, 5037-5051.

(153) Wang, W.; Kourtchev, I.; Graham, B.; Cafmeyer, J.; Maenhaut, W.; Claeys, M. Characterization of oxygenated derivatives of isoprene related to 2-methyltetrols in Amazonian aerosols using trimethylsilylation and gas chromatography/ion trap mass spectrometry. *Rapid Commun Mass Spectrom* **2005**, *19*, 1343-1351.

(154) Kahnt, A.; Iinuma, Y.; Blockhuys, F.; Mutzel, A.; Vermeylen, R.; Kleindienst, T. E.; Jaoui, M.; Offenberg, J. H.; Lewandowski, M.; Böge, O.; Herrmann, H.; Maenhaut, W.; Claeys, M. 2-Hydroxyterpenylic Acid: An Oxygenated Marker Compound for α -Pinene Secondary Organic Aerosol in Ambient Fine Aerosol. *Environmental Science & Technology* **2014**, *48*, 4901-4908.

(155) Kawamura, K. Identification of C₂-C₁₀ .omega.-oxocarboxylic acids, pyruvic acid, and C₂-C₃ .alpha.-dicarbonyls in wet precipitation and aerosol samples by capillary GC and GC/MS. *Analytical Chemistry* **1993**, *65*, 3505-3511.

(156) Jaoui, M.; Kleindienst, T. E.; Lewandowski, M.; Edney, E. O. Identification and quantification of aerosol polar oxygenated compounds bearing carboxylic or hydroxyl groups. 1. Method development. *Analytical chemistry* **2004**, *76*, 4765-4778.

(157) Gao, S.; Surratt, J. D.; Knipping, E. M.; Edgerton, E. S.; Shahgholi, M.; Seinfeld, J. H. Characterization of polar organic components in fine aerosols in the southeastern United States: Identity, origin, and evolution. *Journal of Geophysical Research* **2006**, *111*.

(158) Olson, C. N.; Galloway, M. M.; Yu, G.; Hedman, C. J.; Lockett, M. R.; Yoon, T.; Stone, E. A.; Smith, L. M.; Keutsch, F. N. Hydroxycarboxylic acid-derived organosulfates: synthesis, stability, and quantification in ambient aerosol. *Environ Sci Technol* **2011**, *45*, 6468-6474.

(159) Renard, P.; Siekmann, F.; Salque, G.; Demelas, C.; Coulomb, B.; Vassalo, L.; Ravier, S.; Temime-Roussel, B.; Voisin, D.; Monod, A. Aqueous-phase oligomerization of methyl vinyl ketone through photooxidation - Part 1: Aging processes of oligomers. *Atmospheric Chemistry and Physics* **2015**, *15*, 21-35.

(160) Takáts, Z.; Wiseman, J. M.; Gologan, B.; Cooks, R. G. Mass Spectrometry Sampling Under Ambient Conditions with Desorption Electrospray Ionization. *Science* **2004**, *306*, 471-473.

(161) Roach, P. J.; Laskin, J.; Laskin, A. Molecular Characterization of Organic Aerosols Using Nanospray-Desorption/Electrospray Ionization-Mass Spectrometry. *Analytical Chemistry* **2010**, *82*, 7979-7986.

(162) Laskin, J.; Laskin, A.; Roach, P. J.; Slys, G. W.; Anderson, G. A.; Nizkorodov, S. A.; Bones, D. L.; Nguyen, L. Q. High-Resolution Desorption Electrospray Ionization Mass Spectrometry for Chemical Characterization of Organic Aerosols. *Analytical Chemistry* **2010**, *82*, 2048-2058.

(163) Flores, J. M.; Washenfelder, R. A.; Adler, G.; Lee, H. J.; Segev, L.; Laskin, J.; Laskin, A.; Nizkorodov, S. A.; Brown, S. S.; Rudich, Y. Complex refractive indices in the near-ultraviolet spectral region of biogenic secondary organic aerosol aged with ammonia. *Physical Chemistry Chemical Physics* **2014**, *16*, 10629-10642.

(164) Lin, P.; Liu, J.; Shilling, J. E.; Kathmann, S. M.; Laskin, J.; Laskin, A. Molecular characterization of brown carbon (BrC) chromophores in secondary organic aerosol generated from photo-oxidation of toluene. *Physical Chemistry Chemical Physics* **2015**, *17*, 23312-23325.

(165) Kückelmann, U.; Warscheid, B.; Hoffmann, T. On-Line Characterization of Organic Aerosols Formed from Biogenic Precursors Using Atmospheric Pressure Chemical Ionization Mass Spectrometry. *Analytical Chemistry* **2000**, *72*, 1905-1912.

- (166) Zuth, C.; Vogel, A. L.; Ockenfeld, S.; Huesmann, R.; Hoffmann, T. Ultrahigh-Resolution Mass Spectrometry in Real Time: Atmospheric Pressure Chemical Ionization Orbitrap Mass Spectrometry of Atmospheric Organic Aerosol. *Analytical Chemistry* **2018**, *90*, 8816-8823.
- (167) Hanold, K. A.; Fischer, S. M.; Cormia, P. H.; Miller, C. E.; Syage, J. A. Atmospheric Pressure Photoionization. 1. General Properties for LC/MS. *Analytical Chemistry* **2004**, *76*, 2842-2851.
- (168) Giorio, C.; Bortolini, C.; Kourtchev, I.; Tapparo, A.; Bogialli, S.; Kalberer, M. Direct target and non-target analysis of urban aerosol sample extracts using atmospheric pressure photoionisation high-resolution mass spectrometry. *Chemosphere* **2019**, *224*, 786-795.
- (169) Yang, F.; Jones, C. A.; Dearden, D. V. Effects of kinetic energy and collision gas on measurement of cross sections by Fourier transform ion cyclotron resonance mass spectrometry. *International Journal of Mass Spectrometry* **2015**, *378*, 143-150.
- (170) Safi Shalamzari, M.; Ryabtsova, O.; Kahnt, A.; Vermeylen, R.; Herent, M. F.; Quetin-Leclercq, J.; Van der Veken, P.; Maenhaut, W.; Claeys, M. Mass spectrometric characterization of organosulfates related to secondary organic aerosol from isoprene. *Rapid Commun Mass Spectrom* **2013**, *27*, 784-794.
- (171) Spólnik, G.; Wach, P.; Wróbel, Z.; Danikiewicz, W. 2-Iodomalondialdehyde is an abundant component of soluble organic iodine in atmospheric wet precipitation. *Science of The Total Environment* **2020**, *730*, 139175.
- (172) Zhang, Z.; Yang, M. J.; Pawliszyn, J. Solid-Phase Microextraction. *Analytical Chemistry* **1994**, *66*, 844A-853A.
- (173) Medeiros, P. M.; Simoneit, B. R. Analysis of sugars in environmental samples by gas chromatography–mass spectrometry. *Journal of Chromatography A* **2007**, *1141*, 271-278.
- (174) Jang, M.; Kamens, R. M. Characterization of secondary aerosol from the photooxidation of toluene in the presence of NO_x and 1-propene. *Environmental Science & Technology* **2001**, *35*, 3626-3639.
- (175) Alam, M. S.; Harrison, R. M. Recent advances in the application of 2-dimensional gas chromatography with soft and hard ionisation time-of-flight mass spectrometry in environmental analysis. *Chemical Science* **2016**, *7*, 3968-3977.
- (176) Surratt, J. D.; Gómez-González, Y.; Chan, A. W. H.; Vermeylen, R.; Shahgholi, M.; Kleindienst, T. E.; Edney, E. O.; Offenberg, J. H.; Lewandowski, M.; Jaoui, M.; Maenhaut, W.; Claeys, M.; Flagan, R. C.; Seinfeld, J. H. Organosulfate Formation in Biogenic Secondary Organic Aerosol. *J. Phys. Chem. A* **2008**, *112*, 8345-8378.
- (177) Lung, S. C.; Liu, C. H. Fast analysis of 29 polycyclic aromatic hydrocarbons (PAHs) and nitro-PAHs with ultra-high performance liquid chromatography-atmospheric pressure photoionization-tandem mass spectrometry. *Sci Rep* **2015**, *5*, 12992.
- (178) Lin, P.; Laskin, J.; Nizkorodov, S. A.; Laskin, A. Revealing Brown Carbon Chromophores Produced in Reactions of Methylglyoxal with Ammonium Sulfate. *Environmental Science & Technology* **2015**, *49*, 14257-14266.
- (179) Laskin, A.; Laskin, J.; Nizkorodov, S. A. Chemistry of Atmospheric Brown Carbon. *Chemical Reviews* **2015**, *115*, 4335-4382.
- (180) Maenhaut, W.; Raes, N.; Chi, X.; Cafmeyer, J.; Wang, W. Chemical composition and mass closure for PM_{2.5} and PM₁₀ aerosols at K-pusztá, Hungary, in summer 2006. *X-Ray Spectrom.* **2008**, *37*, 193-197.
- (181) Jeffries, H.; Kamens, R.; Sexton, K. Early history and rationale for outdoor chamber work at the University of North Carolina. *Environmental Chemistry* **2013**, *10*, 349.
- (182) Ebersviller, S.; Lichtveld, K.; Sexton, K. G.; Zavala, J.; Lin, Y. H.; Jaspers, I.; Jeffries, H. E. Gaseous VOCs rapidly modify particulate matter and its biological effects – Part 1: Simple VOCs and model PM. *Atmos. Chem. Phys.* **2012**, *12*, 12277-12292.

- (183) Rudzinski, K. J. Degradation of Isoprene in the Presence of Sulphoxy Radical Anions. *J. of Atmos. Chem.* **2004**, *48*, 191-216.
- (184) Rudziński, K. J.; Gmachowski, L.; Kuznietsova, I. Reactions of isoprene and sulphony radical-anions—a possible source of atmospheric organosulphites and organosulphates. *Atmos. Chem. Phys.* **2009**, *9*, 2129.
- (185) Glasius, M.; Goldstein, A. H. Recent Discoveries and Future Challenges in Atmospheric Organic Chemistry. *Environ Sci Technol* **2016**, *50*, 2754-2764.
- (186) Hettiyadura, A. P. S.; Jayarathne, T.; Baumann, K.; Goldstein, A. H.; de Gouw, J. A.; Koss, A.; Keutsch, F. N.; Skog, K.; Stone, E. A. Qualitative and quantitative analysis of atmospheric organosulfates in Centreville, Alabama. *Atmos. Chem. Phys.* **2017**, *17*, 1343-1359.
- (187) Hettiyadura, A. P. S.; Al-Naiema, I. M.; Hughes, D. D.; Fang, T.; Stone, E. A. Organosulfates in Atlanta, Georgia: anthropogenic influences on biogenic secondary organic aerosol formation. *Atmos. Chem. Phys.* **2019**, *19*, 3191-3206.
- (188) Attygalle, A. B.; García-Rubio, S.; Ta, J.; Meinwald, J. Collisionally-induced dissociation mass spectra of organic sulfate anions. *Journal of the Chemical Society, Perkin Transactions 2* **2001**, 498-506.
- (189) Gómez-González, Y.; Wang, W.; Vermeylen, R.; Chi, X.; Neiryneck, J.; Janssens, I. A.; Maenhaut, W.; Claeys, M. Chemical characterisation of atmospheric aerosols during a 2007 summer field campaign at Brasschaat, Belgium: sources and source processes of biogenic secondary organic aerosol. *Atmos. Chem. Phys.* **2012**, *12*, 125-138.
- (190) Fringuelli, F.; Germani, R.; Pizzo, F.; Savelli, G. One-Pot Two-Steps Synthesis of 1,2-Diol. *Synthetic Communications* **1989**, *19*, 1939-1943.
- (191) García Ruano, J. L.; Fajardo, C.; Fraile, A.; Martián, M. R. Nucleophilic Epoxidation of α -Sulfonyl- α,β -Unsaturated Esters with m-CPBA. *Phosphorus, Sulfur, and Silicon and the Related Elements* **2005**, *180*, 1489-1490.
- (192) Grzesiak, P. Badania tworzenia składników wtórnego aerozolu atmosferycznego z izoprenu w reakcjach w fazie wodnej inicjowanych autooksydacją siarki (IV) z użyciem sprzężonych technik organicznej spektrometrii mas. **2017**.
- (193) Lam, H. K.; Kwong, K. C.; Poon, H. Y.; Davies, J. F.; Zhang, Z.; Gold, A.; Surratt, J. D.; Chan, M. N. Heterogeneous OH oxidation of isoprene-epoxydiol-derived organosulfates: kinetics, chemistry and formation of inorganic sulfate. *Atmos. Chem. Phys.* **2019**, *19*, 2433-2440.
- (194) Herrmann, H. On the photolysis of simple anions and neutral molecules as sources of O-/OH, SO(x)- and Cl in aqueous solution. *Phys Chem Chem Phys* **2007**, *9*, 3935-3964.
- (195) Claeys, M.; Maenhaut, W. Secondary Organic Aerosol Formation from Isoprene: Selected Research, Historic Account and State of the Art. *Atmosphere* **2021**, *12*, 728.
- (196) Schindelka, J.; Iinuma, Y.; Hoffmann, D.; Herrmann, H. Sulfate radical-initiated formation of isoprene-derived organosulfates in atmospheric aerosols. *Faraday Discuss.* **2013**, 165.
- (197) Nozière, B.; Ekström, S.; Alsberg, T.; Holmström, S. Radical-initiated formation of organosulfates and surfactants in atmospheric aerosols. *Geophys. Res. Lett.* **2010**, *37*.
- (198) Schöne, L.; Herrmann, H. Kinetic measurements of the reactivity of hydrogen peroxide and ozone towards small atmospherically relevant aldehydes, ketones and organic acids in aqueous solutions. *Atmospheric Chemistry and Physics* **2014**, *14*, 4503-4514.
- (199) Townsend, T. M.; Allanic, A.; Noonan, C.; Sodeau, J. R. Characterization of Sulfurous Acid, Sulfite, and Bisulfite Aerosol Systems. *The Journal of Physical Chemistry A* **2012**, *116*, 4035-4046.
- (200) McNeill, V. F. Aqueous organic chemistry in the atmosphere: sources and chemical processing of organic aerosols. *Environ Sci Technol* **2015**, *49*, 1237-1244.
- (201) Blando, J.; Turpin, B. Secondary organic aerosol formation in cloud and fog droplets: A literature evaluation of plausibility. *Atmospheric Environment* **2000**, *34*, 1623-1632.

(202) Ervens, B. A modeling study of aqueous production of dicarboxylic acids: 1. Chemical pathways and speciated organic mass production. *Journal of Geophysical Research* **2004**, *109*.

(203) Bianchi, F.; Tröstl, J.; Junninen, H.; Frege, C.; Henne, S.; Hoyle, C. R.; Molteni, U.; Herrmann, E.; Adamov, A.; Bukowiecki, N.; Chen, X.; Duplissy, J.; Gysel, M.; Hutterli, M.; Kangasluoma, J.; Kontkanen, J.; Kürten, A.; Manninen, H. E.; Münch, S.; Peräkylä, O.; Petäjä, T.; Rondo, L.; Williamson, C.; Weingartner, E.; Curtius, J.; Worsnop, D. R.; Kulmala, M.; Dommen, J.; Baltensperger, U. New particle formation in the free troposphere: A question of chemistry and timing. *Science* **2016**, *352*, 1109-1112.

(204) Herckes, P.; Lee, T.; Trenary, L.; Kang, G.; Chang, H.; Collett, J. L., Jr. Organic matter in central California radiation fogs. *Environ Sci Technol* **2002**, *36*, 4777-4782.

(205) Altieri, K.; Turpin, B.; Seitzinger, S. Oligomers, organosulfates, and nitrooxy organosulfates in rainwater identified by ultra-high resolution electrospray ionization FT-ICR mass spectrometry. *Atmospheric Chemistry and Physics* **2009**, *9*.

(206) Mazzoleni, L. R.; Ehrmann, B. M.; Shen, X.; Marshall, A. G.; Collett, J. L. Water-Soluble Atmospheric Organic Matter in Fog: Exact Masses and Chemical Formula Identification by Ultrahigh-Resolution Fourier Transform Ion Cyclotron Resonance Mass Spectrometry. *Environmental Science & Technology* **2010**, *44*, 3690-3697.

(207) Pratt, K.; Fiddler, M.; Shepson, P.; Carlton, A. M.; Surratt, J. Organosulfates in cloud water above the Ozarks' isoprene source region. *Atmospheric Environment* **2013**, *77*, 231-238.

(208) Bianco, A.; Riva, M.; Baray, J.-L.; Ribeiro, M.; Chaumerliac, N.; George, C.; Bridoux, M.; Deguillaume, L. Chemical Characterization of Cloudwater Collected at Puy de Dôme by FT-ICR MS Reveals the Presence of SOA Components. *ACS Earth and Space Chemistry* **2019**, *3*, 2076-2087.

(209) Chapman, E. G.; Barinaga, C. J.; Udseth, H. R.; Smith, R. D. Confirmation and quantitation of hydroxymethanesulfonate in precipitation by electrospray ionization-tandem mass spectrometry. *Atmospheric Environment. Part A. General Topics* **1990**, *24*, 2951-2957.

(210) Fan, C.; Ding, M.; Wu, P.; Fan, Y. The Relationship between Precipitation and Aerosol: Evidence from Satellite Observation. *arXiv preprint arXiv:1812.02036* **2018**



B.575/24

Biblioteka Instytutu Chemii Fizycznej PAN

F-B.575/24



10000000116289

Institute of Physical Chemistry

Kasprzaka 44/52

www.ichf.edu

Polish Academy of Sciences

01-224 Warsaw, Poland

<http://rcin.org.pl>